ADVANCED MASTERS IN STRUCTURAL ANALYSIS
OF MONUMENTS AND HISTORICAL CONSTRUCTIONS

Master's Thesis

Susana Moreira

Dynamic Monitoring of Monumental Buildings Struck by the April 2009 Abruzzo Earthquake: Pre- and Post-processing Procedures.

This Masters Course has been funded with support from the European Commission. This publication reflects the views only of the author, and the Commission cannot be held responsible for any use which may be made of the information contained therein.

Italy | 2010

DECLARATION

Name: Susana Maria Trindade Moreira

Email: su.moreira.pt@gmail@com

Title of the Msc Dissertation: Dynamic monitoring of monumental buildings struck by the April 2009 Abruzzo earthquake: pre- and post-processing procedures

Supervisor(s): Prof. Claudio Modena, Prof. Filippo Casarin

Year: 2010

I hereby declare that all information in this document has been obtained and presented in accordance with academic rules and ethical conduct. I also declare that, as required by these rules and conduct, I have fully cited and referenced all material and results that are not original to this work.

I hereby declare that the MSc Consortium responsible for the Advanced Masters in Structural Analysis of Monuments and Historical Constructions is allowed to store and make available electronically the present MSc Dissertation.

University: University of Padova, Italy

Date: 22nd July, 2010

Signature: _____

This page is left blank on purpose.

To family and friends

This page is left blank on purpose.

ACKNOWLEDGEMENTS

First I would like to thanks to my supervisor Prof. Claudio Modena and co-supervisor Prof. Filippo Casarin for all the help and advisement provided during these four months, which lead to the feeling of fulfilled work.

Thanks so much to Prof. Luís Ramos, for the interest in the work and especially for explaining and help me with the implementation of ARX models in Matlab. Without his guidance the development of this thesis, it would had been much more complicated.

A special thanks to all the Professors, which accompanied us in Guimarães during the first coursework semester, who I had the privileged to meet and from whom I learned so much.

Also, thanks to the Consortium for the scholarship provided.

Now, a really big thanks to all my family and friends, especially the ones that I met this year in the program and are for life. Sorry, for all the preoccupations and stress that I passed to you all. Mom and dad, as always my biggest supporters and “safe place”, thanks for everything you did for me.

And, finally to Clive for not letting me give up, always expect the best for me and for being the best journey companion for the last 10 months.

This page is left blank on purpose.

ABSTRACT

A year has now passed since the April 6th Abruzzo earthquake and a great amount of work is still in progress, giving the opportunity to gather as much information as possible about the behavior of the structures in the presence of seismic/dynamic action.

Within the several activities that University of Padova is developing in L'Aquila, monitoring of buildings with cultural heritage is one of them. Of the two types of monitoring, static and dynamic, this dissertation focus on the second one, with emphases to a preparatory stage for the installation of a dynamic monitoring systems – pre-processing –, and to another stage consisting in the analysis of the output-input data – post-processing.

The pre-processing phase has the objective of answering questions as "*Where to position the sensors?"*, *"What kind of modal frequencies and mode shapes should be expected?"*. By answering these questions, one is prepared to better capture the behavior of the structure and improve the results, reduce time waste and economical resources. In this thesis, a preliminary structural model of San Domenico church was built, in order to prepare possible setups for the dynamic monitoring. Along with it, a brief historical survey and damage description were carried out.

At the other end of the process, is the post-processing phase, which consists of evaluating the information gathered by the monitoring system and take conclusions about the behavior of the structure, study what happen and what to expect. The analyzed data refers to the Spanish Castle and the first step was to identify the first four modal frequencies and then understand the effects of environment and excitation on the structure. This was accomplished by the use of static and dynamic regression models that reproduce approximately the influence of some inputs like temperature and relative humidity, in the output frequencies. Other important aspect was to compare the obtained modal frequencies with the range of frequencies achieved by minor seismic events and know if they had impact in the behavior of the structure.

This page is left blank on purpose.

ESTRATTO

Più di un anno è oramai passato dal sisma che il 6 Aprile 2009 ha duramente colpito l'Abruzzo, e molte linee di ricerca sono attualmente legate al tema sismico in tale territorio. In tal modo, sarà possibile ottenere un ampio database di informazioni legate al comportamento sismico delle strutture.

Tra le numerose attività svolte dal Dipartimento di Costruzioni e Trasporti dell'Università di Padova in tale senso, si sottolinea l'attività di monitoraggio strutturale dei beni culturali. Tra le due tipologie di monitoraggio, statico (controllo delle lesioni) e dinamico (misurazione delle vibrazioni), la presente tesi analizza il secondo, ed in particolare in relazione alla fase preparatoria dell'installazione del sistema di monitoraggio (definita pre-processing), ed alla fase di analisi dei dati del monitoraggio (post-processing).

La fase di pre-processing si pone come obiettivo di rispondere alle seguenti domande: "*quali sono le posizioni più adatte per installare i sensori di accelerazione?"; "quali forme modali e campo di frequenza sono previsti per la struttura monitorata?*" Nel rispondere a tali domande – essenzialmente mediante modellazione numerica – si può stimare il comportamento atteso delle strutture, migliorando pertanto la fase di monitoraggio vero e proprio, riducendo al contempo eccessive ridondanze nel sistema. Nella presente tesi è stato costruito un modello preliminare per l'analisi modale della chiesa di S. Domenico a l'Aquila, proprio allo scopo di ottenere informazioni circa il comportamento dinamico della struttura ed ottimizzare la fase di posizionamento dei sensori nelle successive fasi di identificazione modale e monitoraggio. La simulazione numerica è stata accompagnata da un'analisi storica e del quadro di danno dell'edificio manifestato in seguito al sisma dell'Aprile 2009.

All'altro capo del processo di conoscenza, si pone la fase di analisi dei dati, che essenzialmente consiste nella valutazione dei dati registrati dal sistema di monitoraggio, potendo trarre delle conclusioni relativamente al comportamento manifestato dall'edificio, e potendo valutare lo stato attuale della struttura in vista del controllo continuativo nel tempo.

I dati analizzati sono relativi al Forte Spagnolo a L'Aquila. Il primo passo dell'analisi è stata l'identificazione delle prime quattro frequenze proprie ed in base a queste il tentativo di comprendere quali potessero essere gli effetti dei parametri ambientali su di queste, e su di loro variazioni legati a tali parametri o ad altri eventi, quali ad esempio la progressione dello stato di danno. Tale analisi ha comportato l'utilizzo di modelli regressivi statici e dinamici, che tendono a depurare le frequenze di output dall'influenza dei parametri ambientali (temperatura ed umidità).

L'analisi è infine proseguita con la comparazione delle frequenze identificate e della loro analisi in relazione all'occorrenza di eventi sismici minori che continuano a manifestarsi nella regione, per valutare possibili variazioni di frequenza residue che potessero indicare dei fenomeni irreversibili di danneggiamento nella struttura.

This page is left blank on purpose.

RESUMO

Passado um ano após o terramoto de 6 de Abril, em Abruzzo, uma grande quantidade de trabalho ainda está por concretizar, dando a oportunidade de reunir a maior quantidade possível de informação, relativa ao comportamento de estruturas na presença de acção sísmica/dinâmica.

Dentro das diferentes actividades desenvolvidas pela Universidade de Pádua em L'Aquila, a monitorização de monumentos é uma delas. Dos dois tipos de monitorização, estática e dinâmica, esta dissertação aborda a segunda, com ênfase para uma fase preparatória para a instalação de sistemas de monitorização - pré-processamento -, e uma outra fase que consiste na análise dos dados resultantes dos sistemas já instalados - pós-processamento.

A fase de pré-processamento tem o objectivo de responder a perguntas como "Onde posicionar os sensores na estrutura?", "Que tipo de frequências modais e formas modais esperar?". Ao responder a estas perguntas, está-se a preparar o sistema para melhor captar o comportamento da estrutura e melhorar os resultados, reduzir o desperdício de tempo e recursos económicos. Nesta tese, um modelo preliminar estrutural da igreja de San Domenico foi construído, a fim de preparar configurações possíveis para a localização dos sensores. Adicionalmente, um breve levantamento histórico e descrição dos danos foram realizados.

Na outra ponta do processo, está a fase de pós-processamento, que consiste em avaliar as informações recolhidas pelo sistema de monitorização e tirar conclusões sobre o comportamento da estrutura, estudar o que aconteceu e o que esperar. Os dados analisados referem-se à Fortaleza Espanhola e o primeiro passo foi identificar as primeiras quatro frequências modais e, em seguida, entender os efeitos do ambiente e da excitação na estrutura. Isto foi conseguido através da utilização de modelos de regressão estática e dinâmica que reproduzem aproximadamente os valores medidos e filtram a influência de alguns factores como a temperatura e humidade relativa do ar, nas frequências (output). Outro aspecto importante foi comparar as frequências modais obtidas com a gama de frequências atingidas por abalos sísmicos de pequena dimensão e saber se eles tiveram qualquer impacto no comportamento da estrutura.

This page is left blank on purpose.

TABLE OF CONTENTS

ANNEX I

ANNEX II

TABLE OF FIGURES

LIST OF TABLES

1. INTRODUCTION

1.1 Motivation

Due to the 6th April 2009 earthquake, a lot of buildings with cultural value suffered severe and irreversible damage. More than an opportunity to see in real structures many damaged conditions until now, only in the theoretical domain, is also the chance of application of different approaches to evaluate a problem. Monitoring is one of them, especially the dynamic, because allows a global understanding of the structure and opens a time window in the life cycle of the structure, giving the opportunity to study it better and choose the best way to solve the problems found.

In severely damaged structures like the ones found in L'Aquila, monitoring can decide what kind of intervention to do and can control the progression of damage. Filtering the environmental effects can open the way to damage identification and location, by observing shifts in the modal frequencies.

Also, the detection of damage using this approach is giving big steps towards a more common application, instead of relying exclusively in visual inspection.

The importance of monitoring has increased in the last years, especially due to the scientific developments that allow continuous acquisition and storage of data and also to the improvement of techniques and software to analyze data.

1.2 Objectives of the Thesis

The main objective of this thesis is the development of procedures and information that can improve the application of dynamic monitoring.

For the pre-processing phase the purpose is to study the structure as much as possible, by doing a brief historical survey, identifying the main damage present at the church and at last constructing a FEM model, which allows the modal characterization and a better knowledge of the structure. All these steps are a preparation to better choose the monitoring configuration for the structure. The FEM model, even being in some aspects preliminary, can be in the future calibrated with the measured frequency values coming from the monitoring system.

The post-processing phase intends to demonstrate how damage can be detected, by filtering the modal parameters that come from the structure from the environmental effects and loading conditions.

1.3 Outline of the Thesis

The thesis is divided in 5 chapters: Chapter 1 - Introduction, Chapter 2 - Overall Seismic Context, Chapter 3 - Dynamic Monitoring, Chapter 4 - Case Studies and Chapter 5 - Conclusions and Future

Works. The second and the third chapters regard mainly the theory applied in the in the Case Studies. A brief description of each chapter is performed next:

Chapter 1 - Introduction – is like a guide to the rest of the thesis, presents the motivation and the purpose of the thesis;

Chapter 2 - Overall Seismic Context – since the thesis is applied to monuments struck by the April 2009 Abruzzo earthquake and in Case Study II, minor seismic events of the region are studied, this chapter intends to present the seismicity history of Italy and specifically the surrounding area of L'Aquila. A brief description of the April 2009 Abruzzo earthquake is also included;

Chapter 3 - Dynamic Monitoring – this chapter points out the differences between static and dynamic monitoring, the advantages and purpose, reflects on the different phases of the process and also introduces theoretical concepts, equipments and techniques applied on the subject;

Chapter 4 - Case Studies – two case studies are presented, San Domenico church and the Spanish fortress; they represent two different phases of a monitoring process, pre-processing and post-processing, respectively.

Chapter 5 - Conclusions and Future Works – this chapter goes over the main conclusions of each chapter and proposes works to complement the already done work or to improve it.

2. OVERAL SEISMIC CONTEX

In order to better understand the event of 6th April and seismicity of the area, a general overview of the European and Italian seismicity is presented.

2.1 Seismicity in Italy

2.1.1 Past Earthquakes

As shown in Figure 1, most of the past earthquakes have been happening along the borders of the tectonic plates: Eurasian, African and North America plates, especially where the first two meet. So, the Mediterranean region has a long history of major earthquakes, being some of the most punished countries: Italy, Greece, Turkey, Albania and Romania.

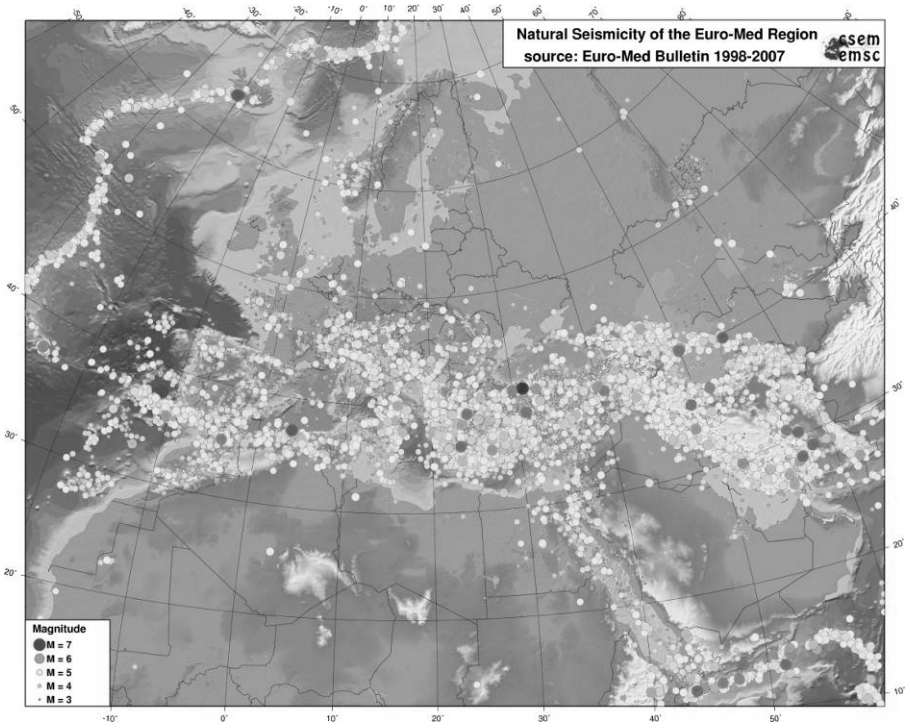

Figure 1 - Registered earthquakes from 1998 to 2007

From past earthquakes, between the most destructive ones, one can refer the earthquake of 1755 in Lisbon, Portugal with an estimated magnitude (Mw) of 9, followed by a tsunami and several fires, in total around 100000 people died.

Other severe earthquakes took place in Greece, on April 3rd 1881, with a magnitude of 6.6, and in Kocaeli (90km east of Istambul), Turkey, on August 17 of 1999, causing irreversible damages to historical buildings and killing thousands of people.

Italy as said before, always presented on of the highest concentration of seismic events and also some of the most destructive. In Table 1, are mentioned some of those earthquakes, as their location, magnitude and fatalities.

Table 1 - Most destructive earthquakes in Italy

Date	Location	Magnitude	Fatalities
25-01-1348	Friuli	n.a.	n.a.
05-12-1456	Molise	6.96	n.a.
17-11-1570	Ferrara	n.a.	70-200
11-01-1693	Sicily	7.41	60000
14-01-1703	Norcia	6.7	6240-9761
16-01-1703	Montereale	6.2	n.a.
12-02-1703	L'Aquila	6.7	2500-5000
05-02-1783	Calabria	6.91	30000
08-02-1832	Crotone	6.48	200+
28-12-1908	Messina	7.24	90000-120000
13-01-1915	Avezzano	6.99	29000+
10-11-1918	Appennino romagnolo	5.79	n.a.
07-09-1920	Garfagnana	6.48	300
23-07-1930	Irpinia	6.72	n.a.
06-05-1976	Friuli	6.43	965
23-11-1980	Irpinia	6.89	2734
26-09-1997	Marche-Umbria	6.05	11
31-10-2002	Molise	5.78	30
06-04-2009	L'Aquila	6.3	308

Observing Table 1 and Figure 2, is noticeable the distribution of earthquakes along the Apennines mountains and also the low depth of the hypocentre, being usually shallow earthquakes.

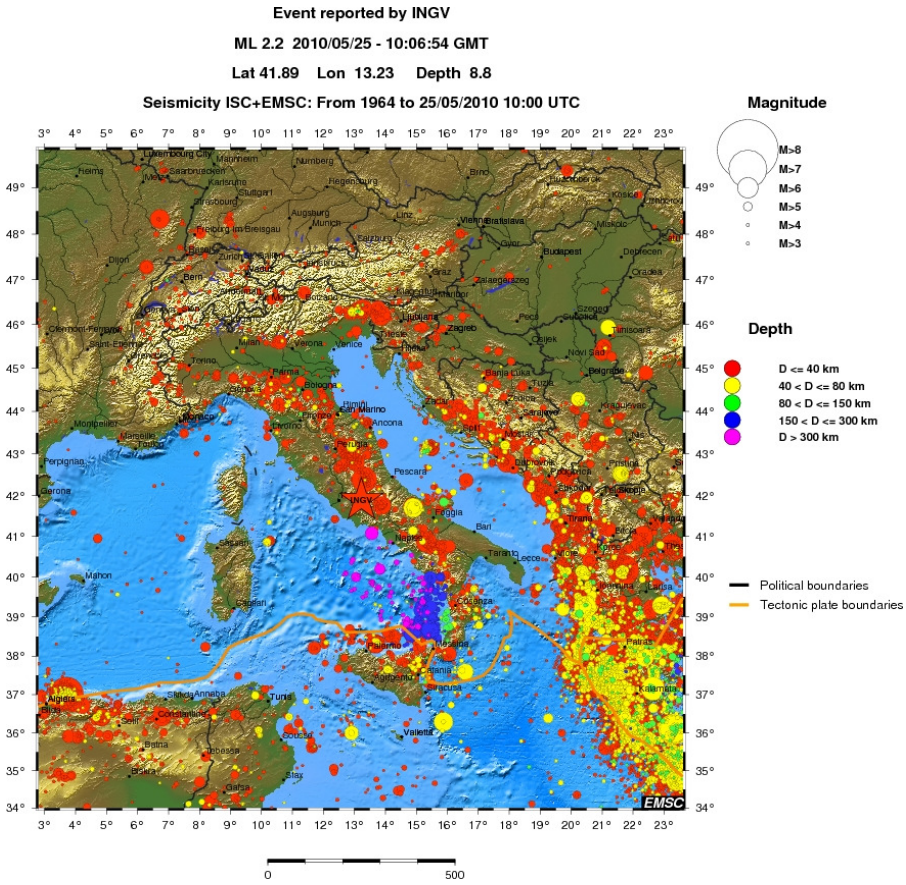

Figure 2 - Seismicity in Italy from 1964 to 25/05/2010

2.1.2 Evolution of seismic zoning

In Italy as in the majority of countries, the occurrence of earthquakes has always been the motivation to create or modify regulations regarding seismicity. Since, Italy is so seismically active the governments always tried to prevent and minimize casualties and severe damages to structures, by introducing legislation and seismic zoning. In 1927, two classes (zones) were applied to the country regarding a low and high level. After the major 1980 Irpinia earthquake, in 1984 the national territory was reclassified in three zones, with the confirmation of the previous classification and with the admission of new municipalities as seismic (see Figure 3 (a)). During 1998, the *Dipartimento della Protezione Civile ("Proposta 1998", pubblicato come Gruppo di Lavoro, 1999)* worked on a new seismic zoning, that was never adopted by the authorities (Stucchi, 2009).

With the San Giuliano di Puglia, in 2002, the attention of the country returned to the seismic zoning, because this location had been left out by the zoning of 1984 but according to "Proposta 1998" (see Figure 3 (b)), it should be classified as zone 2. So, the government with an emergency intervention changed the existing seismic zones, according to the pre-existing classification and the one suggested by "Proposta 1998", defining for the first time a zone 4 and extending the seismic risk to all the territory (see Figure 3 (c)). After that, in 2004 an alteration to the 2003 seismic zones was approved (see

Figure 3 (d)), changing some classifications and with the latest revision came up the zoning of 2006 (see Figure 3 (e)).

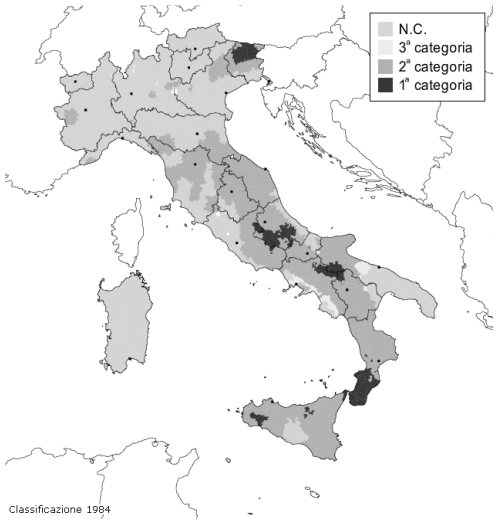

(a) 1984

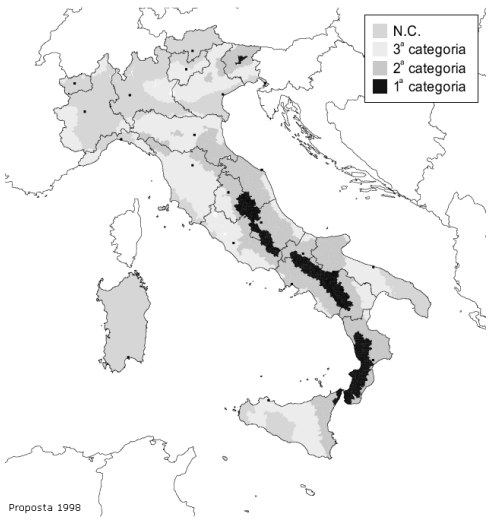

(b) “Proposta 1998”

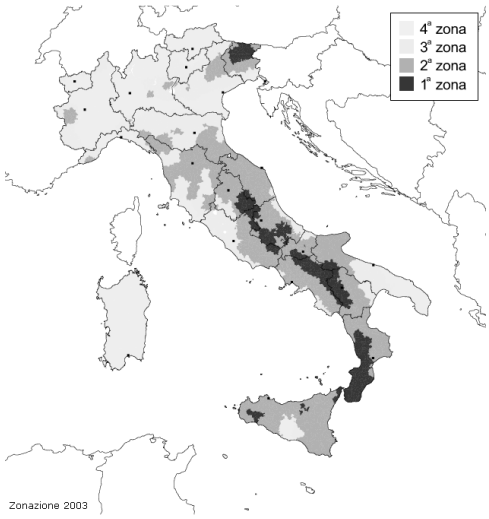

(c) 2003

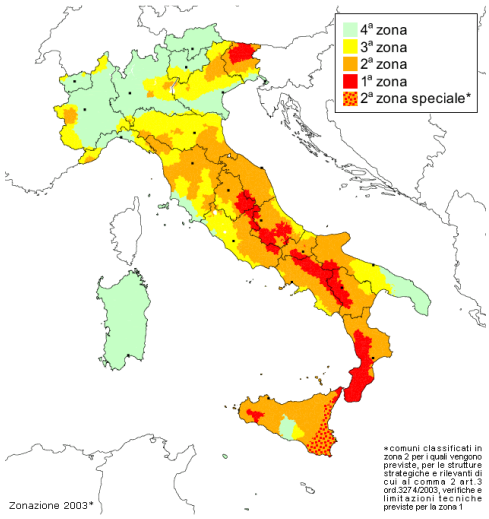

(d) 2003* (Alteration)

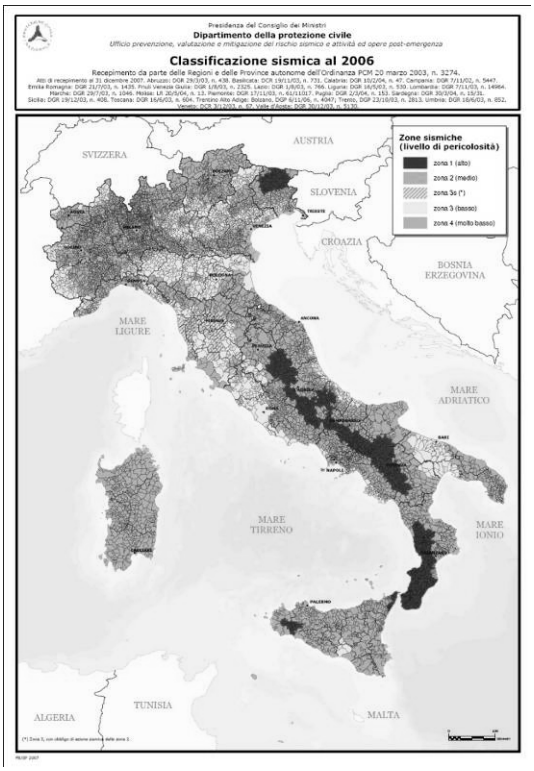

(e) 2006 (Present day)

Figure 3 - Evolution of the Italian seismic zoning: (a) 1984; (b) "Proposta 1998"; (c) 2003; (d) 2003* (Alteration) and (e) 2006 (Present day)

So, the seismic zoning map used nowadays is composed by 4 zones, from 1 to 4, decreasing in seismic risk (Costa, 2009):

- Area 1: Is the most dangerous area, very strong earthquakes can occur. 725 municipalities are included;
- Area 2: Some strong earthquakes are likely to happen. 2344 municipalities are included;
- Area 3: This area can be affected by moderated earthquakes. 1544 municipalities are included;
- Area 4: Is the less dangerous, in which the probabilities of seismic damage are low. 3488 municipalities are included.

The division of the country in sesimic regions is accompanied by the seismic hazard map, which gives the PGA (Ground Peak Acceleration) with a 10% probability of exceedance in 50 years (or 475 years return period), presented in Figure 4. This is the PGA considered by the Eurocode 8 for seismic design and assessement of structures, which is associated with "no-collapse requirements".

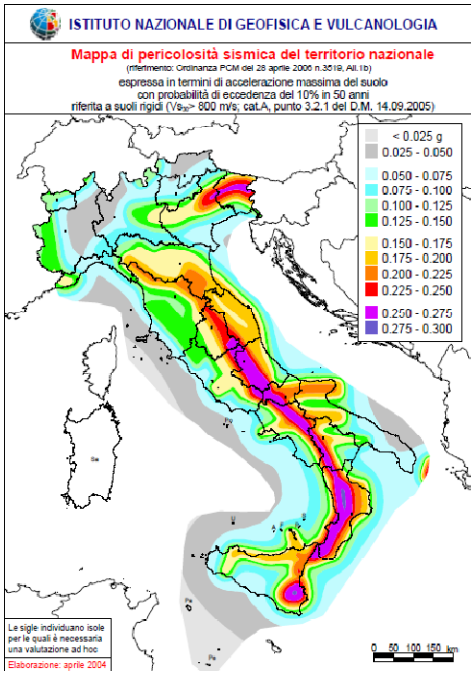

Figure 4 - Italian seismic hazard map

The maximum values of the PGA, 0,275g to 0,300g, represented in dark blue, are applied to Friuli, some areas of the Central and Meridional Apennines, along the Calabric arch until the Messina strait (Lisciotto, 2004).

2.2 Seismicity in Abruzzo Region

2.2.1 Past Earthquakes in the Region

The central Apennines region affected by the April 6th earthquake had experienced in the past several destructive earthquakes, being these documented since 1300. The most severe were the 1703 sequence (Mw >6.7; 14 January, Norcia; 2 February, Aquilano) and the 1915 (Mw>7.0) earthquake that affected Marsica. Other relevant events are: the 1629 earthquake, which damaged the basin of Amatrice; the 1950 and 1951 earthquakes at north of the Gran Sasso; the 1706 and 1903 erthquakes in the Maiella region (see Figure 5). (Rovida et al.,2009).

This area besides the earthquakes that start there, is also affected by two regions: the Umbria-March at Northwest and the Lazio-Molise at Southeast.

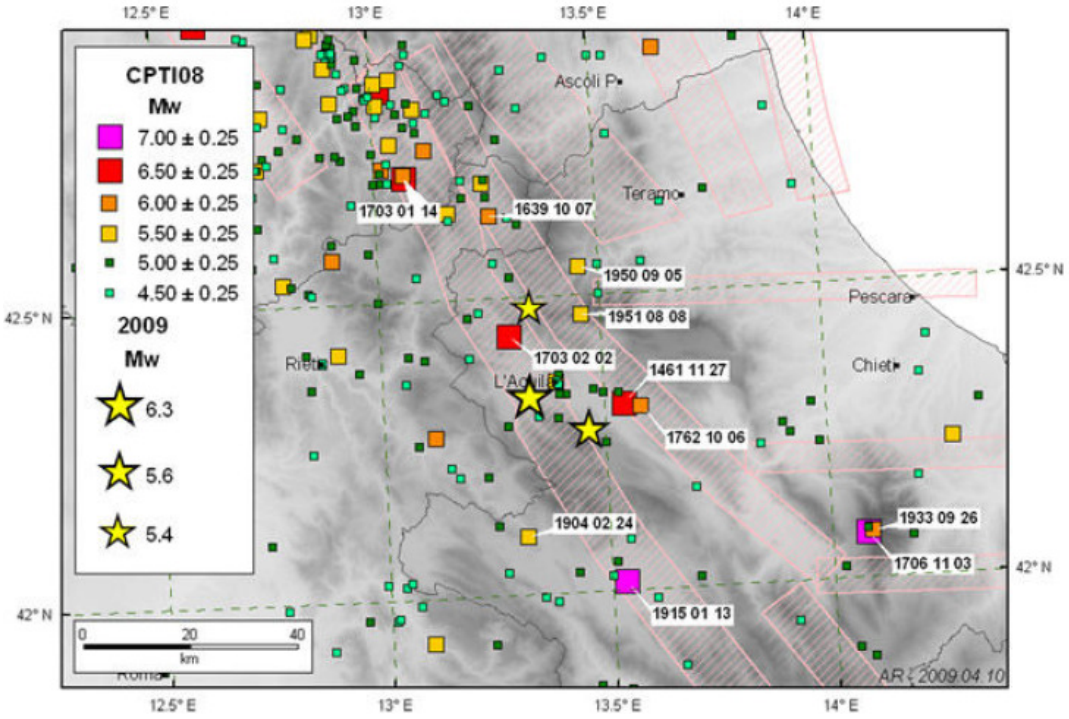

Figure 5 - Historical seismicity of the central Apennines (Rovida et al,2009)

2.2.2 Geology and Soil Characteristics

The local geology and local soil characteristics have a great influence on the intensity of the ground shaking and damage caused by the earthquake. This demonstrates the importance of describing the local geological and soil characteristics.

The soil classification as one can see on the extract of the soil map referring to central Italy is very diverse (see Figure 6). The area surrounding L'Aquila belongs to the category of the *16.4 – Apennine relives on limestone and intra-mountain plains*, which represents 5% of Italy and has the following characteristics according to the Italian National Centre for Soil Mapping:

- "Geology and morphology: Mesozoic and Tertiary limestone, dolomite and marl. Sloping land with included valleys, mean altitude: 889 meters a.s.l (std 464), mean slope: 33% (std 265);
- Main soils: shallow soils (Eutric and Rendzic Leptosols); soils with pedogenetic structure in depth and weekly differential profile (Eutric and Calcaric Cambisols); soils rech in iron ixides and clay accumulation (Haplic and Chromic Luvisols)."

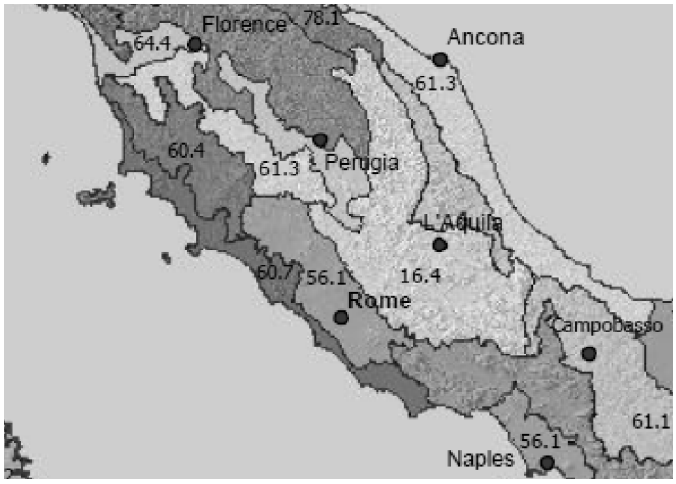

Figure 6 - Soil map of Central Italy

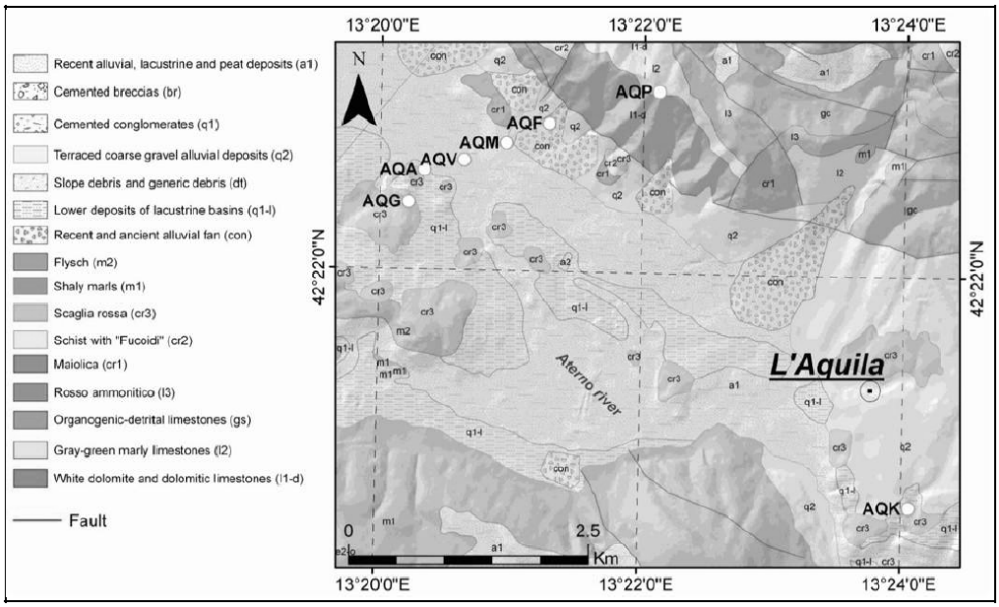

Figure 7 - Geological map of the area around L'Aquila and the location of some of the recording stations

So, combining the soft soil and the fact that L'Aquila is located on a depression area between the Gran Sasso dorsal and the Velino one, the conditions for great seismic hazard are gathered.

2.3 L'Aquila Earthquake – 6th of April

At 6th April 2009 at 01:32:39 (UTC) occurred the main shock of a sequence of events happening for a few a months in the area surrounding L'Aquila. The strong motion was recorded by 55 stations of the Italian Strong Motion Network and it was the most destructive earthquake happening in Italy since

Irpina earthquake in 1980. In sum, 306 people died and a lot of the existent structures collapsed or has severe damage. L'Aquila was one of the most affected locations but others like Paganica, Castelnuovo and Onna also suffered great losses.

The earthquake had a magnitude of 5.8 (Ml), a depth of 8.8 km and it was located at 42.334ºN and 13.334ºE. Figure 8 shows the distribution of PGA around the epicentre, being L'Aquila in the area of higher ground acceleration.

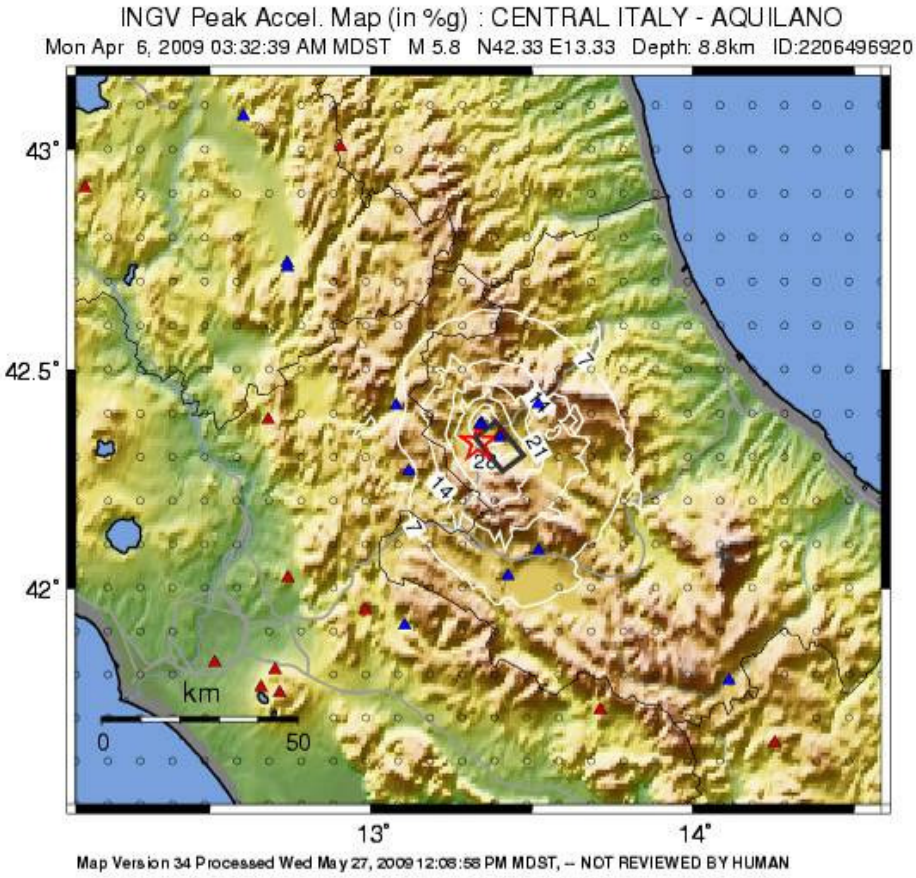

Figure 8 - 6th April PGA map

2.3.1 Cause - Fault Movement

Figure 9 (a) is a representation of the active faults in the surroundings of L'Aquila and responsible for some of the large earthquakes felt in this area (marked with the blue stars). This faults located in the Apennines are normal faults, with a NE-SW direction and with no exception it was one of them, the Paganica fault that caused the 6th April earthquake (see Figure 9 (b)).

Using the radar data coming from the European Space Agency's environmental satellite, ENVISAT, it was possible to create interferograms of the area, which shows a contour of the ground motion waves. Results showed that the area SW of the Paganica fault moved -25cm (downward) and the area NE moved around +8cm (upward) (Walters, 2009).

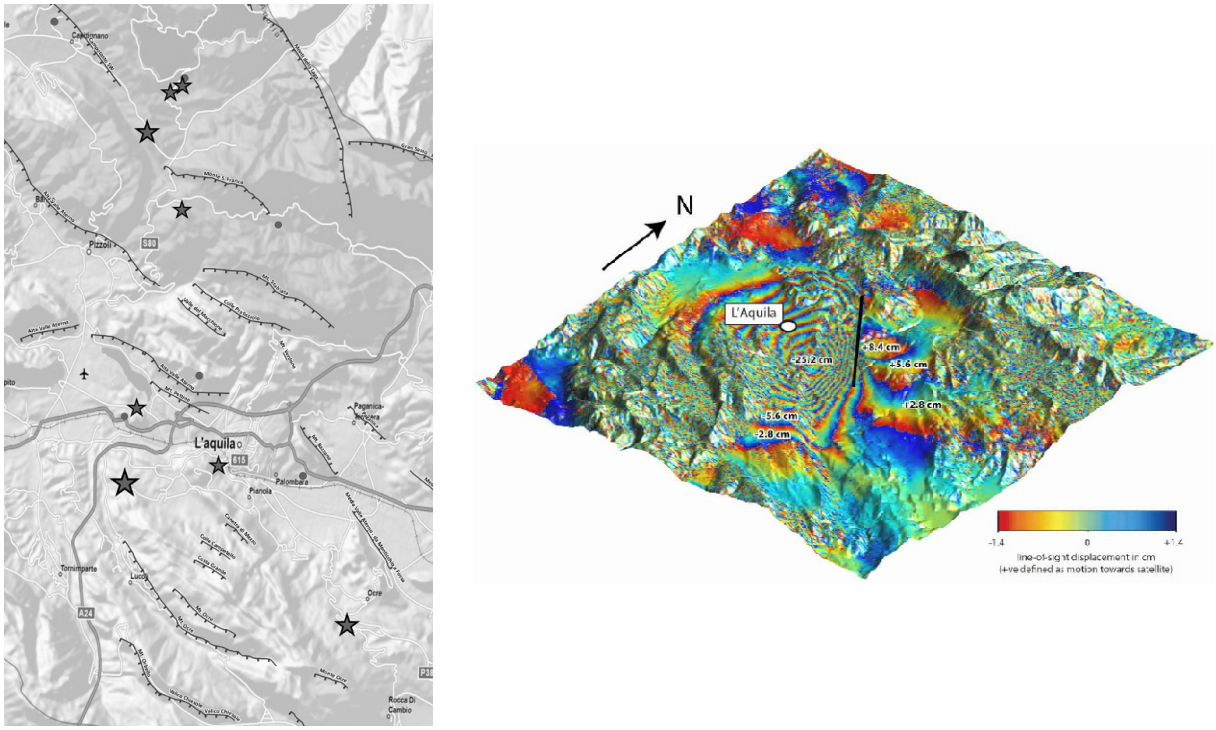

(a) (b)

Figure 9 - (a) Faults in the surroundings of L'Aquila and (b) Earthquake interferogram revealing the surface displacement of the 6th April earthquake (COMET)

2.3.2 Ground Acceleration Data

A lot of recording stations belonging to the national recording network recorded the event, but in order to better assess the ground motion acceleration, only the AQV station was used, which recorded the highest PGA, mainly due to its location in inferior lacustral deposits, formed by sand and conglomerates. Figure 10 shows the accelerograms in two horizontal directions, West-East (WE) and North-South (NS), and also in the vertical one (UP). The highest PGA was recorded in the direction WE, with the value of 646 cm/s^2. An interesting aspect of this earthquake is the high ground acceleration also verified in the vertical direction, which is not very common. With Figure 11 is possible the comparison with the elastic response spectrum recommended by the EC8. Considering a type 2 (near-field) earthquake, a soil type B, a damping coefficient of 5% and a design ground acceleration (a_g) of 0.25g, as recommended by the Italian seismic hazard map and the expressions shown in Chapter 3 of this thesis, it was constructed the elastic response spectrum.

Observe that the response spectrum correspondent to the accelerations of the AQV station, in some regions go beyond the values of the EC8 response spectrum, demonstrating that not even the present day hazard attributed to the area, really describes the possible earthquakes (see Figure 11).

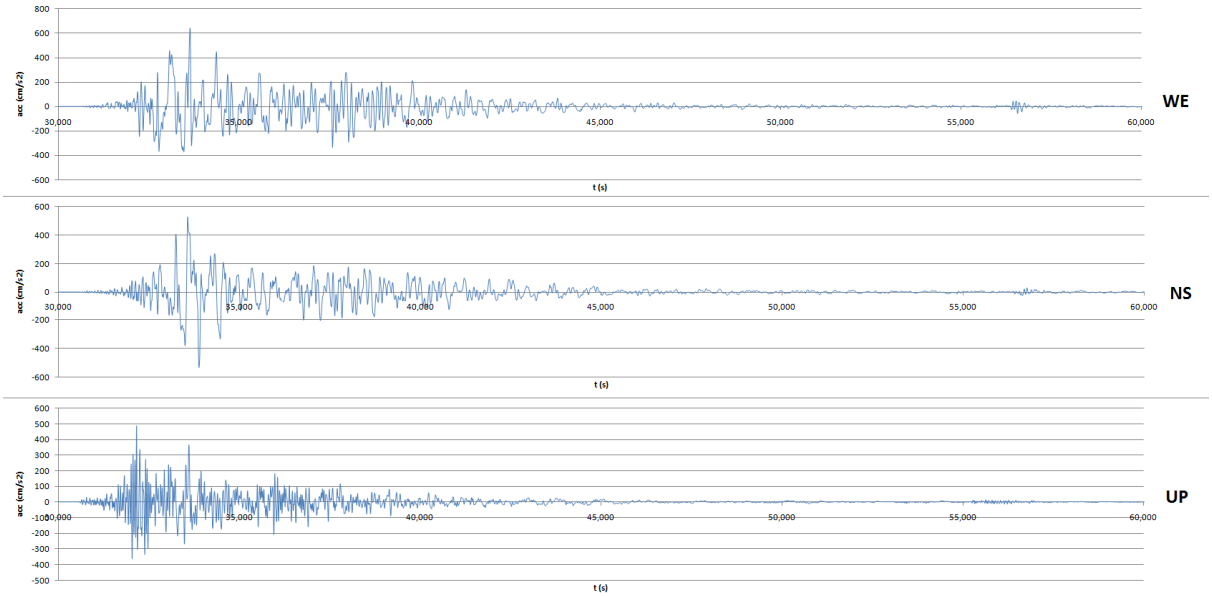

Figure 10 - Accelerograms in the WE (a), NS (b) and UP (c) directions

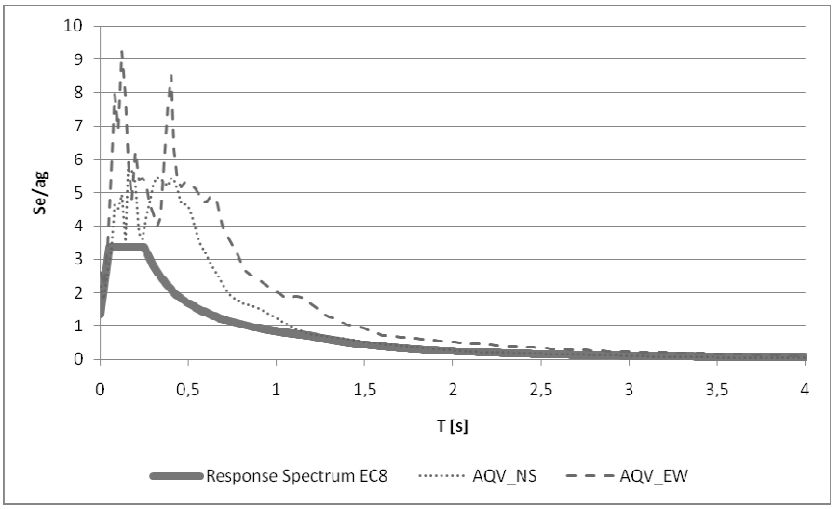

Figure 11 - Response spectra relative to the EC8 recommendation and the accelerations EW for the AQV station

3. DYNAMIC MONITORING

3.1 Introduction

In this chapter a reflection on dynamic monitoring is carried out, pointing out some of the advantages, purposes and how to develop a dynamic monitoring activity.

In order to better understand concepts that will be addressed later in this thesis, a brief presentation of basic dynamic concepts is performed, along with a brief description of the methods and equipments related with dynamic monitoring.

3.2 Dynamic Monitoring

Monitoring is one of the four stages considered by the ISCARSAH recommendations (2001) as necessary to fully understand and analyse the structural. Along with historical investigation, inspection, and structural modelling and analysis of structures, monitoring is everyday more recognized and its true value acknowledge.

The structural model based in hypothesis about the mechanical properties, connections and others, needs to validate them, so it goes to the history, to the inspections and to monitoring to get the empirical values. Especially dynamic monitoring, since evaluates the global behaviour of the structure, is a privileged method to get the validation modal parameters. But it works both ways, since the model is a great way of estimating initial modal frequencies and shapes, which can be a starting point to define the location of sensors e other parameters.

The current practices for structural health assessment are based in visual inspections and damage surveys, but due to recent developments in the area of hardware and software, monitoring has become a more viable option.

Monitoring can be divided in static and dynamic. Static monitoring deals with longer periods of time and with slow-varying parameters, while dynamic monitoring is applied for intensive measurement of high frequency variations and short-lived actions like micro-tremors. So, is required that dynamic monitoring acquires an enormous quantity of data in a short-time period. Is considered that several years are necessary to capture the behaviour of structures requiring a static monitoring system. For dynamic monitoring one year can be enough but fours year is considered the optimum, because abnormalities can be detected.

Conceiving a monitoring program must take into account the purpose of the monitoring system and what information is wanted. Some factors must be bear in mind when deciding what to do: the environment surrounding the structure, level of accuracy, systems reliability, flexibility and maintenance needs (Casarin).

So, dynamic monitoring of masonry structures can be divided in four phases (Ramos, 2007):

1. The first phase, can be considered a pre-processing phase, since the objective is collect the maximum information possible about the structure, by performing a historical survey, non-destructive tests (dynamic tests), damage survey and a numerical model to analyse the modal shapes and frequencies, being calibrated at the end by the values of the monitoring;
2. The second phase is to install the system with limited number of sensors, and the data should be stored periodically and with trigger basis;
3. The third phase is if a threshold is triggered, a full-scale dynamic survey should be performed. After filtering the frequencies of possible environmental and loading effects, if damage exists can be detected and located (post-processing);
4. A fourth phase comprehends complementary non-destructive tests in the area where damage was detected, like for example sonic and radar tests.

3.3 Basic Dynamic Concepts

The three main variables that characterize the dynamic behaviour of a structure are: mass, stiffness and damping. The first two variables are always present in the system, but damping can exist or not. This will lead to damped or undamped systems, which present different behaviour along time. For damped systems, the amplitude of motion tends to zero while for undamped ones the amplitude is constant along time, meaning that the movement will continue indefinitely.

The dynamic analysis also depends if the system is considered continuous or discrete, usually in the civil engineering field is enough to use discrete models, by choosing the points that allow to understand the behaviour of the structure and attribute them the necessary degrees of freedom (in total six, three translations and three rotations).

According to their characteristics and the type of information sought, the approach used to solve dynamic problems varies. The three available mathematical formulations to study the dynamic behaviour are: the Classical Formulation, the Steady-State Formulation and Auto-Regressive Models.

The Steady-State Formulation is applied when damping is not proportional to mass and stiffness of the system, which by consequence doesn't allow the matrix to be diagonalized. Also, Steady-State Formulation is the more adequate approach to study stochastic time series and the noise present in experimental data (Ramos, 2007). Further information can be found Peeters (2000).

Auto-Regressive Models are time-discrete formulations applied when the excitation is characterized by white noise stochastic processes. For single degree of freedom problems, Auto-Regressive Moving Average models (ARMA) are used otherwise, Auto-Regressive Moving Average Vector models (ARMAV) are applied. This mathematical formulation it's based in the input-output relation at

determined instant (Ramos, 2007). Further information can be found in Ljung (1999) and Peeters (2000).

Classical Formulation is the one more common one and some concepts related with it are going to be presented next.

3.3.1 Classical Formulation

Discrete systems can be divided in Single Degree of Freedom Systems (SDOF) or in Multiple Degree of Freedom Systems (MDOF) and can be characterize by the equation of motion, which describes as the name says the motion of the system, relating mass, damping and stiffness with the time dependant displacement , its derivatives, velocity and acceleration and the load vector. The expression doesn't change with the number of degrees of freedom, only the dimension of the variables. The expression of the equation of motion is, for MDOF:

$$M\ddot{q}(t) + C_2 q(t) + Kq(t) = p(t) \tag{1}$$

To solve the equation of motion four methods can be used: classical solution (analytical solution), Duhamel's Integral, Transform methods and Numerical methods. The first three are only applicable with linear elastic systems and only Transform methods work in the frequency domain.

When the force *p(t)* is varying arbitrarily in time, as it happens in earthquakes, it can be described as a sequence of infinitesimal short impulses. The sum of the response to all of those impulses is known as the *convolution integral* and when applied to a SDF gives the *Duhamel's integral* for damped systems (Chopra, 2001):

$$q(t) = \frac{1}{m\omega_D}\int_0^{\tau} p(\tau) e^{-\xi\omega_n(t-\tau)} \sin\left[\omega_D(t-\tau)\right] d\tau, \qquad t > \tau \tag{2}$$

Where τ is determined instant, ω_D is the damping frequency and can be calculated by expression (3):

$$\omega_D = \omega_n\sqrt{1-\xi^2} \tag{3}$$

And ξ is the damping coefficient, which is equal to:

$$\xi = \frac{c}{2m\omega_n} \tag{4}$$

Where *c* is the damping constant.

In the frequency domain the equation of motion, with a arbitrary non periodic function, can be solved with the Fourier Transformation. After applying this method to both sides of the equation and manipulating the intermediate expressions, the Frequency Response Function (FRF), *H(ω)*, is

obtained. The following expression describes the *H(ω)* parameter, which is the ration between the response and the excitation, corresponding to an amplification factor:

$$H(\omega) = \frac{U(\omega)}{P(\omega)} = \frac{1}{k}\frac{1}{1-(\frac{\omega}{\omega_n})^2 + i\left[2\xi(\frac{\omega}{\omega_n})\right]} \quad (5)$$

3.3.2 Response Spectrum

So, by using the expression (2) is possible to compute the displacements caused by an earthquake and consequently build the response spectra of the ground motion. These can be related to the pseudo-spectral acceleration, pseudo-spectral velocity and pseudo-spectral displacement, being the first two very close to the real spectral variables. The direct relation that exists between them defines the following expressions:

$$\begin{cases} S_d = max|u(t)| \\ S_v = max|\dot{u}(t)| \approx S_{v,pseudo} = \omega_n S_d \\ S_a = max|\ddot{u}(t)| \approx S_{a,pseudo} = \omega_n^2 S_d \end{cases} \quad (6)$$

To construct a response spectrum, the following steps are necessary (Abrams, 2010):

1. Definition of the Peak ground Acceleration (PGA);
2. Selection of the parameters T_n and ξ of the SDOF system;
3. Calculation of the response *u(t)* of the system by using the Duhamel integral or a numerical method;
4. Determination of maximum value of S_d;
5. From S_d calculate S_v and S_a, using the relation described above;
6. Repetition of steps 2 to 5 for different values of T_n and ξ;
7. Plotting of the different response spectra.

This opens the possibility of comparing real response spectra with the ones advised by the Eurocode 8 (EC8). The horizontal elastic response spectrum of EC8 has the shape reproduce in Figure 12 and can be reproduce using the expressions for the spectral branches also showed in Figure 12.

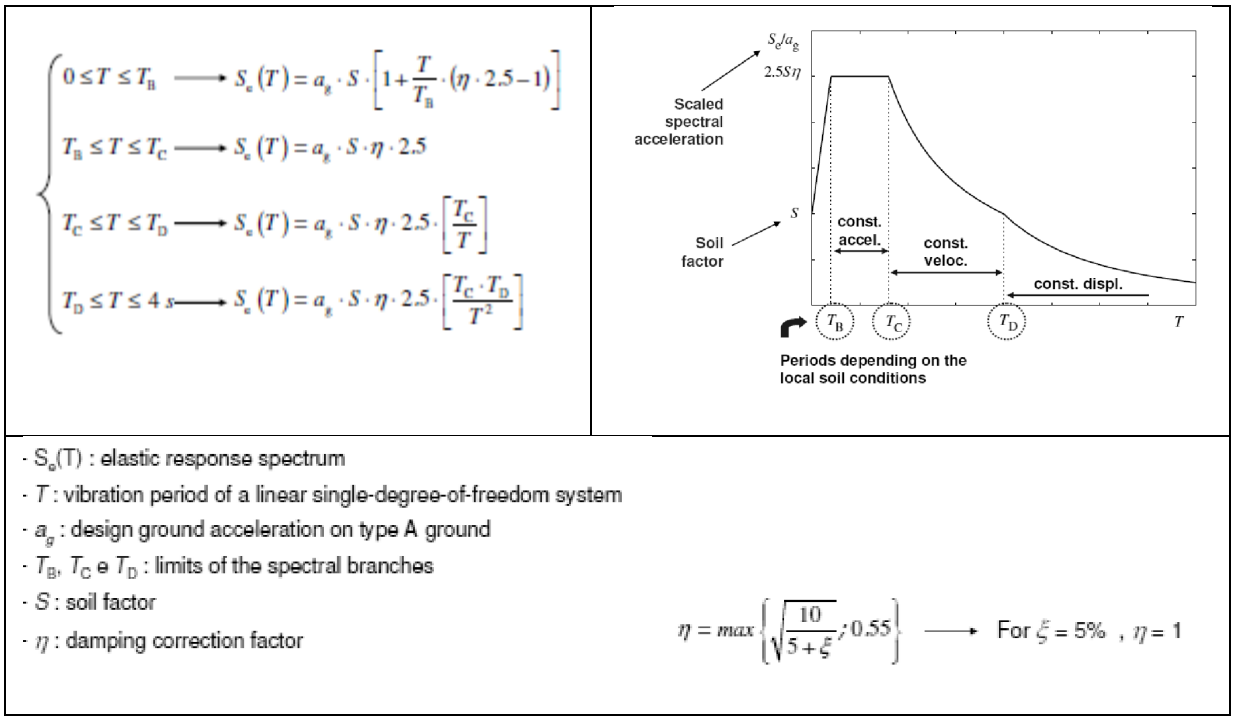

Figure 12 - Sketch of the horizontal elastic response spectrum

EC8 considers seven different types of soils and two types of earthquakes: far-field (Type 1) and near-field (Type 2). Depending on each country seismic risk zoning the ground acceleration a_g is established, for example for L'Aquila the value is 0,25g.

3.4 Experimental Modal Identification

3.4.1 Response Transducers

The response transducers are the responsible for a physical quantity into a proportional electrical signal, which can processed by the data acquisition system. The physical quantity can be displacements, velocities, forces but the most common in dynamic monitoring of structures is accelerations, since is the cheapest solution and also allow the calculation of displacements and velocities by numerical integration. So, piezoelectric accelerometers are the usual equipment and are formed by a quartz crystals or ceramic, which allows the signal production (see Figure 13)

The advantages of the accelerometers are (Ramos, 2007):

- They are active transducers, so don't need external power source;
- Stable;
- Good signal-to-noise ratio;

- Linear over a wide frequency and dynamic range.

Figure 13 - Piezoelectric transducers

There are also other types of transducers: the piezoresistive transducers, the Force-balance transducers and the geophone, which are generally more expensive and have other applications.

3.4.2 Data Acquisition Systems

The Data Acquisition System (DAS) is the equipment responsible for recording the signals sent by the response transducer in the time domain. To directly process the information that comes from a transducer, signal conditioning is performed and some of its main functions are: amplification, isolate the transducer signals from the computer, filtering, excite the transducers and linearization.

Amplification consists in amplifying the signal in order to have the maximum voltage range of the conditioned signal close to the maximum input range of the Analogue Digital Converter (ADC).

The isolation of the transducer signals is necessary to protect the data from differences in ground potentials or common-mode voltages and also due to the possibility of the data contain high-voltage.

Filtering the signals is the separations of undesired signals from the measured one, with the objective of improve accuracy. For example, anti-aliasing filters can be applied when there's the possibility of two different frequencies reproduce the same measured signal, as seen in Figure **14**. The filter must use a sampling frequency equal or higher than 2 times the Nyquist frequency.

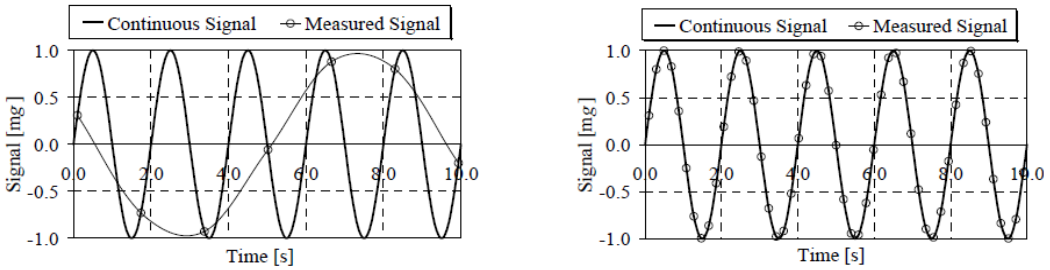

Figure 14 - Anti-aliasing function (Ramos, 2007)

Another type of filter is the noise filter, which clears the signal of high frequencies, which are out of the range of the measured ones.

Other important aspect is the influence of the capacity of the ADC in the accuracy of the digitalized signal. A converter of *n* bits can represent 2^n levels of analog signal, meaning that higher capacity converters assure more accuracy to the signal.

3.4.3 Signal Processing

Signal processing is a post-processing procedure of the signal, which was applied with the use of the software Artemis Extractor. After having the time domain acceleration data is necessary to transform it to the frequency domain using the Discrete Fourier Transform (DFT).

Working in the frequency domain brings problems like the leakage error, which can be reduced by increasing the sampling duration (T_s) or by introducing a process called windowing. The leakage error happens when *"the measuring time is not an integer multiple of the signal period"* (Ramos, 2007), happening always in experimental testing.

For example, as demonstrated in **Figure 15**, for the same signal, two different *Ts* are applied, being the first one a multiple integer of the signal period (at the left) and the second one a random *Ts* (at the right), the resultant spectra are also different. In the first case, a clear and only frequency stands out, while for the second one around the expected frequency there are non-zero values, which means the signal was contaminated.

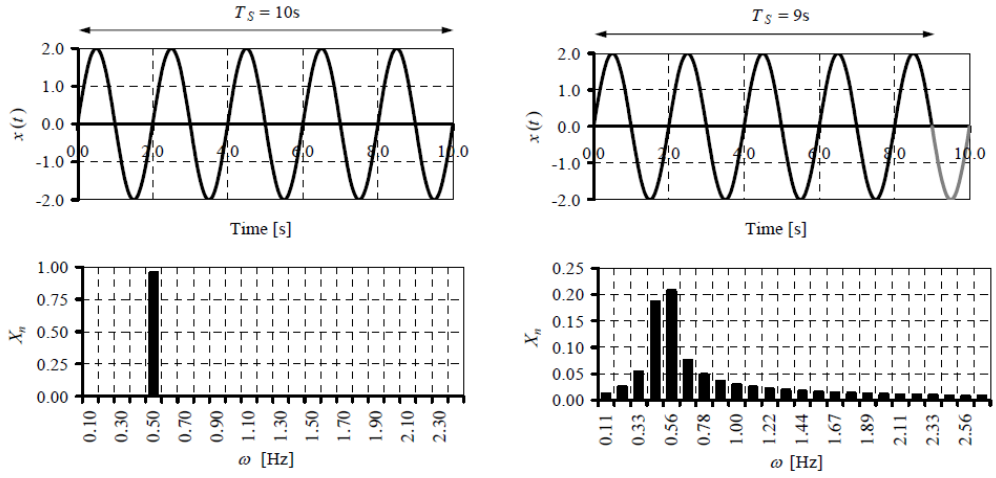

Figure 15 - Example of leakage error (Ramos, 2007)

Of the two solutions mentioned above the most common is the windowing process, which consists in multiplying the measured signal when a non multiple integer Ts is applied (see Figure 16 (a)) by a function, for example Hanning function (see Figure 16 (b)), resulting in an rescaled time series and consequently improved spectrum.

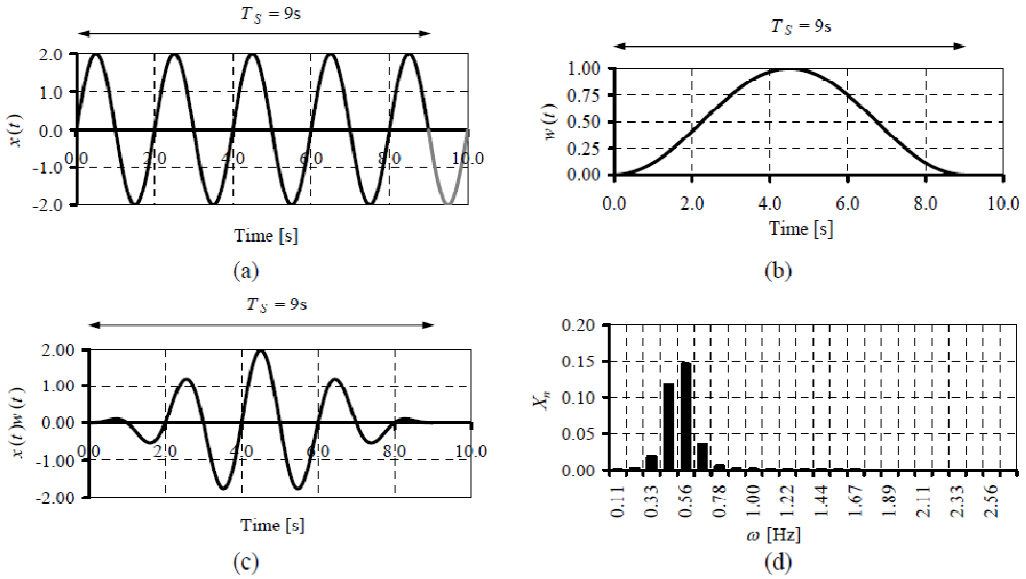

Figure 16 - Windowing process: (a) measured signal when the applied Ts isn't a multiple integer of the signal period; (b) Hanning window; (c) the windowed signal; and (d) the final DFT windoed spectrum (Ramos, 2007)

Other important tool of signal processing is decimation, which allows the alteration of the sampling rate to a lower value, decreasing the number values to process, without losing quality.

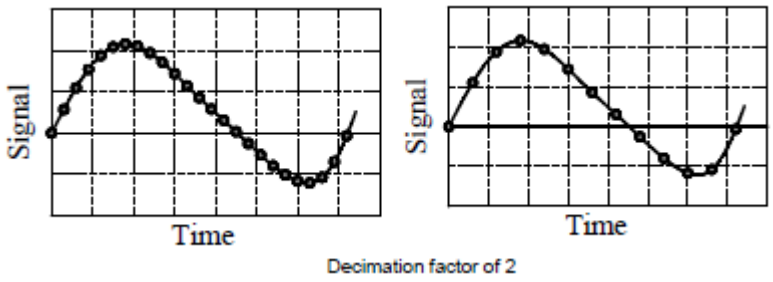

Figure 17 - Example of decimation (Ramos, 2007)

Finally, when the signal is treated in the Fourier transforms, is necessary to apply a procedure known as the Welch method (Welch, 1967), which is described by (Ramos, 2007):

"(...) which involves the signal separation on several individual time records or samples with limited time duration, the application of FFTs for all time records and, finally, the average calculation of every signal transformation, resulting in a final smoothed spectrum. This procedure removes spurious random noise from the signals and gives statistical reliability to the data. (...)"

The application has one disadvantage related with the decrease of the frequency resolution, which can be minimized by overlapping a series of Hanning windows. The best overlapping option is 2/3 but 1/2 on random signals can be also applied.

3.4.4 Output-Only Identification Techniques

There are two possible modal identification techniques, which are differentiated by the type of input data: Input-Output Identification Techniques and Output-Only Identification Techniques.

Input-Output Identification Techniques intent to control the input excitation and then measure the time history response of the structure, while Output-Only Techniques or also called ambient vibration techniques are based on a random nature excitation, in the physical space of the structure or physically local (with enough capacity to excite all the structure), which allows the measurement of the dynamic response of the structure (Ramos, 2007).

Output-Only Techniques are the ones largely applied in the field of monitoring, due to the long periods of time associated, to the necessity of exciting the entire structure and also, with the fact that is less expensive. So, only these ones are going to be explained in more detail.

The base assumption of these techniques is to assume the ambient excitation u_k as a stationary Gaussian white noise stochastic process, which consequently leads to a dynamic response, y_k, reflecting three different contributions from: ambient forces, structural system and noise signals.

In the output-only range, different methods can be applied to the data, being separated into two large groups: frequency domain (non-parametric methods) and time domain (parametric methods), as shown in Table **2**. Since, frequency domain methods are more user- friendly and monitoring requires the analysis of a great amount of data, the Frequency Domain Decomposition (FDD) method was chosen to identify the modes of the Spanish fortress and is presented next.

Table 2 – Classification of some of the relevant output-only identification algorithms (Caetano, 2000)

	Method	Characteristics
Frequency Domain	Peak Picking (PP)	Classical SDOF method
	Frequency Domain Decomposition (FDD)	MDOF method; application of SVD to reduce noise
	Enhanced Frequency Domain Decomposition (EFDD)	MDOF method; application of SVD to reduce noise
	Polimax	MDOF method
Time Domain	Random Decrement (RD)	Operates on time domain series, leading to a free decay curve analysis
	Recussive Techniques (ARMA)	Time series modelling using recursive algorithms
	Maximum Likelihood Methods	Stochastic methods based on the minimization of a covariance matrix
	Stochastic Subspace Identification Methods (SSI-DATA)	Stochastic methods based on the project of state vector on a vector of past realizations

3.4.4.1 Frequency Domain Decomposition Method

The main assumption for this type of technique is that ambient vibration u_k is a stationary Gaussian white noise stochastic process in a frequency range of interest, meaning that the PSD function of excitation is considered constant and the Frequency Response Function (FRF) *H(i,j)(ω)* is determined by the expression:

$$\left|\widehat{H}_{(i,j)}(\omega)\right|^2 = \frac{\hat{S}_{(i,j)}(\omega)}{C} \tag{7}$$

The FDD method is considered an extension of the Peak Picking method, because it also assumes that "resonant frequencies are well spaced in frequency and the contribution of other modes in the vicinity of the resonant frequency is null" (Ramos, 2007).

So, the method is based in the calculation of the Singular Value Decomposition (SVD) of the response spectral density matrix, with the expression:

$$S_y(\omega_k) = \Psi_k \Lambda_k \Psi_k^H \tag{8}$$

Where:

Ψ_k is a complex matrix where each columns contains the mode shape vectors of each spectral peak;

Λ_k is a diagonal matrix with the singular values, positive and real eigenvalues of the matrix $S_y(\omega_k)$.

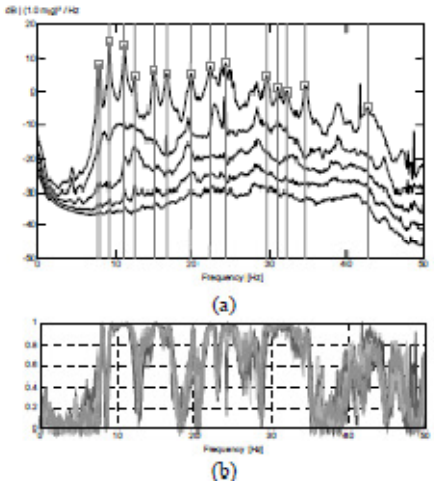

Figure 18 - Application of the FDD, being (a) the SVD lines and (b) the coherence function

To help in the detection of the modes, by indicating the linearity between two measured signals, the coherence function is calculated (see expression (9)). The values can vary between 0 and 1 and when closer to one, it can mean the presence of a mode.

$$\gamma_{i,j}^2(\omega) = \frac{\left|\hat{S}_{y(i,j)}(\omega)\right|^2}{\hat{S}_{y(i,i)}(\omega)\hat{S}_{y(j,j)}(\omega)} \quad (9)$$

3.5 Influence of Environmental and Loading Conditions

Literature recognizes the influence of the environmental factors in the modal frequencies, especially regarding temperature and relative humidity. Peeters (2000) when studying the effects of temperature of different materials in different locations of the Z24 Bridge, showed the enormous importance that this environmental factor has in the variation of the modal frequencies. This demonstrated the necessity of filtering the modal frequencies of the temperature, enabling the assessment of changes in frequency caused by damage.

Also Ramos (2007), in different case studies like the Clock Tower Mogadouro or Church of the Jerónimos Monastery, proved the importance of separating the influence of environmental and loading conditions from the variations in frequencies caused by damage.

In order to allow the detection of damage, a model involving the environmental and loading effects as inputs and the modal frequencies as outputs, needs to be built. The objective is to filter the influence of the inputs and to establish a confidence range, in which the changes in frequency are characterized by the inputs. If the frequencies go out of that interval, it means that something not taken in consideration by the model caused a change, which can be damage or other factor not considered before.

The first step is to calculate the correlations between the different inputs (*x*) and outputs (*y*), which is obtained by determining the estimated covariance, correlation coefficient and coefficient of determination as follows:

$$\hat{r}_{xy} = \frac{\hat{R}_{xy}}{\hat{\sigma}_x \hat{\sigma}_y}$$

$$\hat{R}_{xy} = \frac{1}{N-1}\sum_{k=1}^{N}(x_k - \bar{x})(y_k - \bar{y}) \quad (10)$$

$$\hat{\sigma}_x = \sqrt{\frac{1}{N-1}\sum_{k=1}^{N}(x_k - \bar{x})^2} \quad , the\ same\ for\ y$$

This can be useful in the case of having a lot of inputs, choosing the ones with higher correlation factor to be modelled.

Next, two different ways of correlating the environmental effects and modal parameters are presented: linear regression - the static approach - and ARX models - the dynamic approach. While static models consider just the input at instant *k* for the calculation of the response at instant *k*, the dynamic models take into consideration the previous inputs and outputs. This can be an advantage to model modal parameters influenced by temperature, because thermal inertia can be accounted for.

3.5.1 Linear Regression

Linear or multi-linear regression is one of the easiest ways to correlate the environmental effects ($u_{1,k}^{env}$) and the modal frequencies by minimising the Least Square Method. This way is possible to determine the coefficients a_i and establish the function that estimates$\hat{y}_k$:

$$\hat{y}_k = a_0 + a_1 u_{1,k}^{env} + a_2 u_{2,k}^{env} + \cdots + e_k \tag{11}$$

Then the error, e_k, is the difference between the measured value and the estimated one for the same instant:

$$e_k = y_k - \hat{y}_k \tag{12}$$

The confidence intervals *ci* are calculated by (13), because the residuals are assumed to have a normal distribution and for a 95% confidence interval α is 0.05:

$$ci = \pm z(1 - \frac{\alpha}{2})\hat{\sigma} \tag{13}$$

Figure **19** shows an application of a bilinear regression with 95% confidence intervals.

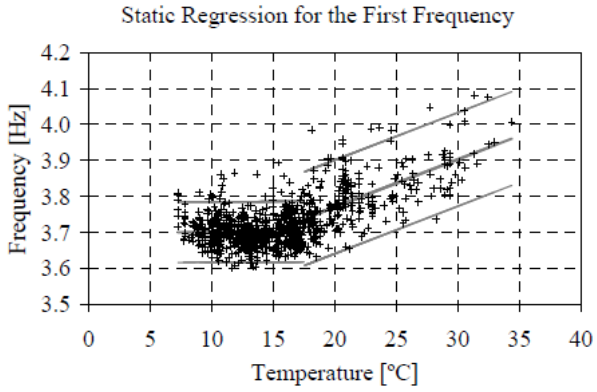

Figure 19 - Bilinear static regression applied in the case of the Church of the Jerónimos Monastery

Besides linear regressions also higher polynomial orders and non-linear regressions can be used to better describe the relation between environmental effects and frequencies, being applied the same considerations and changing the function which estimates the response of the structure, y.

3.5.2 ARX Models

ARX models stand for AutoRegressive output with an eXogeneous input part, and as said before, are dynamic models which allow to consider the influence of previous inputs and outputs to instant k, in its response y. By applying also the Least Square method to the expression (14) is possible to calculate the coefficients a_i and b_i, respectively the autoregressive and exogeneous part. The indexes n_a, n_b and n_k are characterized for being: the autoregressive order (number of poles), the exogeneous order (number of zeros+1) and number of samples before the input affects the output (delay), respectively. The error is assumed as a Gaussian distribution, so the confidence intervals are calculated as before.

$$\hat{y}_k + a_1 y_{k-1} + \cdots + a_{na} y_{k-na} = b_1 u_{k-nk}^{env} + b_2 u_{k-nk-1}^{env} + \cdots + b_{nb} u_{k-nk-nb+1}^{env} + e_k \quad (14)$$

To expression (14) is applied a shift operator $q^{-1} y_k = y_{k-1}$, which transforms it to the form:

$$A_q \hat{y}_k = B_q u_{k-nk}^{env} + e_k \quad (15)$$

, with the following polynomials A_q and B_q:

$$\begin{aligned} A_q &= 1 + a_1 q^{-1} + \cdots + a_{na} q^{-na} \\ B_q &= b_1 + b_2 q^{-1} + \cdots + b_{nb} q^{-nb+1} \end{aligned} \quad (16)$$

Peeters (2000) presents a procedure to simulate and predict the response of the structure depending in the environmental outputs and from there detect damage. Ramos (2007) proposed the following brif description:

1. “The normalization of the inputs and outputs:

$$\begin{aligned} u_k^{env} &= \frac{u_k^{env,m} - \bar{u}}{\sigma_u} \\ y_k &= \frac{y_k^m - \bar{y}}{\sigma_y} \end{aligned} \quad (17)$$

Where $u_k^{env,m}$ and y_k^m are the measuring values, $\bar{u}$ and $\bar{y}$ are the average values and σ_u and σ_y are the standard deviations;

2. The estimation of several ARX models (e.g. ARX[0,1,0], ARX [2,1,0], ARX [3,1,0], etc.) and their statiscal properties;

3. The selection of the “best” model based on quality criteria, like the loss function V or the Akaike’s Final Predition Error (FPE), see Ljung (1999), given by:

$$V = \frac{1}{N}\sum_{k=1}^{N} e_k^2$$
$$FPE = V\frac{1 + d/N}{1 - d/N} \tag{18}$$

Where *d* is the number of estimated parameters;

4. The simulation of the expected response with the previous selected model;
5. The calculation of simulation error and its statistics;

$$e_k = y_k - \hat{y}_k \quad and \quad \hat{R}_{xy} \tag{19}$$

6. The establishing of confidence intervals ci and detect the outliers:"

$$\left[\hat{y}_k - z\left(1 - \frac{\alpha}{2}\right)\sqrt{\hat{R}_{xy}} \quad , \quad \hat{y}_k + z(1 - \frac{\alpha}{2})\sqrt{\hat{R}_{xy}}\right] \tag{20}$$

4. CASE STUDIES

As seen before, dynamic monitoring requires pre- and post-processing. The two following case studies intend to reflect this two phases of the dynamic identification process:

- Case Study 1: The Saint Domenico Church – Preliminary structural model as base for dynamic monitoring;
- Case Study 2: The Spanish Fortress – Influence of environmental and loading conditions in the dynamic behaviour, using monitoring data.

At present day, the Spanish fortress has already the monitoring equipment installed and acquiring data, so is on post-processing that the study will be developed. It will be accompanied by brief descriptions of the history of the building, the interventions carried out since the earthquake and the detected damage, to better understand the actual behaviour.

For the Saint Domenico Church, it will be performed a brief historical survey, an inspection of the damages, completing an existing post-seismic damage map and finally a preliminary structural model, for future use in dynamic testing and remedial interventions.

Both monuments were struck by the April 2009 Abruzzo earthquake.

4.1 Case Study 1: San Domenico Church

San Domenico Church is located in the East part of the city centre of L'Aquila. The main entrance is oriented S-W and turned to Angioina square and the S-E lateral door opens to San Domenico square, being both accessible by several streets. At North, the church has also several street accesses but at N-E is connected to the rest of the monastery.

Figure 20 – (a) Location and (b) Façade of San Domenico church

The monumental church is part of the Complex of San Domenico, which comprehends besides the church a monastery with two porticoed cloisters. The Complex was converted from a royal palace which was a gift of Charles II of Anjou to the Dominican Fathers of Prayer in 1309, as a way to fulfil the promise that he made when he was a prisoner of King Peter of Aragon. The medieval style church is located on the hill and it was dedicated initially to Mary Magdalene. During many years the church kept its initial configuration, but due to the pressure of the House of Anjou some changes were performed leading to a more elaborated medieval architecture. As shown in Figure 21, the church is divided in three naves that are crossed by a vaulted transept, finishing with five polygonal apses (instead of the semi-circular ones common in medieval churches). Columns have a cruciform shape, as well as the entire church, and the spans are achieved with arches, vaults and domes. The Presbytery was covered with a ribbed, cross-vaulted ceiling, which is typical of mature gothic style, brought by Charles of Anjou.

In terms of exterior, to the South-West wall (main façade) was added a cover of ashlar stonework and also some decorative aspects like the cornice. This façade was finished later and its style is mainly Romanesque, due to its plain aspect, only broke by the elaborated and majestic doorway, similar in composition to others like Porta Santa or the main doorway in basilica of Collemagio. Other distinguishable features from the exterior are the two doors that give access to the lateral naves and present complex sculptural decorations.

Other changes were made during the centuries XVI and XVII, being these mainly decorative, but it was the 1703 earthquake that caused the collapse of the church, killing 600 people, and the consequently reconstruction, in 1712. The reconstruction work is attributed to Piazzola, whom kept the medieval basilical form, but changed the interior to a late Baroque.

The most recent alterations are connected with the concrete beam at the top of the second level walls and the concrete trusses and beams that compose the roof frame, which substituted the original timber elements.

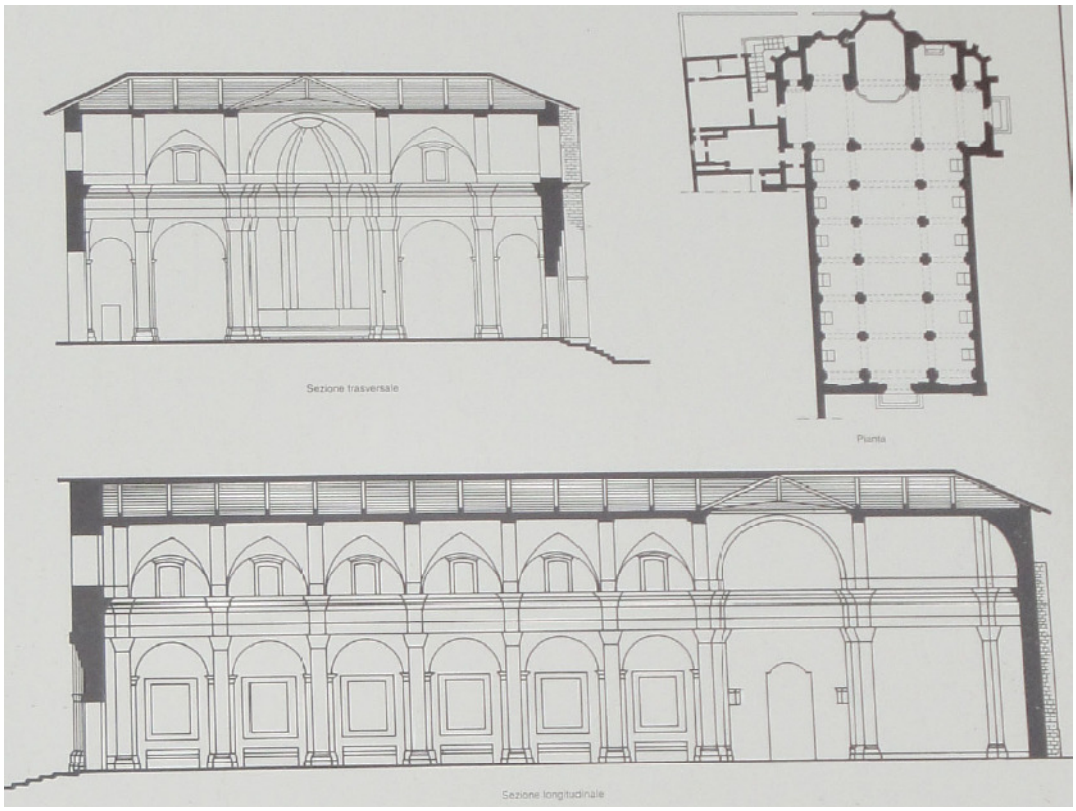

Figure 21 - Drawings of San Domenico church from the XIV cent. to XVIII cent. (Adapted from "Progetto Mirabila")

4.1.1 Damage Description

San Domenico church suffered some damage due to the 6th April earthquake, but when compared with other churches in city centre of L'Aquila like San Marco or Santa Maria di Paganica churches, it's possible to say that it was not as severely affected.

An explanation can be the fact that a similar damage as the other churches suffered now, was presented by San Domenico after the 1703 earthquake, which lead to the reconstruction of the church.

Next, some of the mechanisms present in the "Scheda per il Rilievo del Danno ai Beni Culturali – Chiese", which is a form to evaluate the damage of the churches, based on the macro-elements formed by damaged masonry structures, are compared with some of the mechanisms detected at San Domenico. Here, the mechanisms are presented but the degree of damage is not evaluated:

- Main Façade (S-W façade) – the main façade shows clearly the presence of out-of-plane deformation, Mechanism 1, (see Figure 22 (b)) and overturning of the upper part of the façade, Mechanism 2 (see Figure 22 (a));

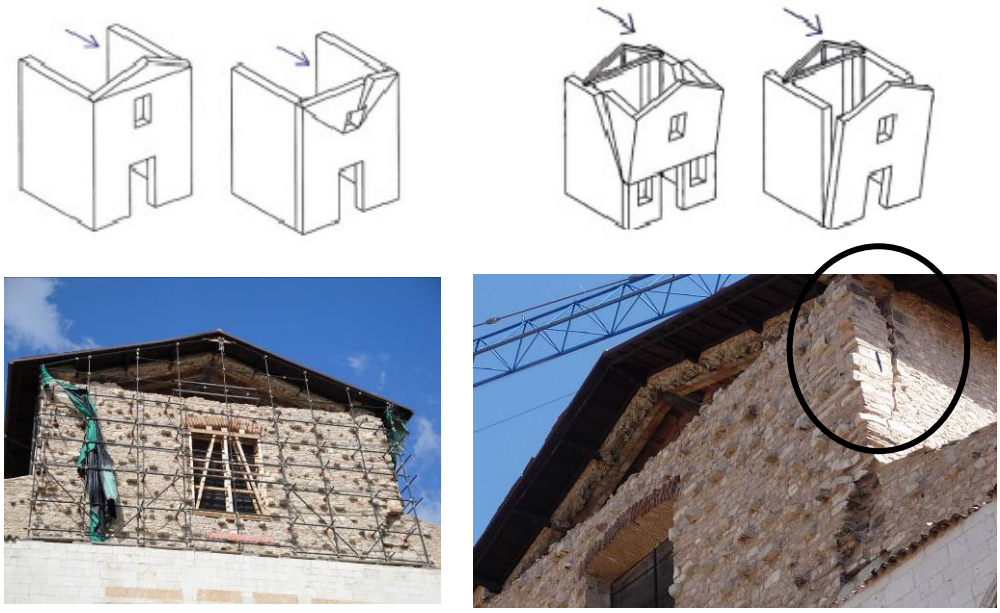

(a) (b)

Figure 22 - (a) M2: Overturning of the upper part of the façade and (b) M1: Out-of-plane deformation

- Central nave vaults – since this vaults are not structural, they don't present the necessary seismic resistant capacity, which can lead to collapse, as verified in San Domenico church, Mechanism 8 (see Figure 23);

Figure 23 - M8: Damage of the central nave

- Transept – this part presents three different types of mechanisms, two in the façades and one in the vaults. The façades show out-of-plane deformation, Mechanism (see Figure 24), and wide spread shear cracks, Mechanism 11 (see Figure 25), both severe. The other mechanism is cracking of the vaults of the transept, Mechanism 12, as shown in Figure 26.

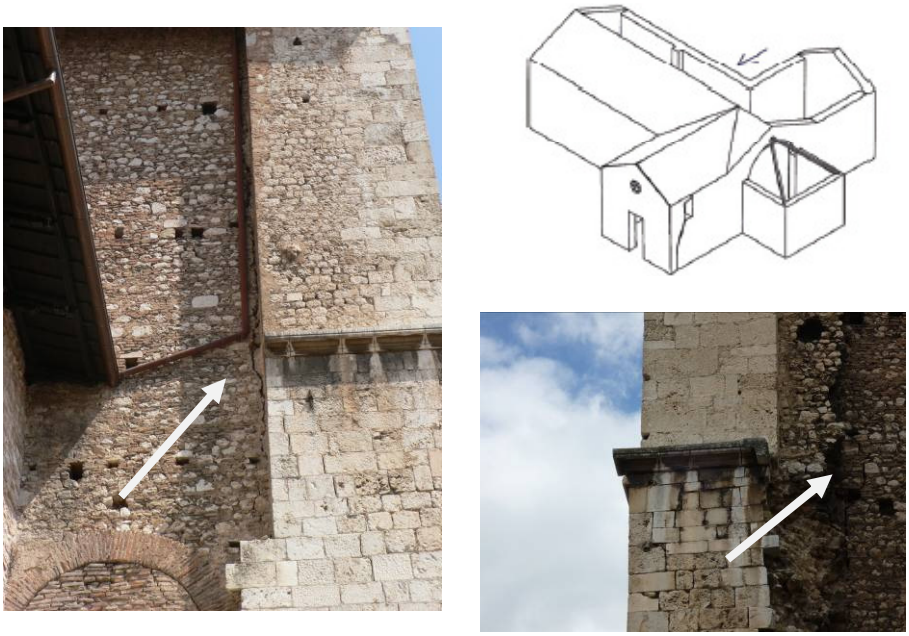

Figure 24 – M10: Out-of-plane deformation of the façades of the transept

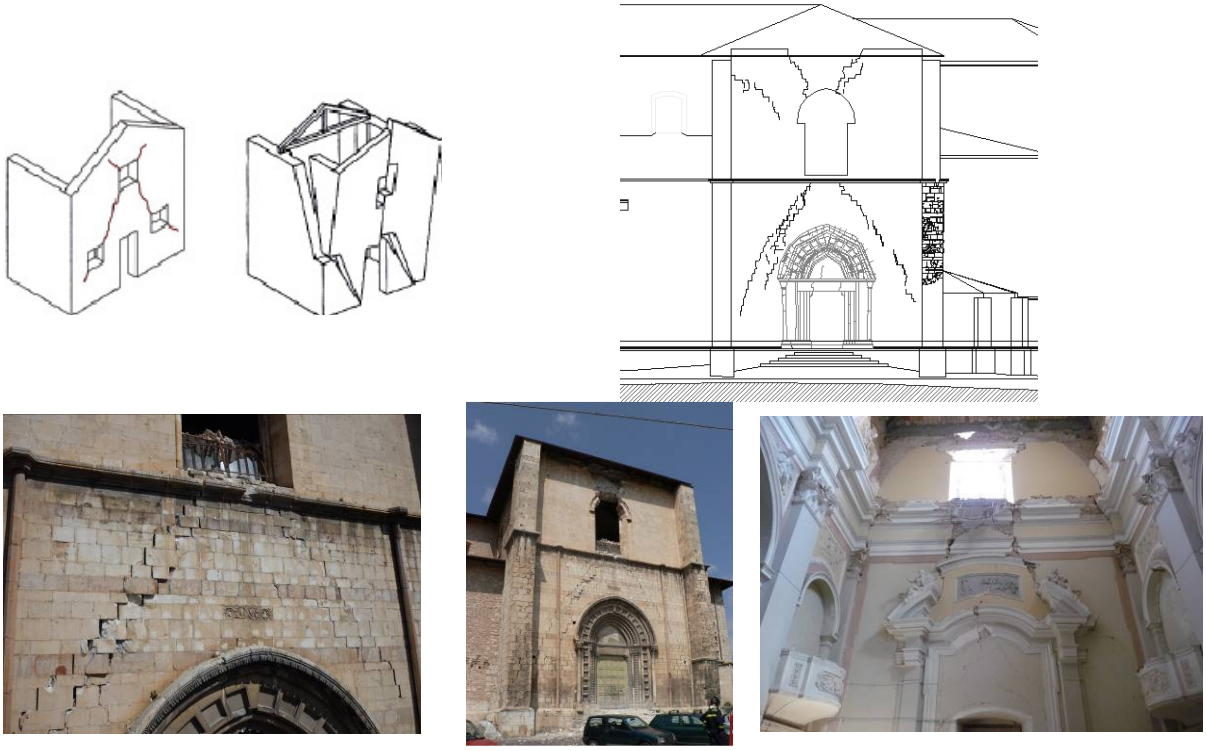

Figure 25 – M11: Shear mechanism of the transept

Figure 26 - M12: Damage in the transept vaults

- Lantern – the lanterns on top of two domes of the smaller apses show horizontal sliding cracks, Mechanism 15, due to the horizontal seismic forces (see Figure 27);

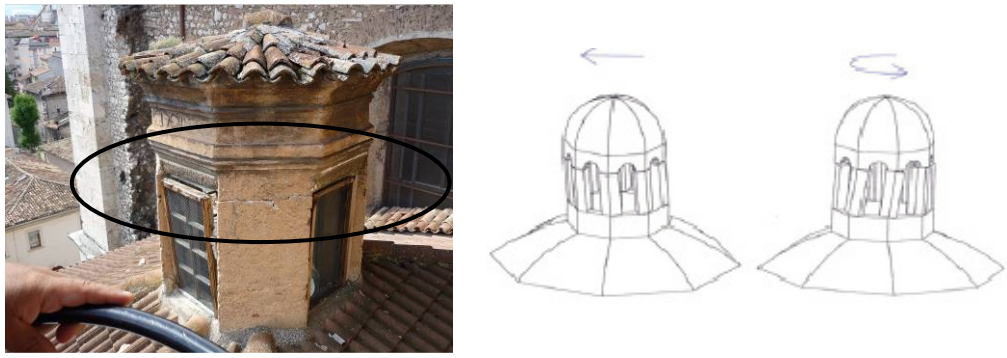

Figure 27 - M15: Horizontal cracks in the lantern

- Apses – this part of the church presented four mechanisms. Observe Figure 28, where is possible to see the horizontal crack formed by the movement of the connections between the roof and the walls, Mechanism 21. The other mechanisms are out-of-plane deformation of the walls, Mechanism 16 (see Figure 29 (b)), shear cracks, Mechanism 17 (see Figure 29 (a)), and damage of the apse vault, Mechanism 18 (see Figure 30).

Figure 28 - M21 – Damage to the connection between the roof and walls of the apse

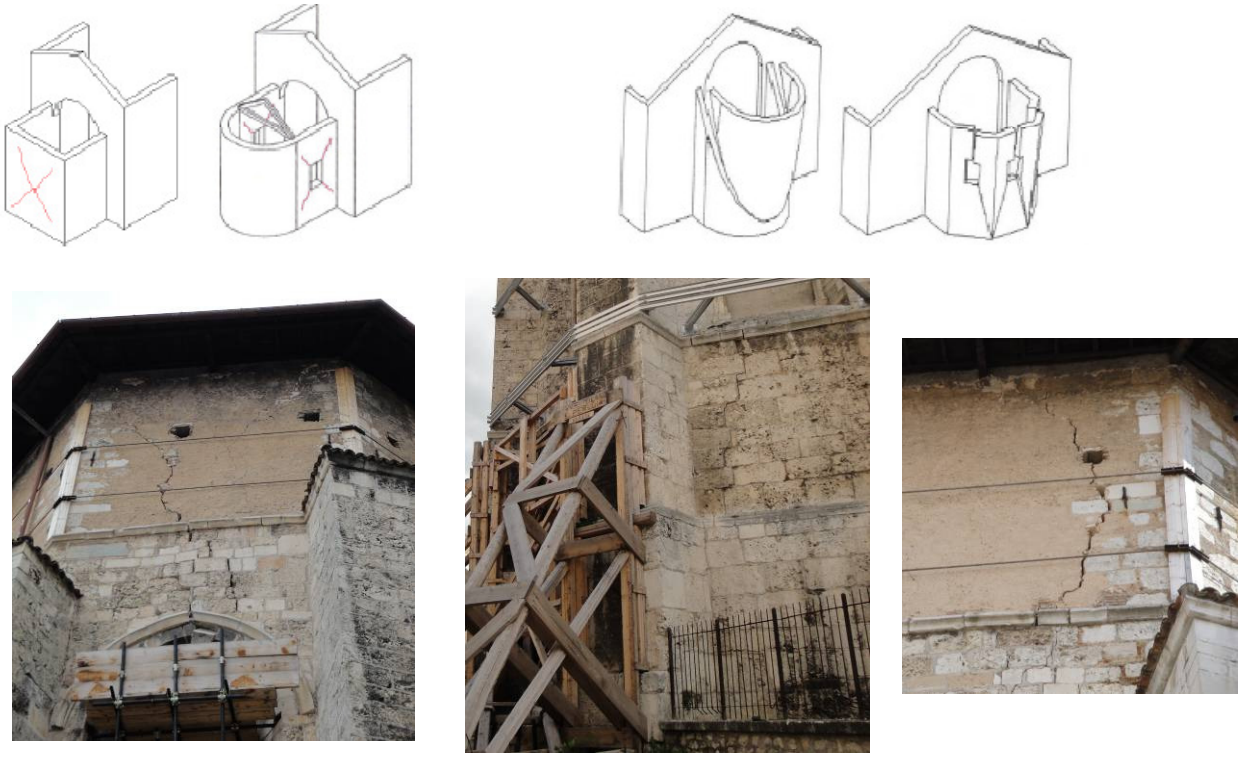

(a) (b)

Figure 29 - (a) M17: Shear mechanism of the apses and (b) M16: Out-of-plane deformation of the apses

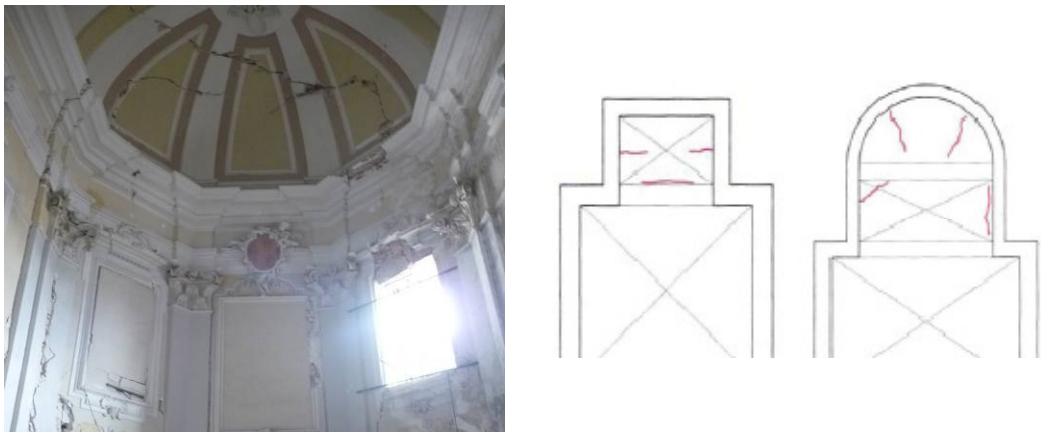

Figure 30 - M18: Damage in the apses' vaults

Cracks and tilting of elements are also present in other elements, as for example the arches and domes of the lateral domes, as shown in Figure 31. This photographic survey is complemented with a damage map (see Annex I) performed right after the earthquake.

Figure 31 - Cracks in the arches and domes of the lateral naves

4.1.2 Structural Arrangement

This enormous church presents in general a symmetrical disposition along direction SW-NE, the long central axis of the church, due to the crossed shape in plan and can be considered to have 2 levels and the roof. The second level has a smaller area that comprehends the central nave, the transept and the central apse.

All the exterior walls are structural and present the thicknesses showed in Table 5 (walls are named according to the direction they are facing and the part of the church they belong). SW apse and NE nave walls achieve the two levels, while SE and NW nave walls finish at the first. Then, in terms of walls, there are the ones of the transept and also inner walls, which become exterior at the second level.

The lateral naves are composed by six structural elliptical domes on each side, which are supported by four arches that meet the columns. The columns are crossed shape, being seven embedded in the exterior walls and other seven independent, for each side.

The central nave has seven arches, connected by timber beams and with infill applied. The vault along the nave is not structural, being built with a technique which mixtures small stripes of timber with plaster.

The transept has a central circular dome supported by four arches based in columns, which are connected to inner walls. From the central dome start two structural vaults that meet the exterior walls of the transept. In the continuity of the NW and SE exterior walls of the nave, there are two arches that act as intermediate support for the vaults.

At the opposite side of the main entrance, may one say, at the end of the church, there are five apses, but only the central one reaches the two levels. The central apse is formed by a vault, starting from the main dome to a semi-circular dome. The vault and dome are supported by walls, shared with other two apses. Each of these apses contains four small arches connected to the walls and serve as starting base to a dome.

The top of the masonry walls that reach the second level supports a concrete beam, with the exception of the SW wall, this way the beam doesn't to a closed circuit. The two concrete beams present at the central nave are connected by steel ties that span across the nave, spaced by approximate 1m.

The roof is framed, formed by concrete trusses along the transept and apse, and beams that combine brick units and a concrete layer along the nave. The roofing is composed by bricks, tiles and a layer of thermal insulation. The roof of the lower levels is achieved with timber elements and tiles.

4.1.3 Construction of the FEM Model

The construction of the FEM model is being done in a preliminary stage of the dynamic monitoring, so the main objective is to capture the first modes of the structure and consequently choose possible setups for the position of the sensors.

After studying the geometry and the structural arrangement of the structure, it is now possible to come up with a model closest possible to reality. The program chosen to recreate the structure was Straus7, due its user friendly interface and to the fact that the purpose is in the linear elastic range.

In the presence of very different structural elements, the type of entity chosen to model them depended on the type of element and on the easiest way to conjugate them all together. For walls, domes and vaults, the evident entity is "*plates"*, which ended up conditioning the choice of other elements. To facilitate the structural arrangement, the entity "*plates"* was extended also to columns and arches. The exception are the intermediate arches supporting the vaults of the transept, the arches supporting the domes of the smaller apses and the roof frame, which were accomplished with *"beams"*. The final configuration of the model is presented in Figure 32.

So, from the plans and elevations provided by the architectural part (see Annex I), a base plan of the structural elements was created, considering the mid-plane projection and from there, the elements were extruded to their heights, as shown in Figure 33.

The eccentricities between elements were respected when superior to 5cm, which lead to the use of "*rigid links"* to connect elements. This option was taken in order to respect the effect of eccentricities in the dynamic behaviour of the structure.

Also, in the connection between arches and walls/columns, the distance between middle lines was kept and achieved with "*rigid links"* because, uniting them and consequently change the radius of the

arch, would increase a lot the spans of the arches in proportion to the original distance. For example, the arches of the central nave which have a span of 10m, if connected to the columns, would have the span increased of almost 2m (1/5 of span).

Another advantage of using *"rigid links"*, regards the superposition of elements' thickness. This entity avoids the concentration of stiffness and mass in connections between elements, contributing to a better approximation of reality.

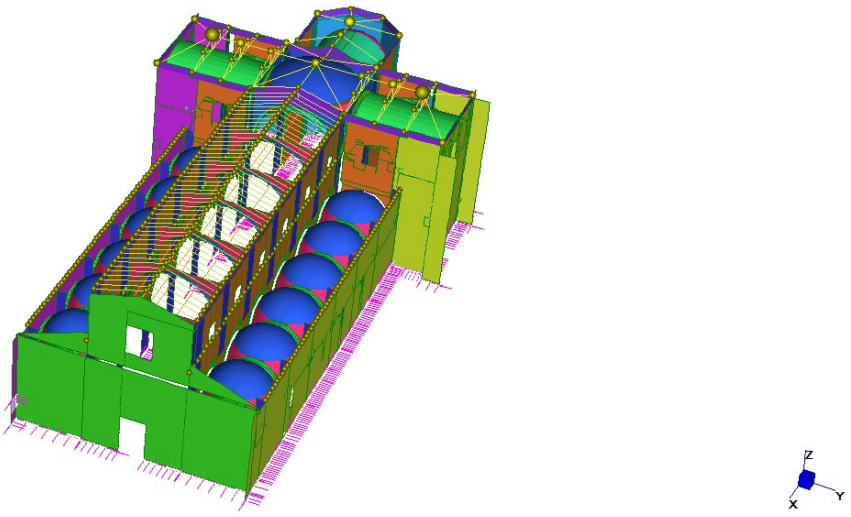

Figure 32 - Perspective of San Domenico church model

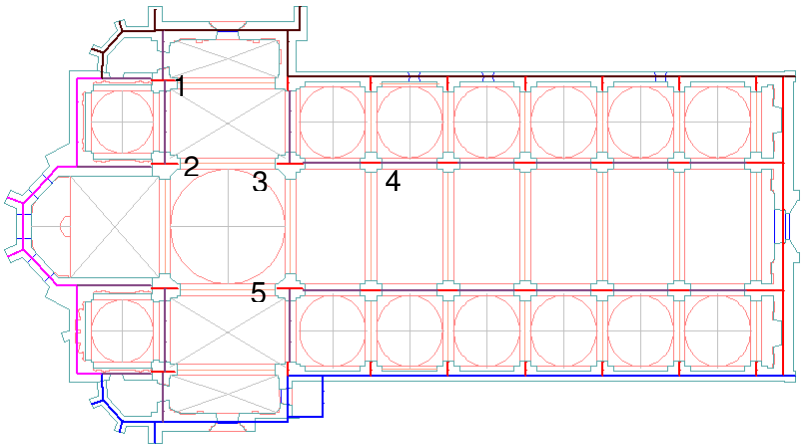

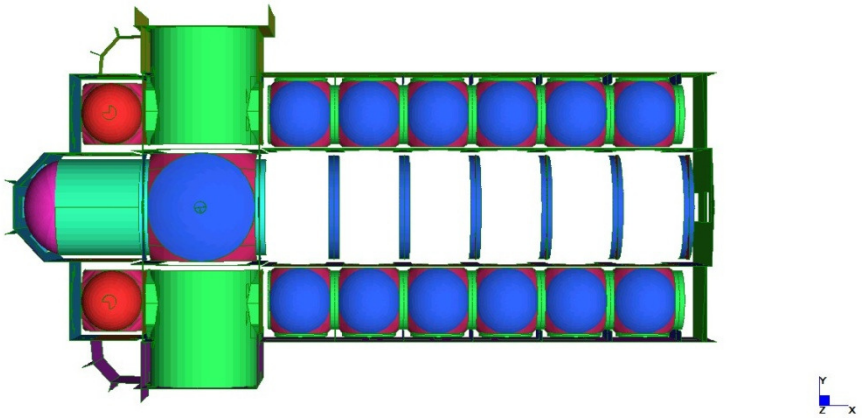

Figure 33 - At the top plan containing the mid-plane projection lines more pronounced and the bottom *xy* view of the plan

So, the first elements to be created were the walls and columns, being then added the arches, domes and finally the roof. The interior of the church presents the configuration shown in Figure 34, achieved mainly with "*plate"* elements and can be compared with the pictures present in the section 4.1.1.

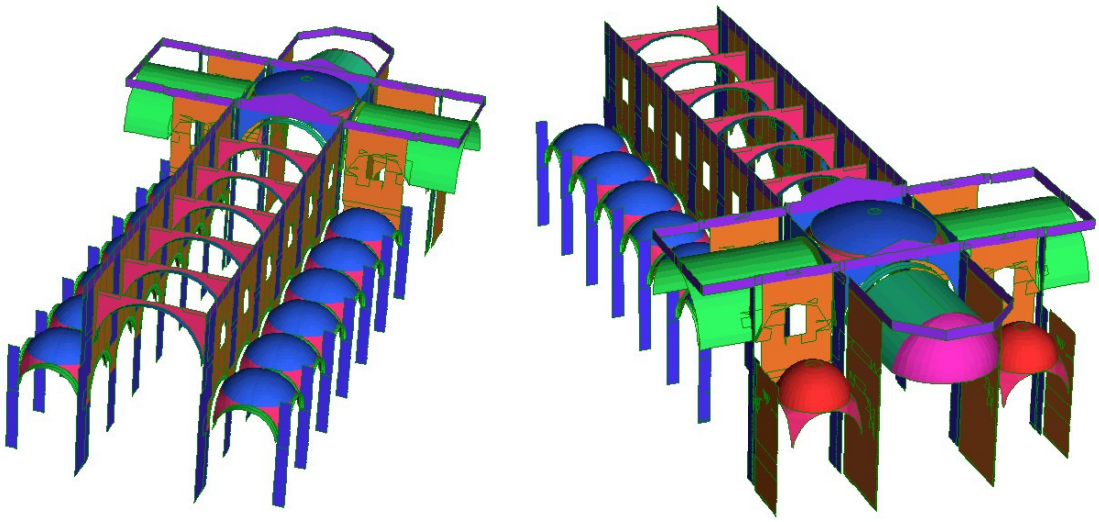

Figure 34 - Views from the inner elements

The roof presents a complex combination of different elements like concrete beams, brick beams combined with a concrete layer, concrete trusses, masonry walls and steel ties (see Figure 35). Since, there's little information about the roof structure a lot of assumptions and considerations were made based on the architectural drawings and photographs of a previous visit to the roof. This part is clearly one of the areas that need future development.

After running a first model where the steel ties were modelled as "*beams"* and this compromised the quality of the modal analysis, they were changed to rigid links. Also, from the photographs is not

possible to see the thin layer of concrete covering the roof, being only the brickwork beams visible. This lead to at first just modelling the brickwork beams and then to accomplish the transversal stiffness that the concrete cover provides, every four beams, rigid links forming a cross connected the beams.

Instead of modelling the roof as *"plates"*, which would create problems to the mesh, it was chosen to recreate the roof frame as beams and add non-structural masses to the nodes of the beams.

Figure 35 - Transposition of the roof from reality to the model

4.1.3.1 Elements' Thickness, Material Properties and Roof Masses

The majority of the elements previously described are in masonry, but there are other materials like concrete, timber and steel. Since no tests to the materials were performed, the material properties were chosen according to existing codes and similar monuments already analysed.

For the elements in masonry, the choice was based in the NTC 08 recommendations. The masonry elements seem to be composed by consistent rubble masonry, with an exterior layer of brickwork. By now it's not possible to know the extent of brickwork in the masonry elements, so the properties were chosen in order to describe a combination of both and are presented in Table 3.

For the main façade, it was adopted the same characteristics along the entire thickness, because it was not possible to assess the connection between the ashlar stonework and the inner layer, and also the influence of this exterior layer in the resistance capacity of the wall. By assuming the previous values, the conservative option is taken.

The properties of the timber beams and concrete elements are shown in Table 3. For the timber beams were adopted values of C18 (softwood) recommended in Eurocode 5, which corresponds for example to pine beams. The category chosen for the concrete it was 20MPa and the default values from the program were kept.

To characterize the brickwork beams with a thin layer of concrete on top, the stiffness and density were considered to be closer to the one of the bricks. Ahead in this chapter is explained how the effect of the concrete layer was modelled.

Table 3 - Material properties

Material	E [MPa]	ν	γ [kg/m3]	G [MPa]
Masonry (consistent rubble masonry with brickwork)	2400	0.2	2000	-
Concrete		0.2		-
Timber	9000	-	380	560
Brick beams with thin layer of concrete	2400	0.2	1900	-

The church presents a great variety of sections and thicknesses.

Table **5** and Table 4 contain the dimensions of the elements, according to the type of entity chosen to represent them in the model. The numeration of the truss beams and the correspondence between letters and dimensions is presented in Figure 36.

Table 4 - Thicknesses of *"beam"* entities

Beam Elements	Cross-section	Dimensions (bxh or d)
Timber beams	Circular	0.200
Concrete truss (B1 and B 2)	Rectangular	0.180 x 0.200
Concrete truss (B3,B4 and B5)	Rectangular	0.180 x 0.300
Lateral apses arches	Rectangular	0.561 x 0.484
Intermediate arches of transept vaults	Rectangular	1.070 x 0.580
Masonry beams	Rectangular	0.200 x 0.200

Table 5 - Thicknesses of the different *"plate"* entities

Plate Elements	Thickness (m)
S-W nave wall (bottom)	1.910
S-W nave wall (top)	0.952
S-E nave wall	0.919
N-E central apse wall	1.400
N-W nave wall	0.756
Inner walls	1.070
Main and lateral domes	0.200
Lateral arches	0.484
Lateral apses domes	0.545
Apse's semi-circular dome	0.418
Apse's vault (in x, cylindrical part)	0.240
Transept's vaults (in y)	0.150
Main arches, in zy plane	1.040
Main arches, in zx plane	0.952
Nave arches	0.415
Concrete beam	0.900
Infill	0.200
S-E transept façade	1.65
N-W transept façade	1.00
Lateral apses exterior walls	1.546
S-E transept window wall	0.808
N-W transept window wall	0.65
N-E apse window walls	0.836
Columns (1)	2.000
Columns (2)	2.280
Columns (3)	2.090
Central nave columns (4)	1.930

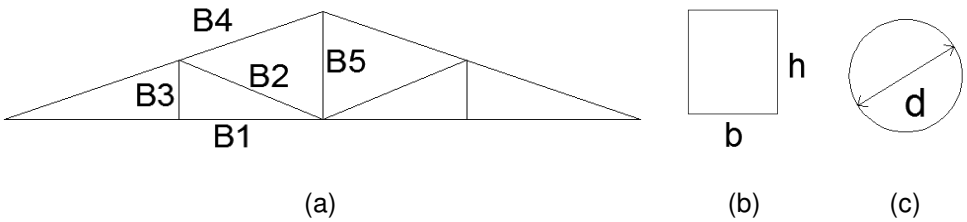

Figure 36 - (a) Numeration of the truss beams, (b) Corresponding dimensions of a rectangular cross-section and (c) Corresponding diameter of a circular cross-section

Since the columns have a crossed shape cross-section, it was necessary to approximate them to a quadrangular shape, which could be used with *"plate"* entity. The equivalent cross-section, was determined to maintain the moment of inertia around x and y axis with approximated values and proportion.

The mass of the non-structural materials of the roof (tiles, timber elements, thermal insulation) was considered 145kg/m^2. Estimating the area of the roof, this was multiplied by the mass and then distributed by the modes.

For the roof of the lateral naves, considering that the load goes to the exterior walls (S-E and N-W) and for the support on the walls of the central nave, the mass per node at the first was 455kg and at the second was 562kg.

For the apses, except the central one the masses were (from right to left) and the roof of the naves:

- First apse: exterior wall - 417kg/node; inner wall (only one node) – 1668kg;
- Second apse: exterior wall (x direction) – 492kg/node; exterior wall (y direction) – 574kg/node; inner wall (only one node) – 6887kg;
- Fourth apse: exterior wall (x direction) – 492kg/node; exterior wall (y direction) – 530kg/node; inner wall (only one node) – 6887kg;
- Fifth apse: 416kg/node; inner wall (only one node) – 1667kg;
- Central nave: exterior walls (concrete beam) – 130kg; concrete beam top – 260kg.

The roof at the second level is little more complex so a more precise distribution had to be done, as shown in Figure 37. The areas of distribution, calculated considering the inclined length of the roof, and the attributed masses are presented in Table 6.

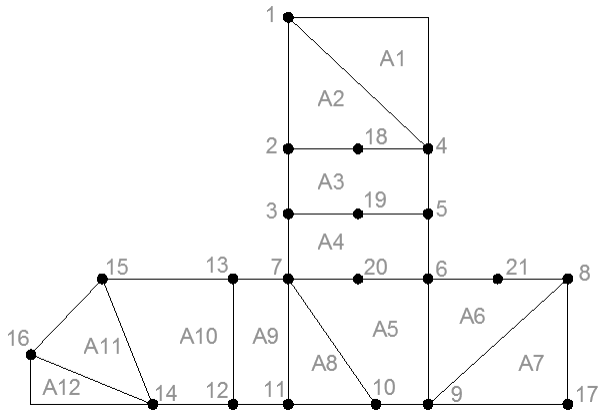

Figure 37 - Nodes considered for the non-structural masses

Table 6 - Distributive areas and nodes with masses in the transept and central apse

Name	Area [m2]	Nodes	Mass [kg]	Nodes	Mass [kg]
A1	29.691	1	3226	13	1828
A2	29.691	2	1763	14	6528
A3	43.357	3	2096	15	3729
A4	43.357	4	9988	16	1400
A5	27.408	5	4191	17	1378
A6	19.01	6	3295	18	1763
A7	19.01	7	3173	19	2096
A8	9.969	8	3574	20	1787
A9	18.297	9	4515	21	1787
A10	32.13	10	2478		
A11	19.306	11	2049		
A12	9.653	12	3656		

4.1.3.2 Boundary Conditions

The interaction soil/structure is very important to the behaviour of the structure under seismic loads. In this case, no information was available about the soil, so the boundary condition assumed was fixed.

Other important aspect is the fact that the church shares a wall with monastery. The only information available was that the monastery has two floors, meaning perpendicular slab to the wall. This was transposed to the model, by fixing the nodes at the height of 3.153m.

Both boundary conditions are important and were modelled roughly, an opportunity of improvement of the model is to know more about this interactions and modelled them as translational springs.

4.1.4 Analysis of the results

Since the main purpose is to study the mode shapes and respective modal frequencies, two types of analysis were performed in the elastic range: a linear elastic analysis, with the structure subjected only to dead load and a natural frequency analysis.

4.1.4.1 Linear Elastic Analysis

The main objective of running a linear elastic analysis, with only dead load, is to check if the structure is deforming properly and the concentration of stresses. As seen in Figure 38, the structure has higher displacements at the second level, as expected, and the maximum combined displacement (xyz) is 4.782mm at the mid-span of the arches of the central nave. The exterior walls due to their big thicknesses and to the fact that the bases are fixed, present a very stiff behaviour and as seen, deform much less than the rest. As seen the external elements are bending towards the interior of the church, because the interior is deforming under its own weight and dragging the surrounding elements.

When it comes to stresses, the church also shows a predictable behaviour. The church in general is in compression (see Figure 39), with exception of some parts of elements, like the middle span of some arches, domes, infills and segments of the concrete elements.

The concentration of compression stresses, for masonry elements, is located at the base of the walls and in the columns of the central nave, at the base and at the place when they meet the arches, as seen in Figure 40. The maximum compression is 0.187MPa and it occurs where the column 5 (see Figure 33) joins the arch coming from the central nave. At the base of the columns supporting the main dome, the stress is around 0.152MPa and for the base of the columns at the naves is around 0.142MPa.

The maximum tension in the masonry elements is in the element connecting the main dome with the arches and is around 3 MPa.

The highest compression stress is associated with the concrete beam at the top of the walls with a value of 0.670MPa (at the lower fibres of the cross-section of one of the supports). The concrete beam is behaving as continuous beams pinned at intermediate supports, the columns, introducing tension at the lower fibres of the mid-span and top fibres at the supports, and compression at the opposite fibres of the same locations. Also, the highest value in tension (1.926MPa) occurs in the top fibres at one of the supports in the transept.

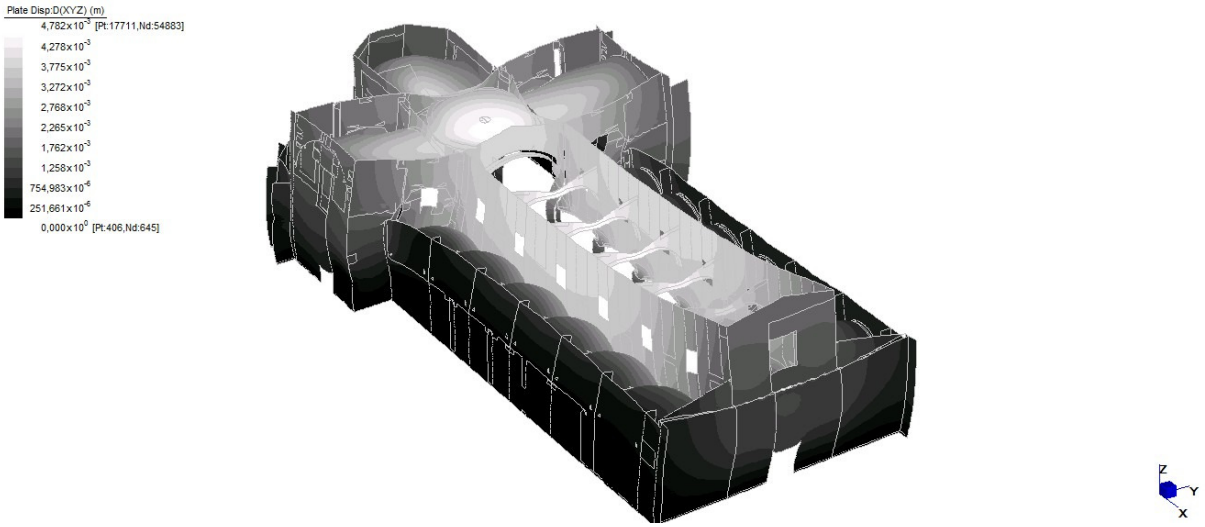

Figure 38 - Linear elastic deformation, under dead load

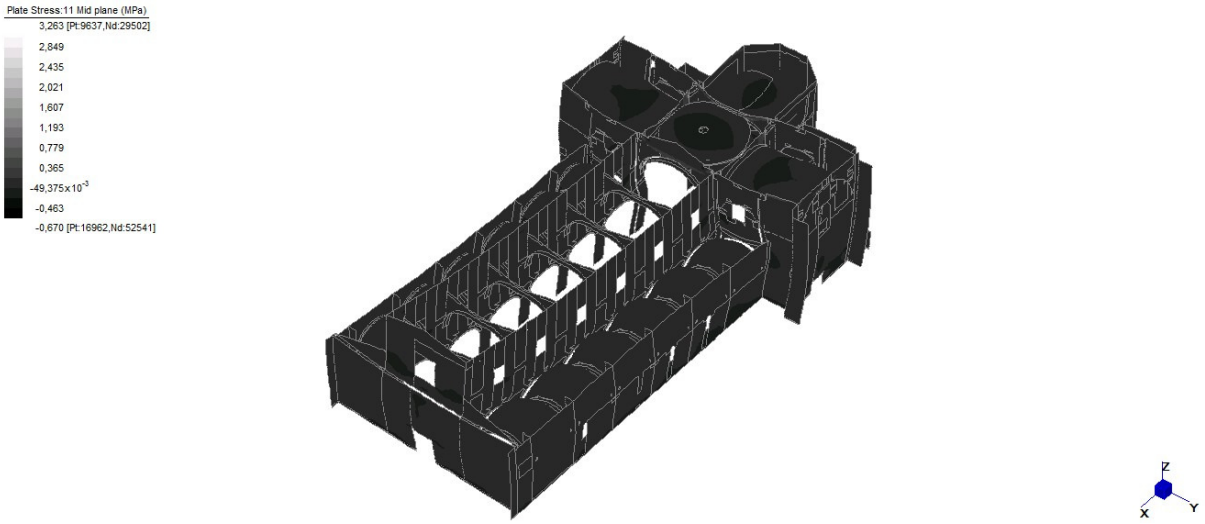

Figure 39 – Principal stresses for the entire structure

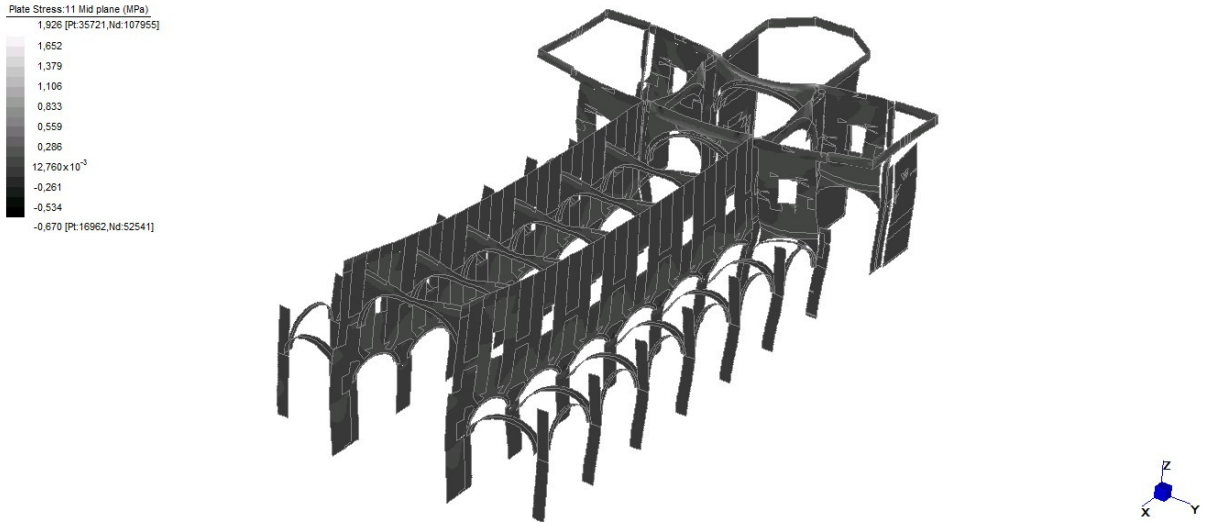

Figure 40 – Principal stresses of some of the inner elements

4.1.4.2 Natural Frequencies Analysis

The first four modes that characterize the structure are the ones presented in Table 7, presenting values in the expected range for this kind of structures.

After running an analysis asking for 100 modes, the cumulative mass participation factors reached in the x direction, 74% and in the y direction 80%, not reaching the 85% necessary to determine the overall seismic response. A possibility to mobilize more mass is fro example to change the boundary conditions, substituting the present fixed condition for a less stiff interaction. At 100 modes the frequency was around 5.9 Hz.

Table 7 - First four modal frequencies and respective mass participation factors

Mode	Frequency	Mass Participation Factor		
		x	y	z
	[Hz]	[%]	[%]	[%]
1	2.710	0.000	48.762	0.002
2	3.548	3.071	4.366	0.001
3	3.747	29.823	1.595	0.001
4	3.800	19.270	0.424	0.000

The first mode is clearly, as one can see by the mass participation factor (see Table 7), a translational mode in the y direction. This is also shown by the modal shape, presented in Figure 41, being the right lateral nave the one to show higher displacements in y, reaching the maximum of 719.165×10^{-6}m, at the top of the 4th column, counting from the right. The higher displacements are extended to the surrounding area: 2nd level of the central nave, especially near the windows, lateral domes and central arches.

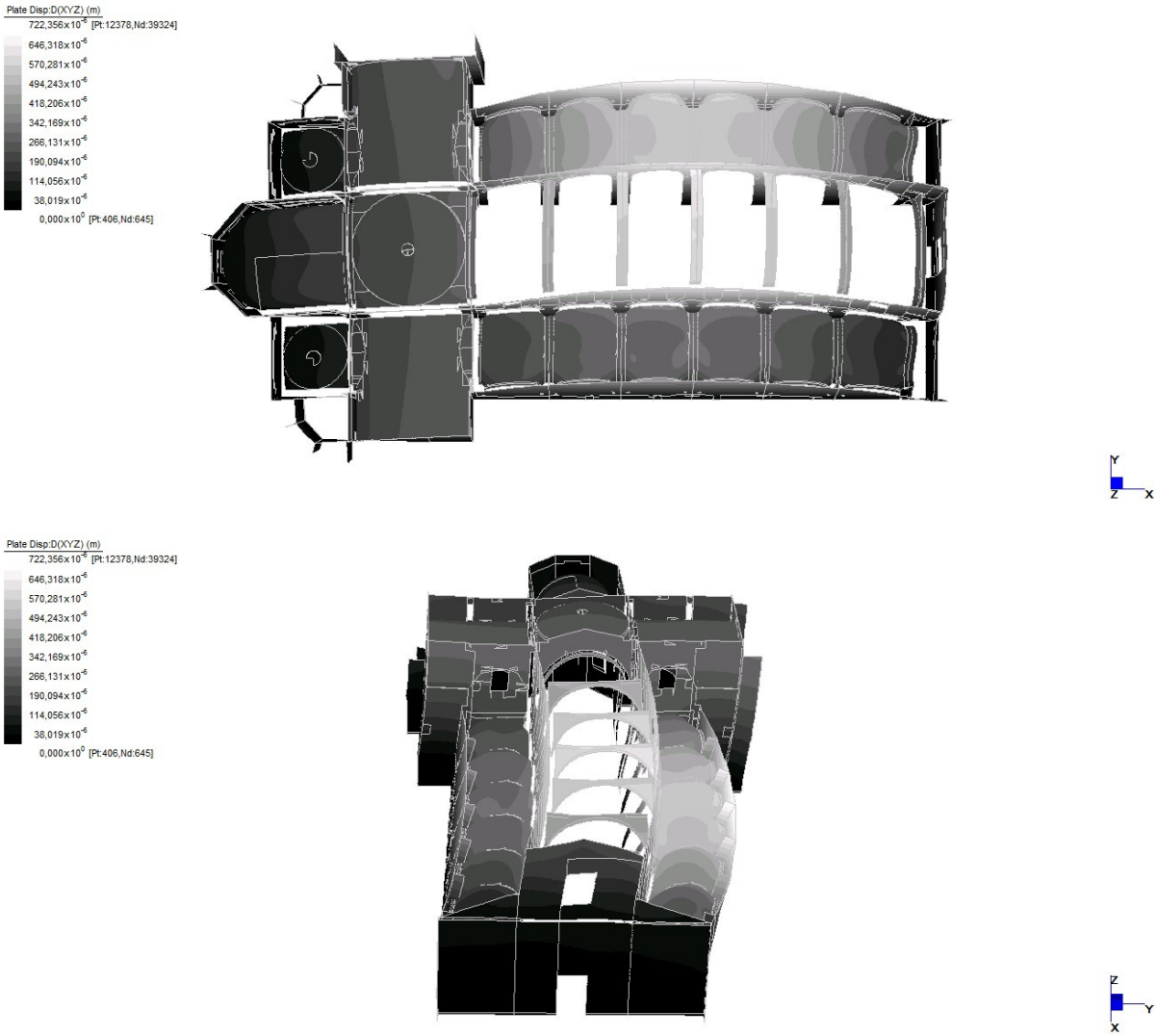

Figure 41 - Mode shape 1

The second modal frequency is not as clear as the first one. The modal shape can be described as follows: the apse, transept, left lateral nave and left part of the central nave are moving in one way and the right part of the central nave and right lateral nave are moving in the opposite way (see Figure 42). The mid-span of the central nave arches is acting as a hinge, allowing the opposite behaviour. The maximum displacement in the y direction is 1.238×10^{-3}m, at the top of the 3rd column at the right, counting from the main entrance. This value is much higher than the previous detected in Mode 1.

For the x direction, the maximum displacement was detected at the top of the S-W walls, one of the parts of the church that fell due to out-of-plane mechanism during the 6th April earthquake.

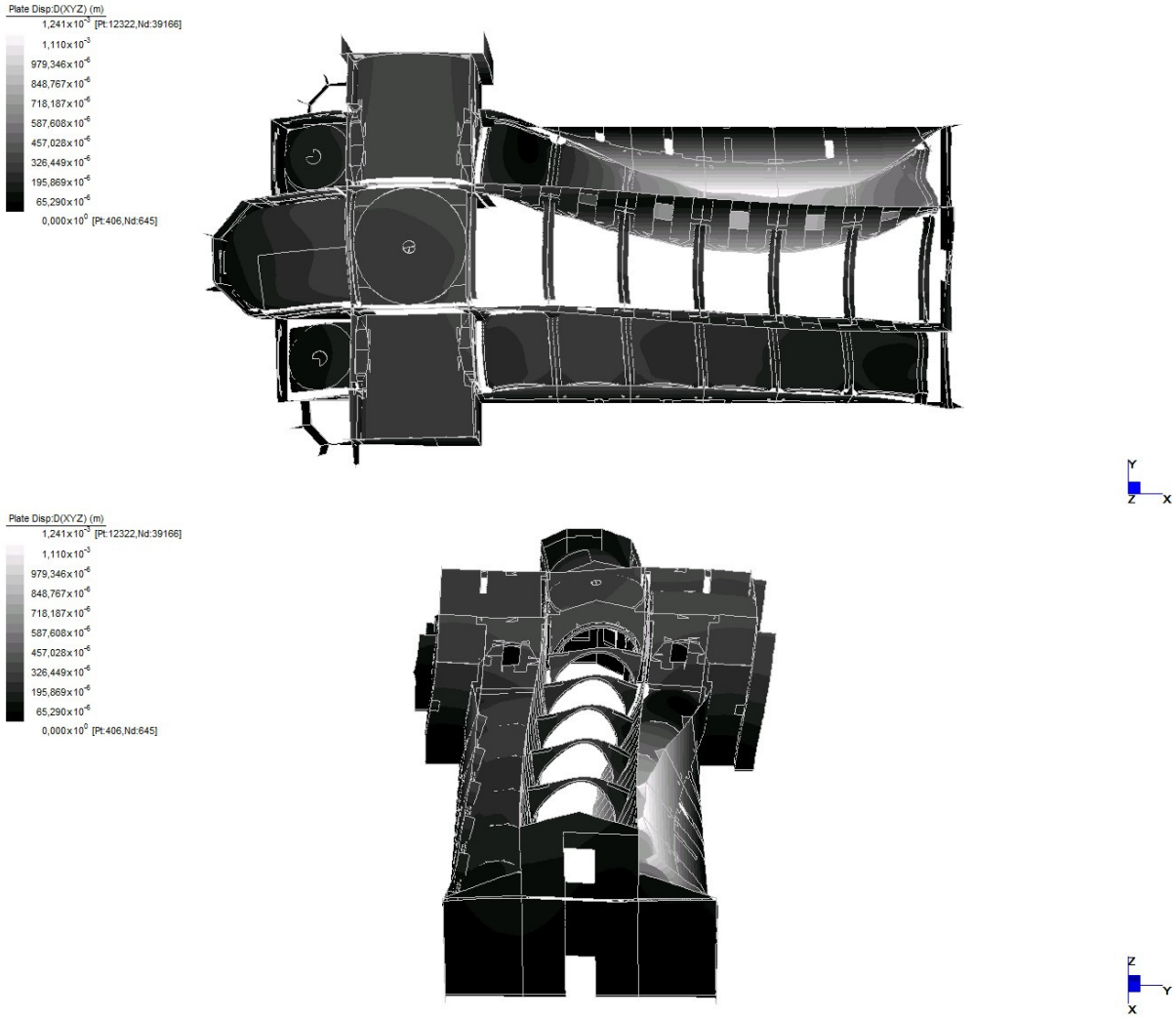

Figure 42 - Mode shape 2

The third mode is a mainly a translation mode in x, proved by the mass participation factor (see Table 7) and the mode shape (see Figure 43). This mode shows the movement in x of the S-W wall and the apse and transept (Group 1), which behave as a block and by consequence influences the movement of the naves. Taking into consideration the coordinate system displayed at the lower right corner of Figure 43, when Group 1 moves in the positive direction of x, the right side of the nave moves in negative direction of y and the left side moves towards the positive.

In this particular mode, the biggest displacements in y are in the left lateral nave and the highest is 664.583×10^{-6}m, at the top of the third column, counting from the entrance. The maximum displacement in x is in the top part of S-W wall, with the value of 639.523×10^{-6}m.

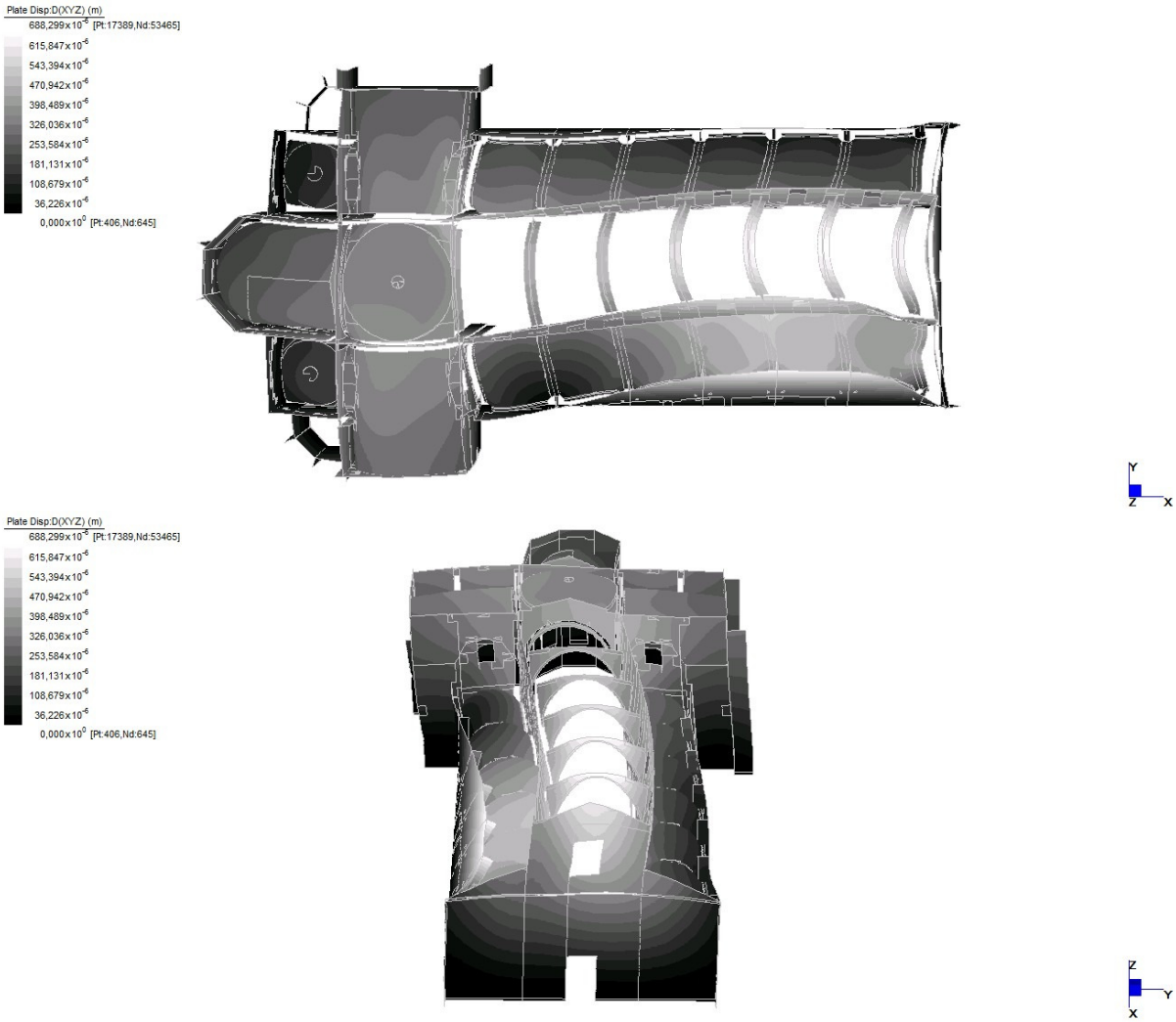

Figure 43 - Mode shape 3

The fourth mode is again translational in x, as expressed by the mass participation factor (see Table 7) and modal shape (see Figure 44). The difference from the third mode is in the movement of Group 1 (apse, transept and S-W wall), which for this particular mode move in the positive direction of x. The naves behave in an approximated way as described for the third mode.

The maximum displacement in y is 827.024×10^{-6}m and happens for the node at the top of the fourth column, at left, counting from the entrance and the displacement in the x direction is again in the triangular area at the top of the S-W wall, the one collapsed during the 6th April earthquake.

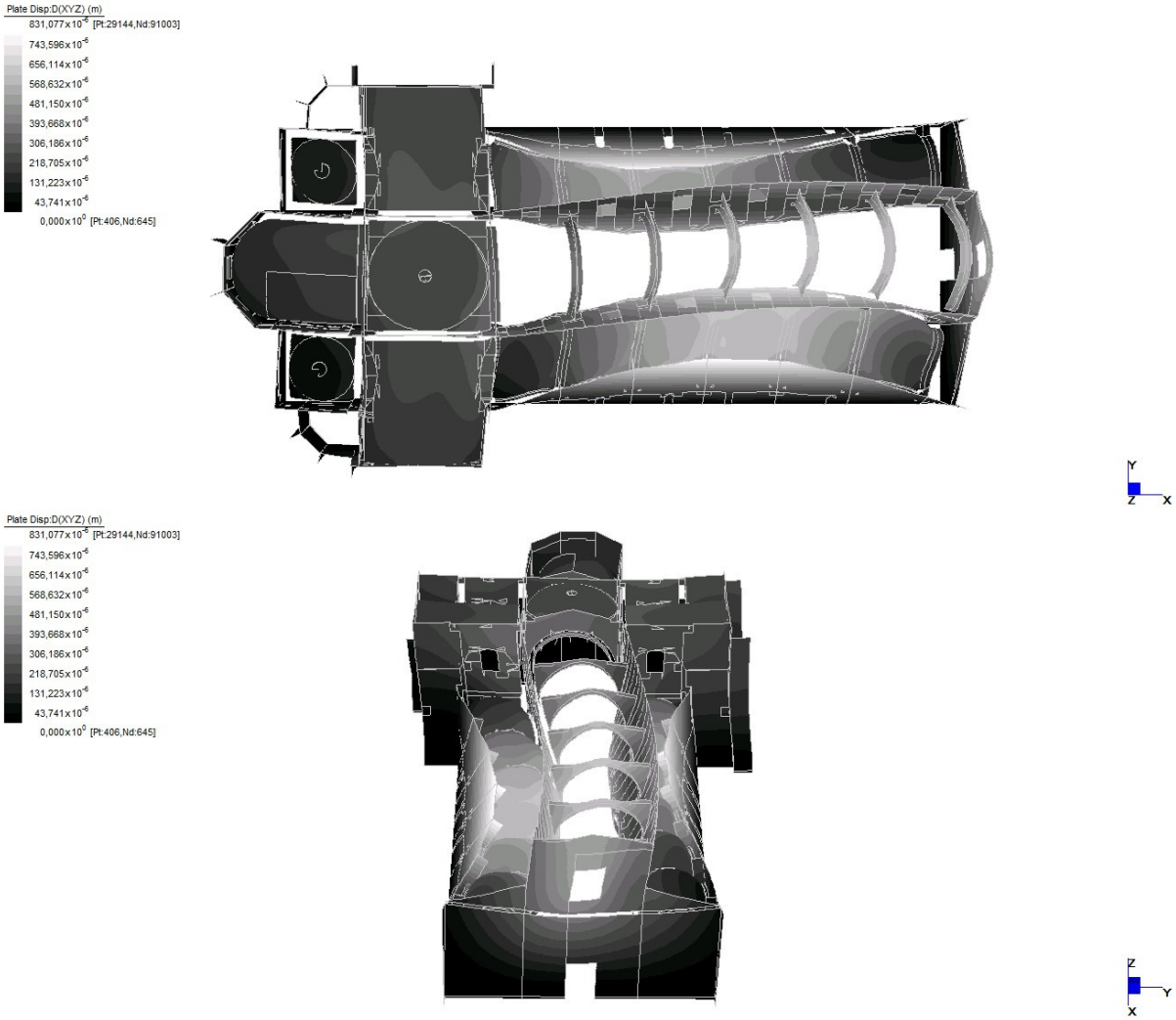

Figure 44 - Mode shape 4

A brief reference can be made to the 5th mode, with a frequency of 4.542Hz, because in its predecessors the apse and transept always moved as a block in the same direction, but in this mode torsion is their principal movement.

The higher modes show local behaviours of the different elements of the structure.

4.1.5 Discussion of possible setup

Regarding the modal analysis performed is advisable to locate sensors in the points with higher displacement in x and y. This means doing a possible setup mainly to control the accelerations at the top of the third and fourth column of each side of the lateral naves, enabling also a better understanding of the type of connection existent between the church and the rest of the monastery. At the top of the central nave, one sensor on each side maybe aligned with one of the previous sensors or placed in one of the windows, and one more at the base of the S-E wall, also aligned with one from

the columns. The sensors at the base should have two channels, one parallel to the wall and the other one perpendicular. The sensors at the top of the lateral naves and central nave can have only one channel perpendicular to the wall. This setup would have 8 sensors permanently in the church. A sketch is presented in

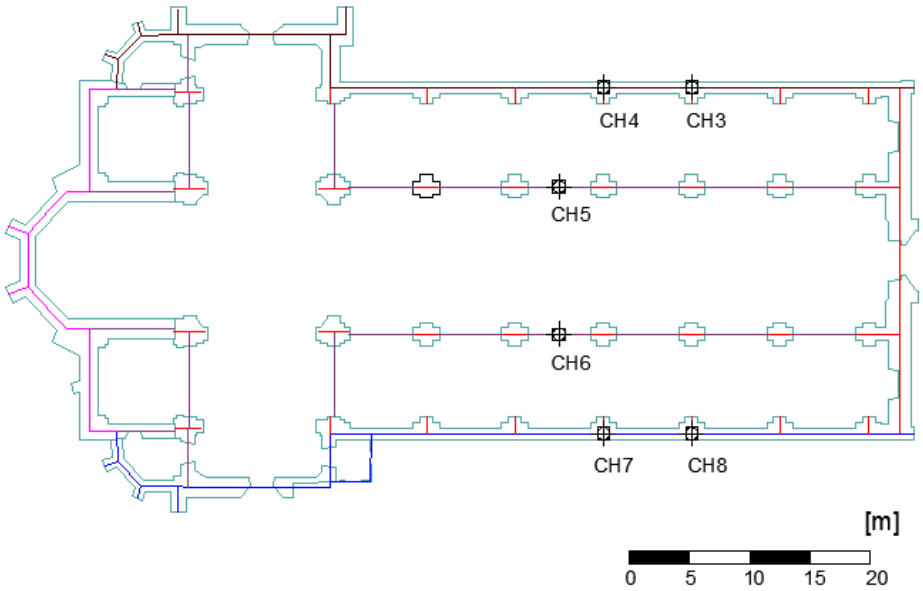

Figure 45 - Plan with the possible locations of the sensors

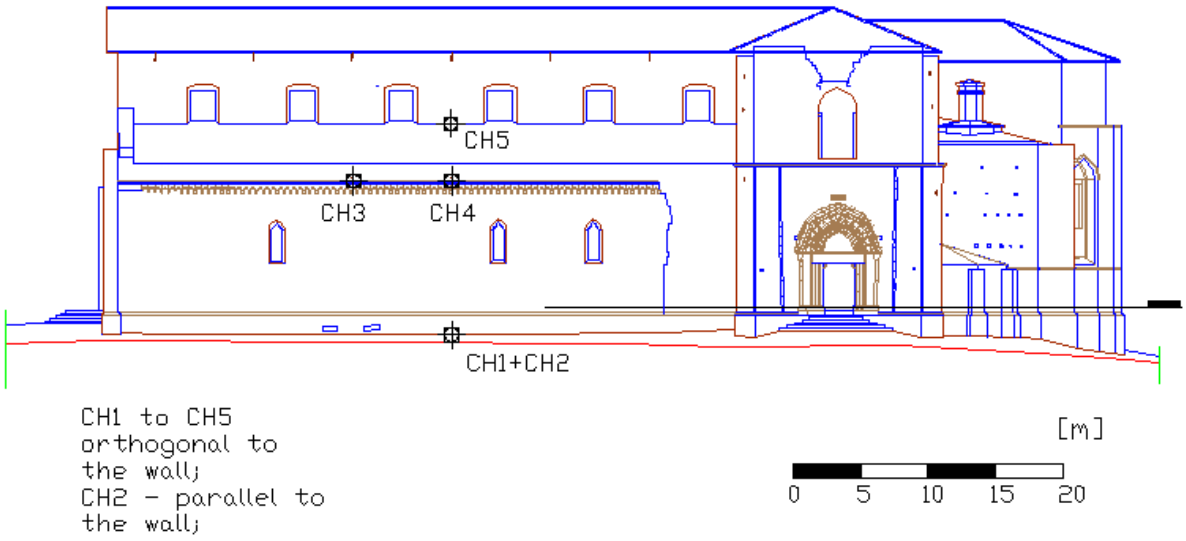

Figure 46 – Elevation with the possible setup for the sensors

Other possibility is to conjugate the previous setup with: two sensors at the top of each transept wall perpendicular to the naves (channels in the x direction), another sensor in the S-E façade of the transept (channel in the y direction), near to the collapsed part and a last one on the top of the S-W wall, also near the collapsed part (channel in the x direction). This would allow recording the behaviour

of the structure near the parts that collapsed due to out-of-plane mechanisms and to capture higher modes. Higher modes present local modal shapes that enable an easier detection of damage.

As recommended by Ramos (1998), the measuring duration should be 2000 times the highest natural period, which correspond to the lowest frequency, in this case 2.71Hz. So, the measuring duration should be around 13 min.

4.2 Case Study 2: Spanish Fortress

As presented in and Figure 47, the Spanish fortress is located in the North-East side of the city centre of L'Aquila and the street surrounding it is Benedetto Croce street.

(a) (b)

Figure 47 – (a) Location of the Spanish Fortress and (b) 3D sketch of the Spanish Fortress (adapted of Google Earth)

The Spanish fortress, as the name sais, was built during the Spanish domination of the south of Italy and is one of the most impressive castles of the Renaissance period. In order to control the citizens of L'Aquila, in 1534, the fortress stated to be built, based on a project of Don Pirro Aloisio Escrivà, famous for his military constructions and by order of Viceroy Filiberto d'Orange. Nowadays is still visible that the canons were pointed to the city and not to the outside.

From 1534 to 1575 only the military structure was complete and only in 1870, all the wings were finished and the ditch created. Also, only by this time, the timber bridge that crosses over the ditch was demolished and substituted with one in masonry. Since then till 1913, the structure suffered different changes, which lead to the present day configuration.

Between 1949 and 1951, the fortress was restored and today is the occupied by the National Museum of Abruzzo.

The enormous fortress is formed by four bastions, pointing to the four cardinal directions, connected by walls 60m long and 30m wide at the bottom and 5m wide at the top. The ditch around the fortress is 14m deep and 23m wide (Casarin, 2010).

4.2.1 Damage Description

Due to the 6th April earthquake, the Spanish fortress was severely damage and its load bearing capacity and consequently stability were compromised. Next, a brief description of each wing is presented.

Figure 48 - Views of the S-E façade (main façade) before and after the 6th April earthquake (Casarin, 2010)

The S-E wing, which corresponds to the main façade, was the one that suffer the most destructive effects. In what regards the external face of the wing the main damages were (Casarin, 2010):

- Overturning of the upper masonry walls (see Figure 48);
- Several collapses on the 2nd floor;
- Separation of the floors from the longitudinal walls.

In the inner face, the main damages detected were:

- Pillars failing by crushing (see Figure 49 (a));
- Damaged walls of the 1st floor;
- Longitudinal crack in the barrel vault of the arcade, which goes through the entire thickness of the slab;
- Shear cracks on the transverse bearing walls.

(a) (b) (c)

Figure 49 - (a) Pillars of the arcade, (b) and (c) internal walls (Casarin, 2010)

The S-W wing presents also considerable damage, regarding specifically:

- Overturning of the two façades;
- Cracks on vaults and shear cracks on the transverse walls;
- Separation between external perimeter walls and internal walls and floors of the 1st and 2nd floors (see Figure 50).

Figure 50 - Separation between walls and floors (Casarin, 2010)

The two wings left, the N-W and the N-E, suffer less damage. In fact, the N-W wing resisted quite well to the overturning of the façades and to the consequent disconnection of elements, mainly due to a previous intervention that inserted a system of tie rods in this wing (see Figure 51 (a)). So, the damage was concentrated in the shear walls (see Figure 51 (b)) and on the masonry walls and slabs of the 2nd floor, which present partial collapse (see Figure 51 (c)), (Casarin, 2010).

The N-E wing presents a slight overturn of its two façades and shear cracks in the transverse walls, being the elements of the 2nd floor the most affected.

(a) (b) (c)

Figure 51 - (a) Tie rods inserted in the structure, (b) Cracked shear walls and (c) Partial collapse of a floor slab (Casarin, 2010)

Summing up, according to the damage survey performed with the form regarding palaces, the overall damage comprehends: overturning and flexural mechanisms on the external walls, disconnection of floors from walls, shear cracks in external and internal walls, damages in vaults and arches, partial collapses of floors and vaults and pillars crushing.

4.2.2 Emergency Intervention

With the damage survey, was possible to observe that one main problem was the overturning of the exterior walls and since aftershocks were still a worry, a temporary intervention to stabilize the S-E and S-W wings (most affected wings) was carried out. The strengthening intervention consists of connecting the two exterior walls of each wing, by means of stainless steel cables and take advantage of the remaining resisting capacity of the structure.

For the S-E wall was still necessary to rebuild the roof with hollow section steel frame covered by a light structure made of wood. For the S-W wing a steel framed structure was built against both façades, to better distribute the stresses that would come from the cables in tension.

Figure 52 - Provisional stability intervention

4.2.3 Dynamic Monitoring System

Prior to the installation of the monitoring system some on site non-destructive tests were performed. The experimental campaign comprehended: sonic pulse, velocity tests, radar tests, thermographic tests, single and double flat-jack tests and dynamic identification tests.

To the ambit of this thesis, the most important one is the dynamic test and is the only one which is going to be briefly described.

The objective was to evaluate the behaviour of the perimeter walls of the structure (facing the courtyard and the ditch), since overturning mechanisms were activated in the 6th April earthquake.

On September 8th and 9th were dynamic tests were performed in the S-E wing of the castle, the one same one where is installed the monitoring system. They were carried with ambient vibration excitation, with five configuration setups, with 27 points of acquisition and usually eight sensors were used, counting with the ones fixed at the base (reference sensors). The sampling rate was 100 SPS and 3 records of 65'536 points each were made for each setup.

The resultant modal identification identified four modes with frequencies around: 2.93Hz (present in all the setups), 4.15-4.18Hz (not very clear), 5.20 - 5.4Hz and finally 8.7 - 8.8Hz. The modal shapes described for the first, second and third modes are out-of-plane bending shape and the fourth is a considered a local mode at the top of the second level. The determined modal shapes are presented in the Figure **53**

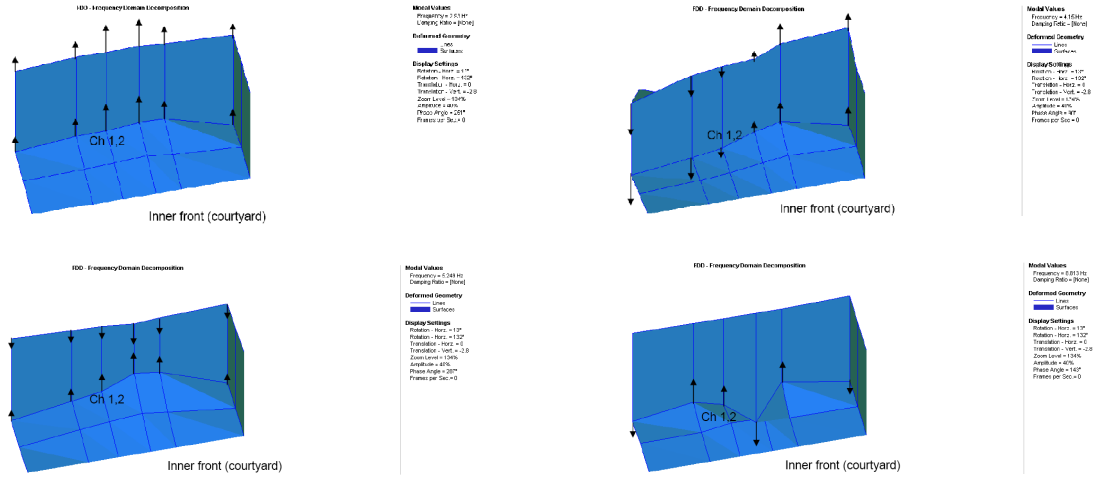

Figure 53 - The four modal determined modal shapes (Casarin, 2010)

The actual dynamic monitoring system was installed after the dynamic test, from the 17 till the 19 of December 2009, in order to complement a pre-existing static monitoring system, which was controlling the crack pattern evolution and the environmental parameters.

The system is composed by an acquisition unit connected to eight high sensitivity piezoelectric accelerometers, a central unit located in the second floor of the S-E wing and a wi-fi router for remote transmission of data (Casarin, 2010). The overall location of the accelerometers is presented in Figure **54**, and the accelerometers are described as follows:

- CH1 (orthogonal) + CH2 (parallel) are fixed at the base of the S-E wing internal wall (see Figure **55** (a))
- CH3 + CH5 are orthogonal to the internal wall of the S-E wing, placed along the elevation, aligned along a vertical line (see Figure **55** (b) and (c));
- CH4 is orthogonal to the external wall of the S-E wing, aligned with CH7 vertically (see Figure **55** (b) and (c));
- CH6 + CH7 + CH8 are orthogonal to the wall (external) of the S-E wing and are aligned horizontally at the 2nd level (see Figure **55** (b) and (c)).

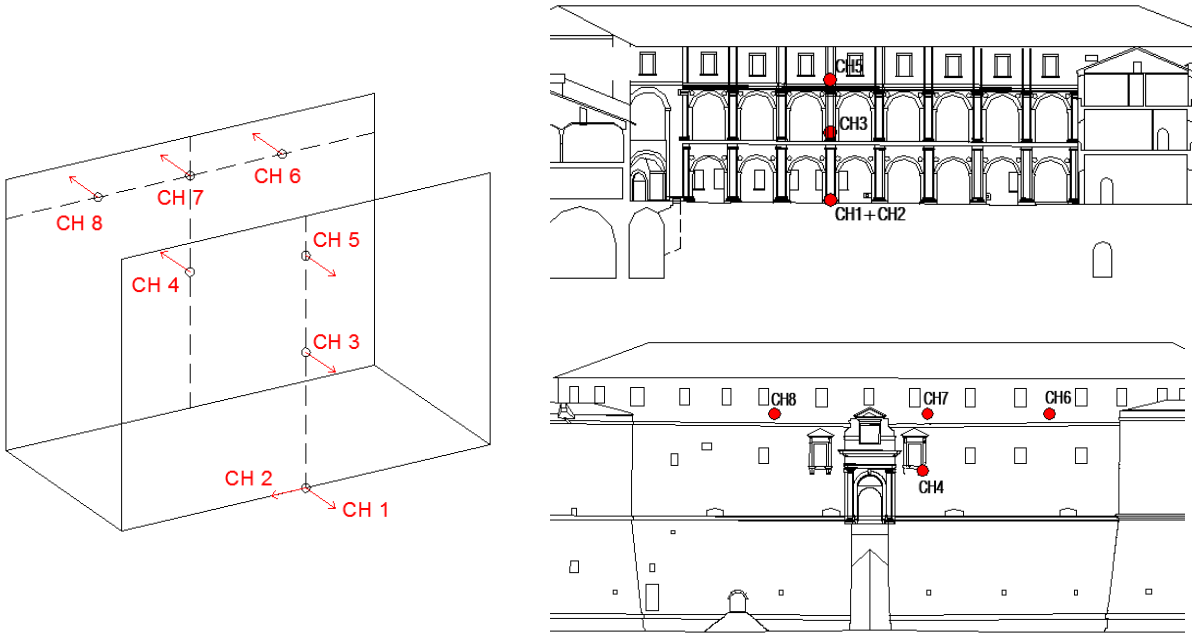

(a) (b)

Figure 54 - (a) Sketch of the location of the sensors and (b) Position in the elevations of the fortress

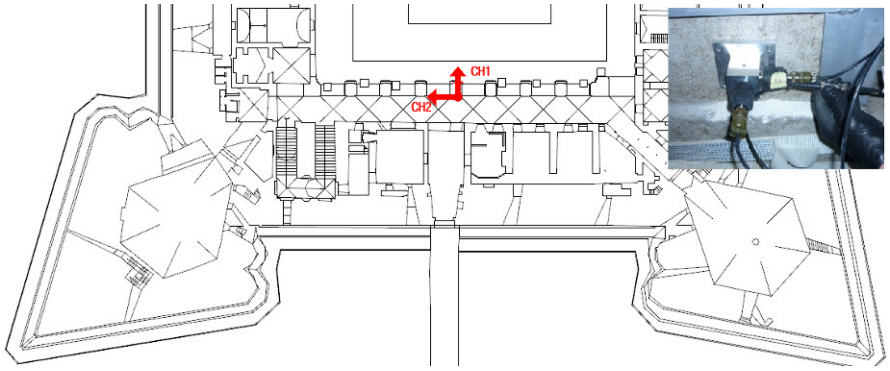

(a)

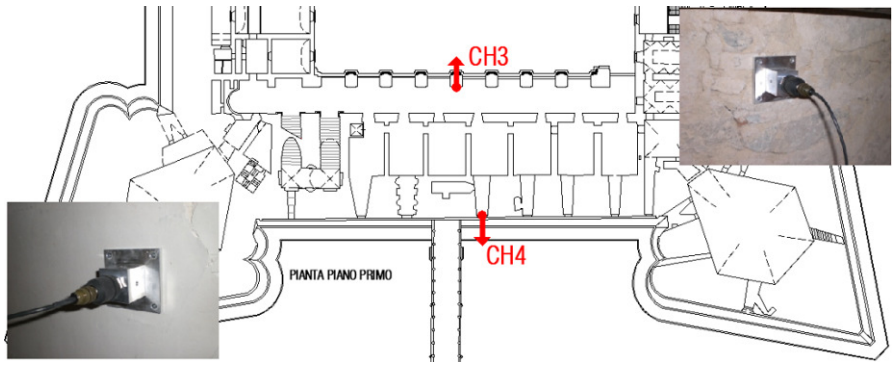

(b)

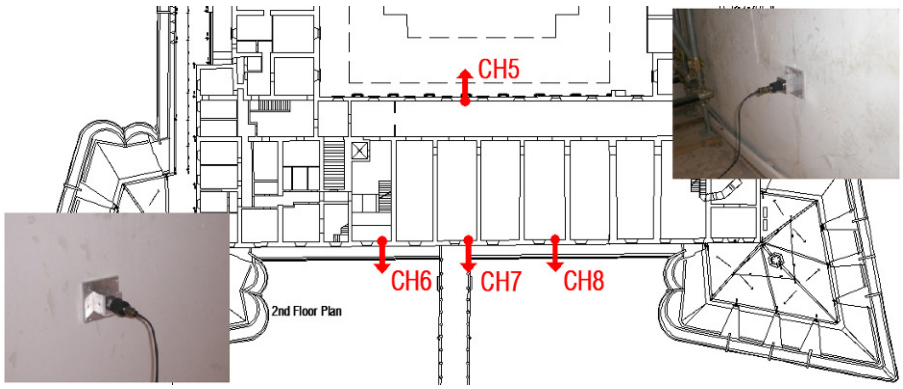

(c)

Figure 55 - (a) Location in plan of CH1 and CH2; (b) Location in plan of CH3 and CH4 and (c) Location in plan of CH5, CH6, CH7 and CH8 (Casarin, 2010)

The system allows fixed time interval recordings and trigger basis ones, the first are “long” acquisition, corresponding to 131’072 points, or 21’51’’ of recording, with a sampling interval of 100 Hz, each hour of the day; the second one is a “shorter” recorder of 3’35’’ at sampling frequency of 100Hz, that is triggered when determined thresholds, for each sensor, are crossed. Specifically, for channels 1 and 2, the trigger is at +/- 5E-3 m/s^2 and for the remaining is +/-2E-2 m/s^2.

When one of the sensors is triggered, the system records data 1’42’’ before the event (keeping 10 windows of 1024 points each, at a sampling of 100 Hz) and 1’42’’ after the values return to the signal range below the threshold.

4.2.4 Dynamic Identification

For the dynamic identification, the software used was ARTeMIS Extractor and the method selected was the Frequency Domain Decomposition, FDD.

When it comes to signal processing of the data series, it was applied a high-pass filter, the spectral density was 2048 points, with a 66.7% overlap and a decimation of 2.

Then were selected the peaks of the SVD, that could describe a mode, having in memory the previous dynamic identification, the phase angle and the coherence function. As said before, when the coherence value is closer to one the possibility of existing a mode there is bigger.

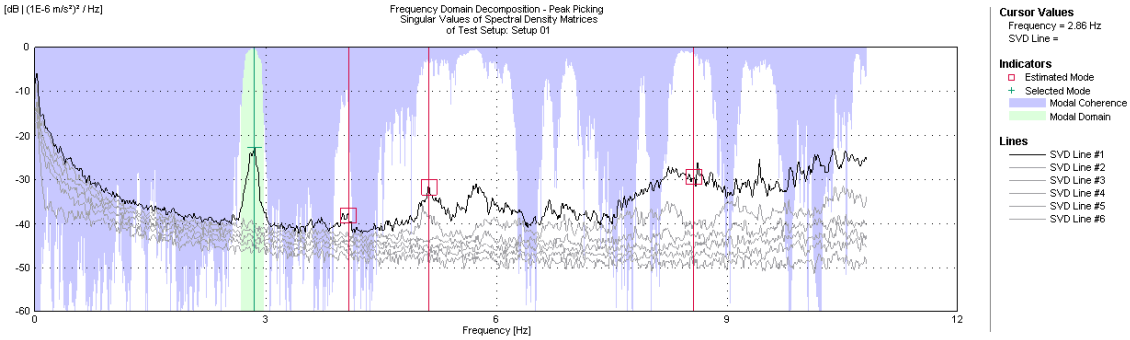

Figure 56 - FDD - Peak peeking

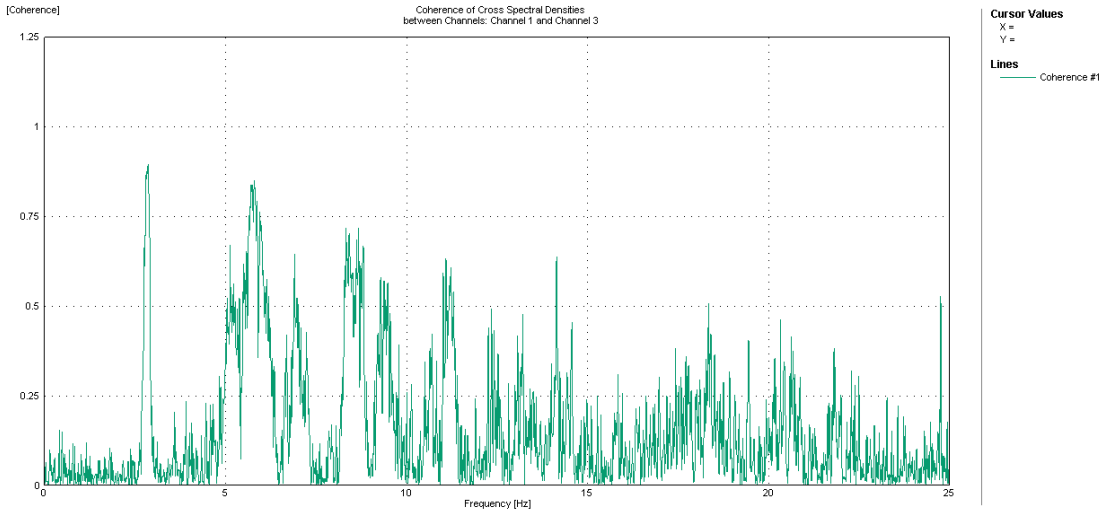

Figure 57 - Coherence function for a channel at the base (CH1) and the other on the first floor (CH3)

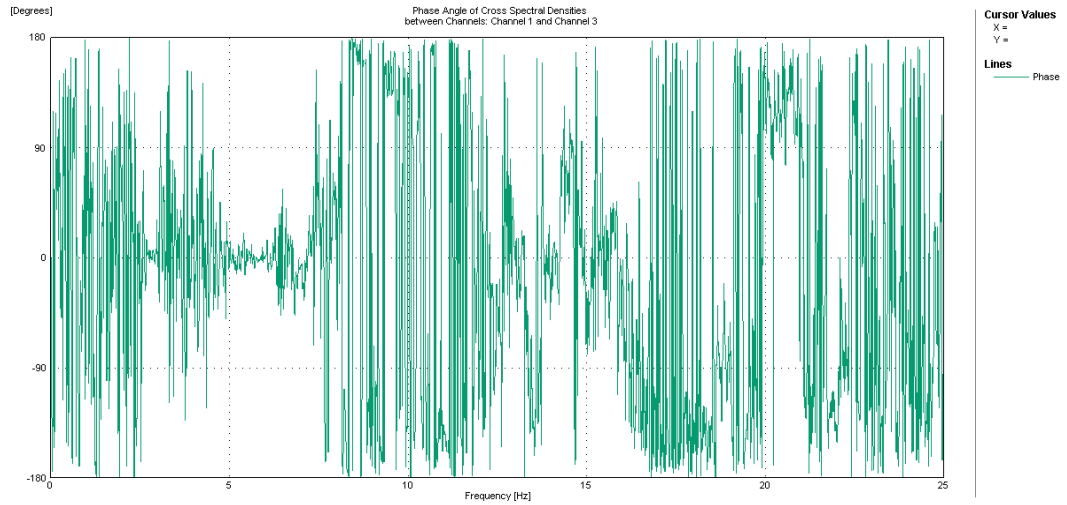

Figure 58 - Phase angle between CH1 and CH3

The frequencies were determined in two phases, resulting in the first, from 22/12/2010 to 08/04/2010, and second sets of data, from 11-04-2010 to 29-05-2010 (this data is presented in Annex II). All frequencies were determined for the first data set, but for the second due to the excessive time it takes to detect the two last modes and their low relation with the environmental effects, as seen in the next section, only the two first frequencies were determined. In Figure 59, the range of frequencies is presented for the four modes analysed, as seen, the frequencies seem to find a sinusoidal trend more clearly for the last two thirds of the events.

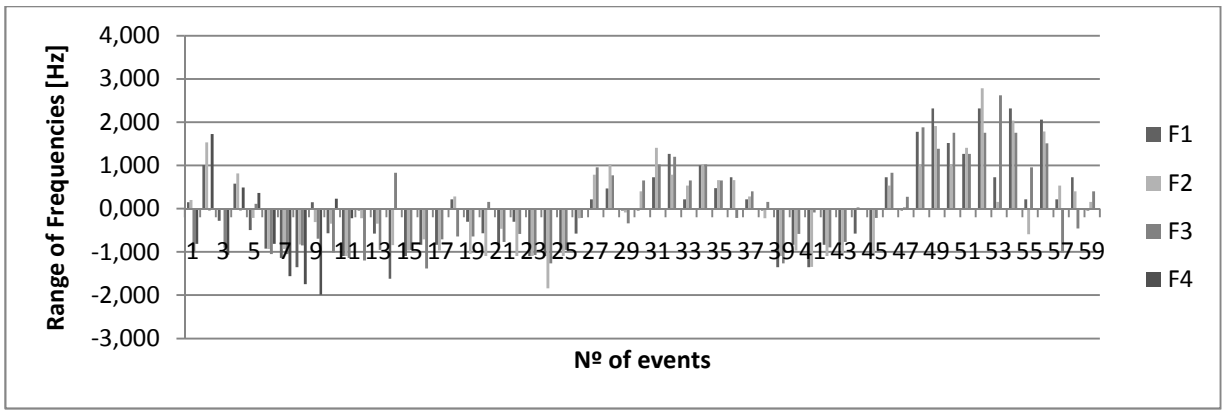

Figure 59 - Range of frequencies determined for the first set

The modal shapes detected for the each mode were:

- Mode 1 – all the nodes moving the same way, describing a out-of-plane bending movement, as seen in Figure **60**;

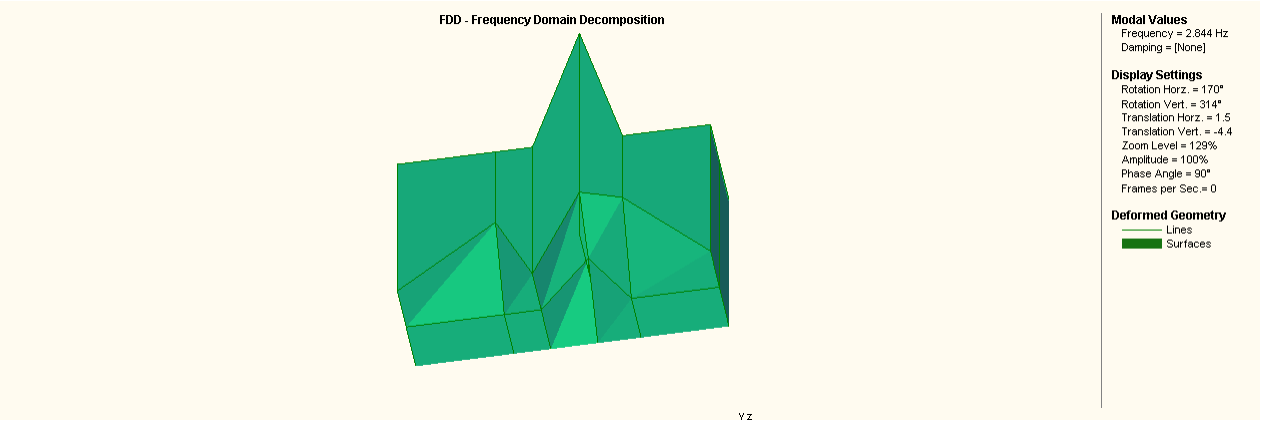

Figure 60 - Modal shape 1

- Mode 2 – describes a torsional mode, moving at the top three nodes in one way and the other node goes in the opposite way, as shown in Figure **61**;

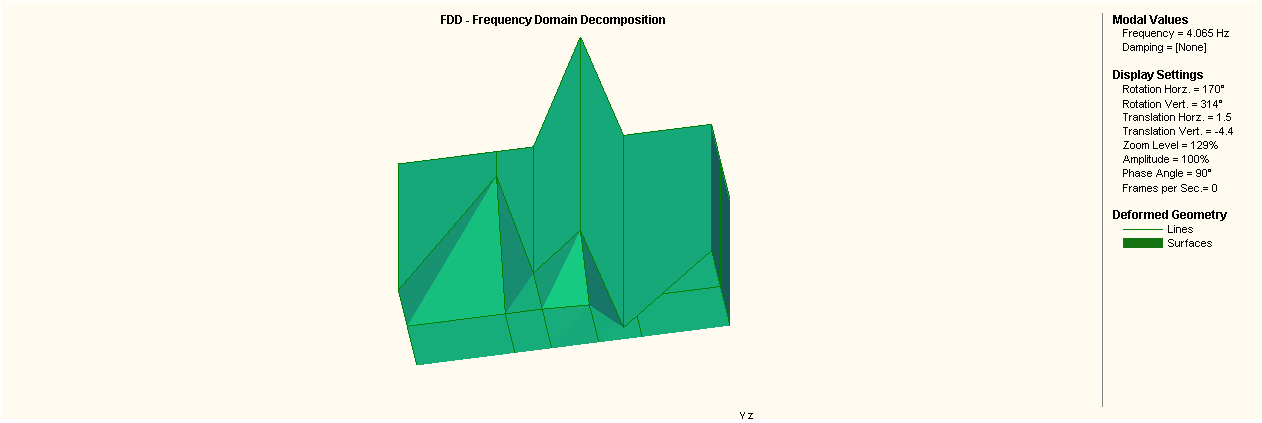

Figure 61 - Modal shape 2

- Mode 3 – is a out-of-plane bending movement, with the nodes in different faces of the wing going in opposite ways, as shown in Figure **62**;

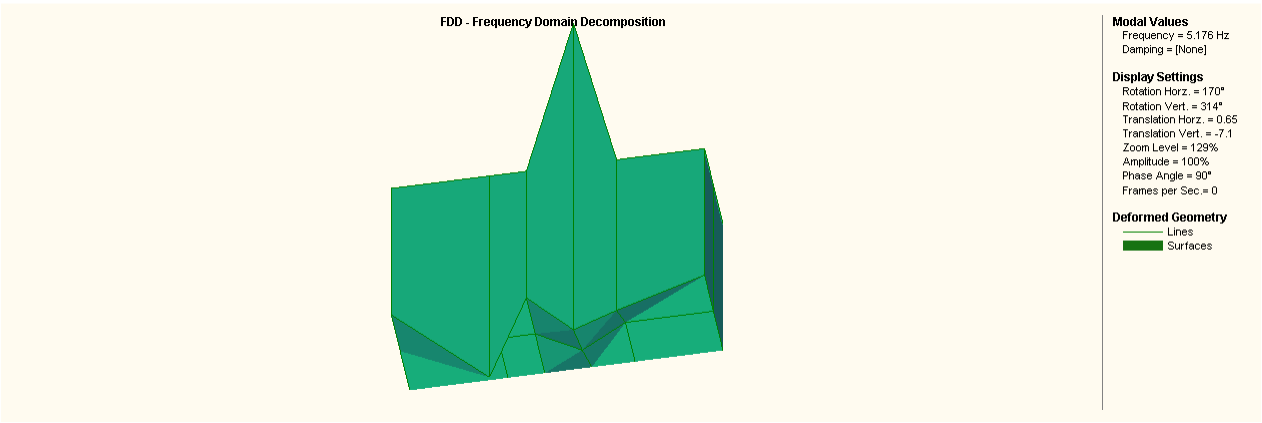

Figure 62 - Modal shape 3

- Mode 4 – represents a local mode of the top of the wall, facing the courtyard, as seen in Figure **63**

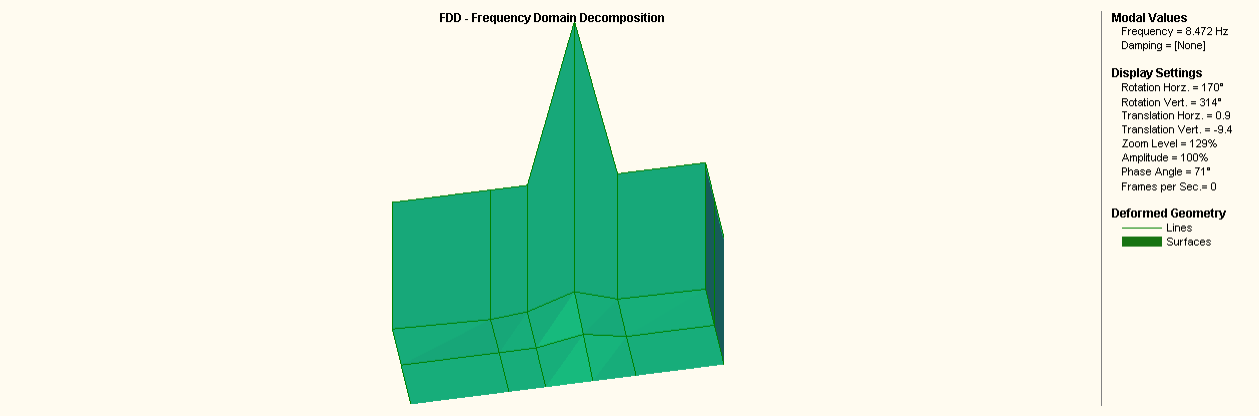

Figure 63 - Modal shape 4

A final comment regards the accuracy of the modes. The first mode was always very easy to detect, with a clear peak and high values of the coherence function, while the others are not so consistent, especially the fourth mode. In some cases, this last mode was not possible to detect. Due to this lack of quality, the next section is going to be developed mainly around the 1st mode.

4.2.5 Environmental and Loading Effects

As explained before, the dynamic response of the structure is mainly influenced by environmental actions and level of excitation. In this particular case, the two studied environmental effects are the temperature (T) and the relative humidity (RH). The level of excitation is going to be quantified by the mean of the Root Mean Square (RMS) of the two ground acceleration channels, by the expression:

$$RMS = \sqrt{\frac{1}{N}\sum_{i=1}^{N} x_i^2} \qquad (21)$$

It is important to stress that the temperature and relative humidity measurements belong to the monitoring sensors in San Marco church, which is not far from the fortress. It is reasonable to use this data because if there is any shift in the values of temperature and humidity, it applies to all the values, keeping the relative relation. The recordings are made every hour of the day, summing up 24 recordings per day.

Figure **64** and Figure **65** help to better understand the variations in time of the temperature and relative humidity. As can be seen the temperature is starting to increase, as expected, and a part of the cycle of temperatures is already represented. The relative humidity is following the opposite trend, decreasing its values from November to May. In the comparison day by day, is possible to observe that between the end of December and the end of February, the values of the temperature and of the relative humidity seem to vary in the same way, behaving in opposite ways the remaining time.

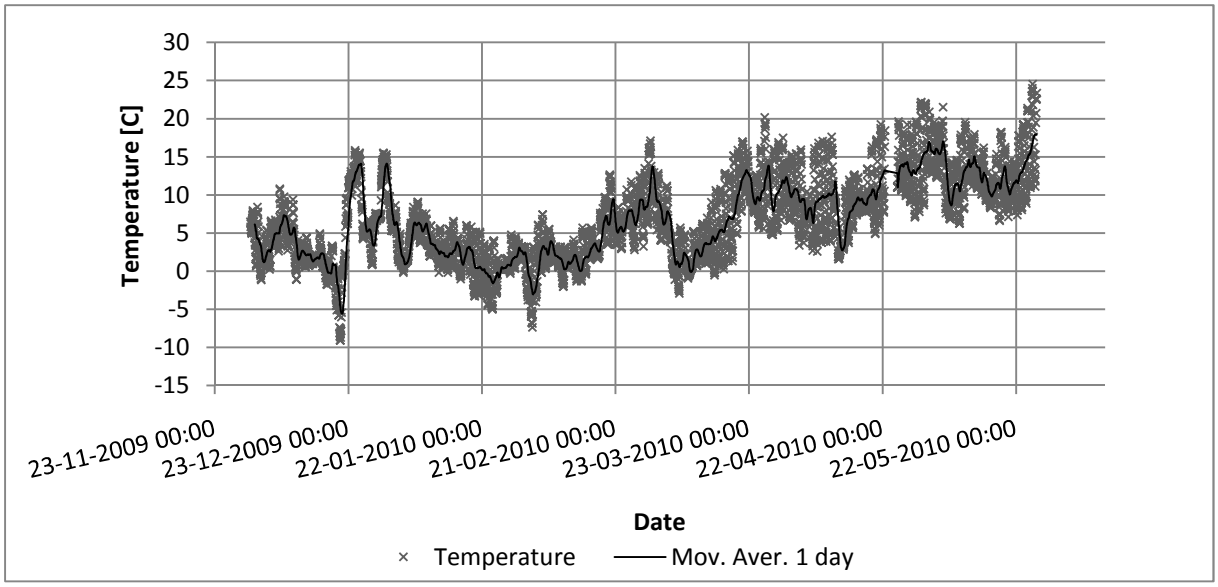

Figure 64 - Variation of temperature along time

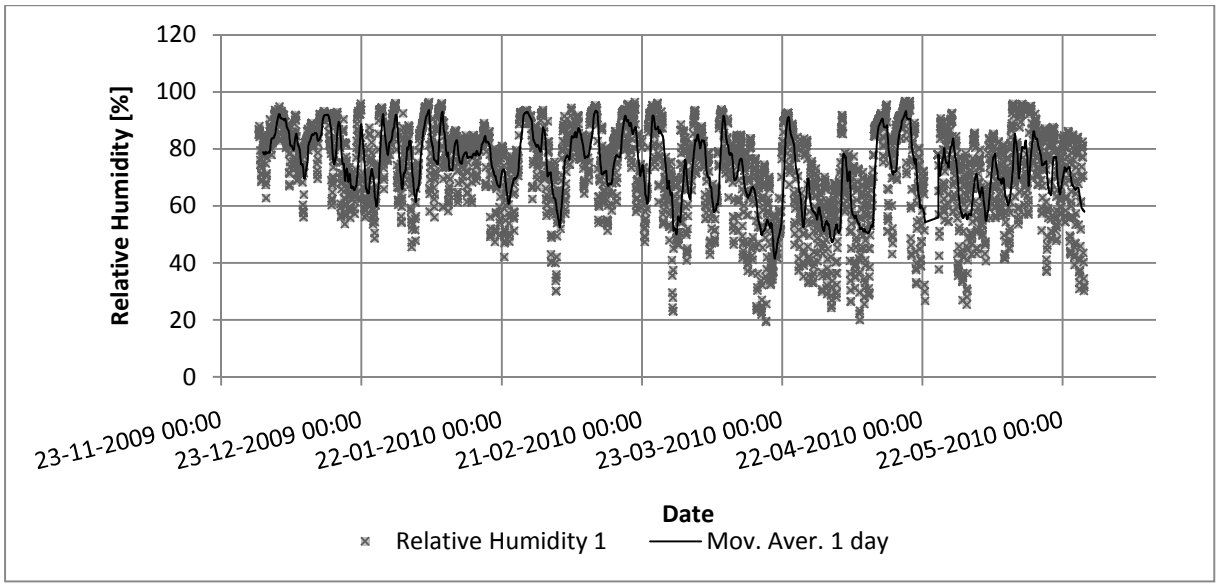

Figure 65 - Variation of relative humidity along time

A first modal identification and comparison with T and RH, was performed in the time interval of 21/12/2009 to 21/01/2010, every three days, if possible. So, the decision was to keep with “every three days” sampling interval, with two readings per day.

The data from 22/12/2010 to 08/04/2010 was the first to be available for analysis, so a preliminary statiscal analysis was performed, presenting the results showed in Table **8**.

Table 8 - Statistical results of Inputs and Outputs

	Inputs			Output			
	T	RH	RMS	ω1	ω2	ω3	ω4
	[°C]	[%]	[mg]	[Hz]	[Hz]	[Hz]	[Hz]
N	59.000	59.000	59.000	59.000	59.000	59.000	53.000
Mean	4.905	72.274	0.043	2.883	4.111	5.328	8.531
σ	4.336	13.352	0.007	0.047	0.098	0.198	0.161
Max	16.000	96.101	0.064	2.991	4.382	5.847	8.984
Min	-2.515	41.596	0.036	2.808	3.931	5.054	8.118

Temperature presents a mean value of 4.905°C, with values varying between -2.515°C to 16°C. The RH shows a mean value around 72%, but the range of values can go from 42% to 96%. RH also presents the highest standard deviation (σ), being more scattered than the other inputs. When it comes to the RMS the values vary from a minimum of 0.036mg to a maximum of 0.064mg, which are relatively low excitation levels and mean goes around 0.043mg.

As shown for the outputs, the dispersion is bigger for the modes 3 and 4, which is accompanied by the difficulty in detecting theses modes for some days, adds great uncertainty to their definition.

In order to establish possible relations between the modal frequencies and the different inputs, graphs were plotted along time and correlations were calculated, as shown in Table **9**. The graphs relative to the first frequency are presented here, the remaining can be found in Annex II

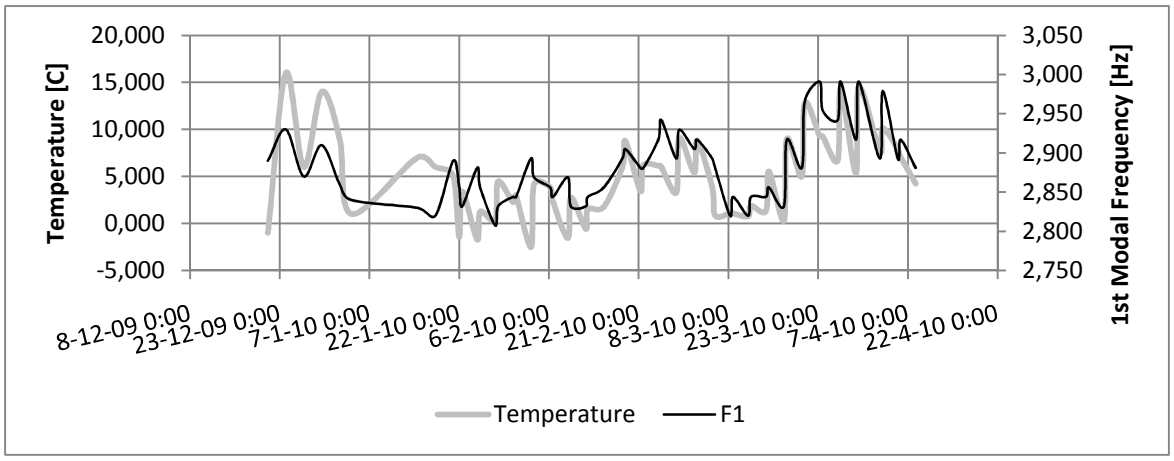

Figure 66 – Temperature effect on the first frequency

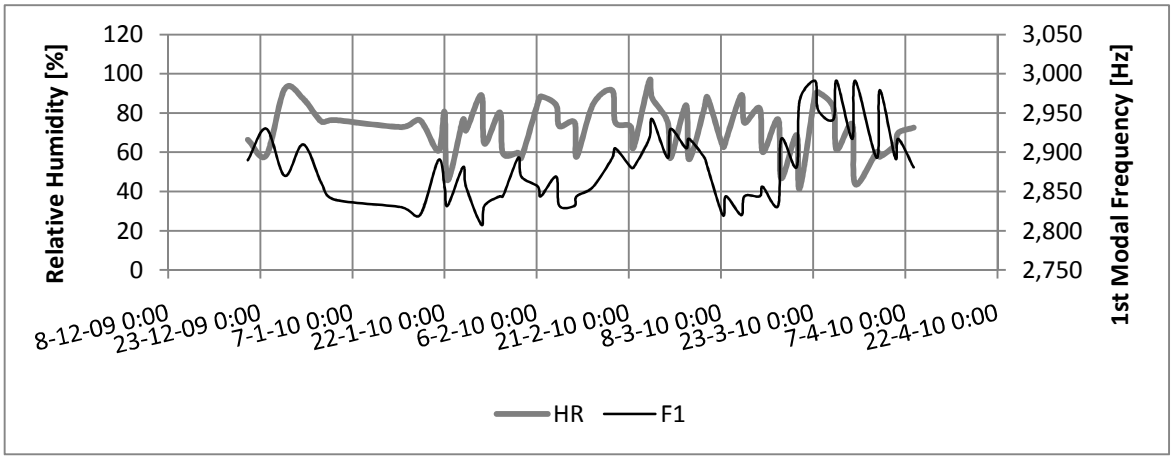

Figure 67 – Relative humidity effect on the first frequency

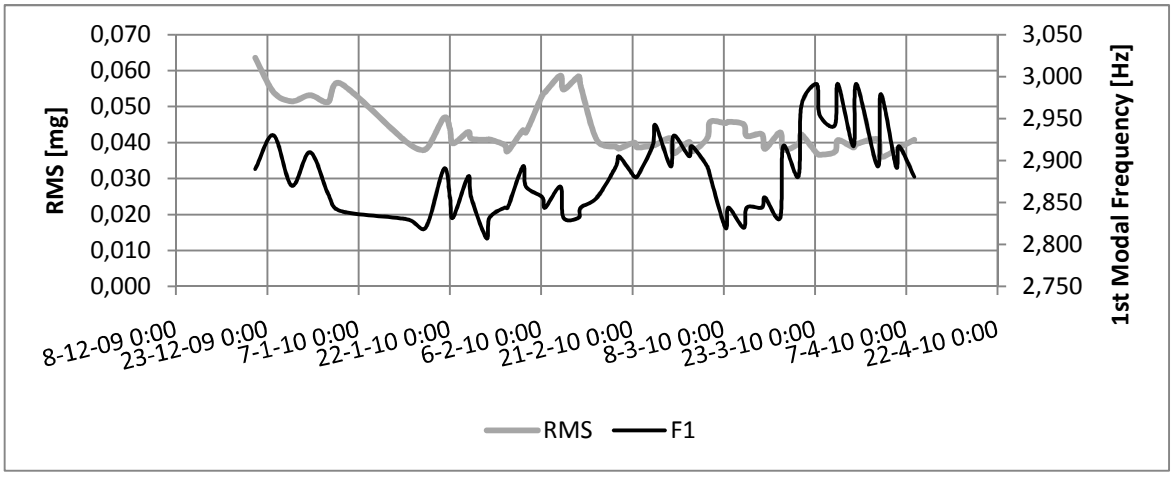

Figure 68 – RMS effect on the first frequency

Table 9 – Covariance, correlation and determination coefficients

T	Output frequencies			
	ω1	ω2	ω3	ω4
R_{xy}	0.14098	0.30637	0.50171	0.03298
r_{xy}	0.70881	0.73629	0.59402	0.04750
R^2	0.50241	0.54213	0.35286	0.00226
RH	**ω1**	**ω2**	**ω3**	**ω4**
R_{xy}	-0.11424	-0.13193	-0.00859	-0.08201
r_{xy}	-0.18653	-0.10297	-0.00330	-0.03803
R^2	0.03479	0.01060	0.00001	0.00145
RMS	**ω1**	**ω2**	**ω3**	**ω4**
R_{xy}	-0.00010	-0.00025	-0.00058	0.00019
r_{xy}	-0.32543	-0.38259	-0.44806	0.17212
R^2	0.10590	0.14637	0.20076	0.02962

As seen in Figure **66** and Table **9**, in general when the temperature increases the modal frequencies tend to increase also, being especially demonstrated in the first and second frequencies.

For values of relative humidity close to 100%, the modal frequencies tend to present lower values, but the correlation coefficient is low, if one considerer all the values of the RH (see Figure **67** and Table **9**).

The RMS presents lower correlation values, but higher than the relative humidity, which means some kind of relation not present in Figure **68**. There is a relation between the capability to detect modes and the values of RMS, not present in the graphs. With lower values of RMS, is much more difficult to detect the modes, since the structure is not very excited.

Since, some of the relations were not so clear, some graphs were plotted with Inputs vs. Frequency. Polynomial regressions were added to the graphs, stating if the values of the variables increase or decrease together. Again, the graphs relative to the environmental effects vs. first frequency are presented here and the remaining can be found in Annex II

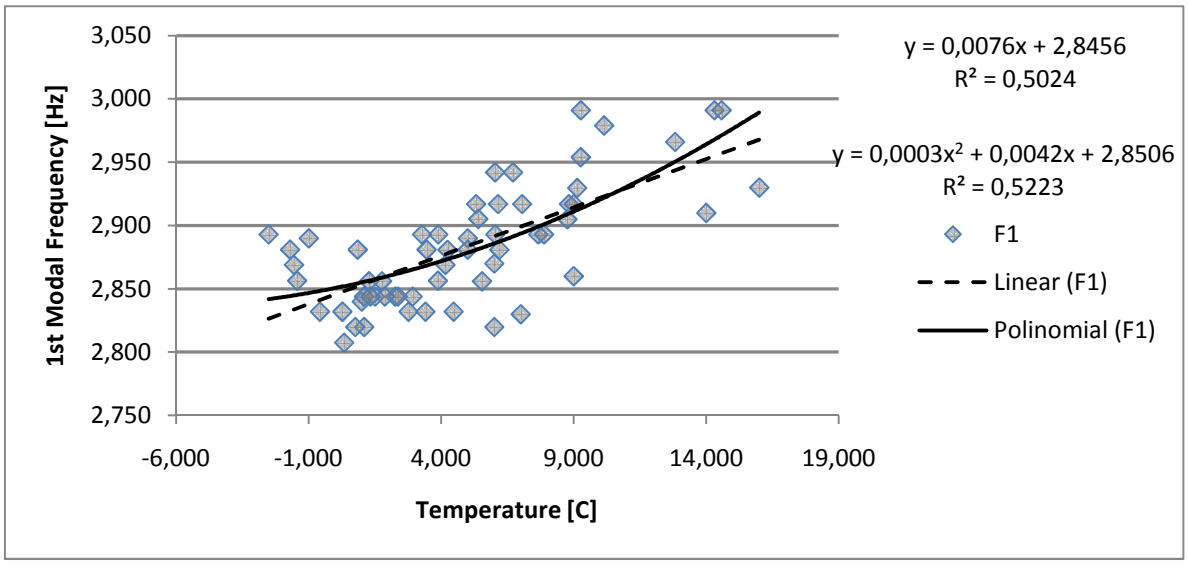

Figure 69 – Frequency 1 vs. Temperature

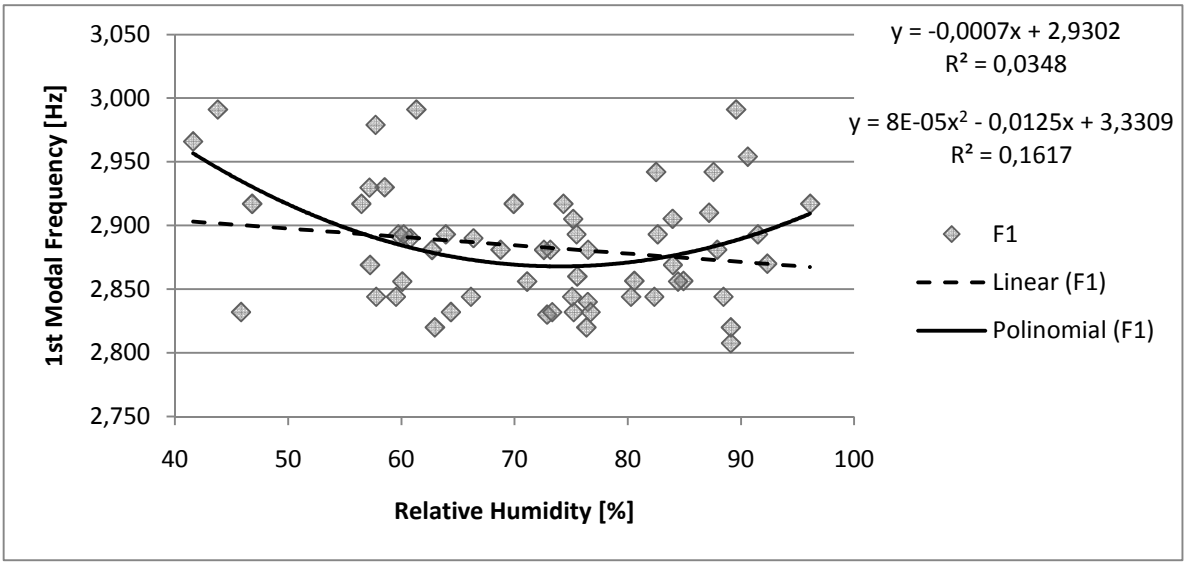

Figure 70 - Frequency 1 vs. Relative Humidity

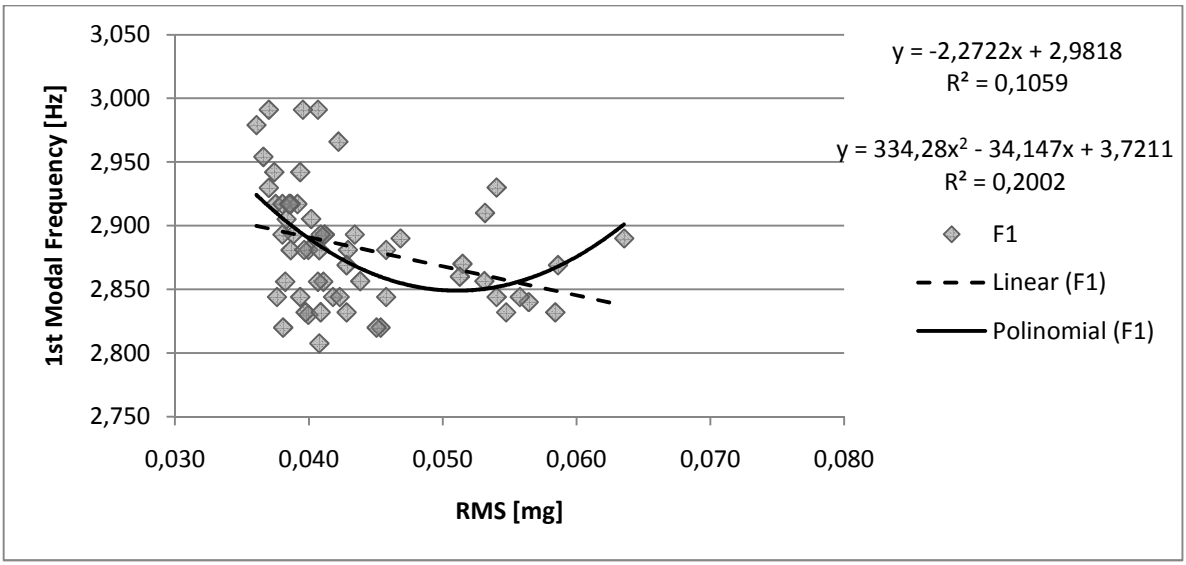

Figure 71 - Frequency 1 vs. RMS

From these to last graphs, Figure **69**, Figure **70** and Figure **71** is possible better evaluation of the relations between variables. So, frequency tends to increase with temperature, to decrease with relative humidity and RMS. These relations tend to be not so clear for the last two frequencies.

With temperature, materials expand and the structure acquires a stiffer configuration, increasing the frequencies, while for relative humidity, if the structure absorbs water, the mass changes increases and the frequencies decrease.

As said before, the minimum time interval necessary to correctly simulate and predict the relation between environmental effects, level of excitation and frequency is one year, so the following models are a “work in progress”, meaning they need to be improved with more data.

Another, time interval (from 11-04-2010 to 29-05-2010) was analysed, constituting a second set of data. To demonstrate, the procedure of simulation and prediction and the application of static and ARX models, twol cases were considered:

- Case 1 – the first set of data works as estimation data (simulation) and the second set as validation data (prediction), only applied to temperature and first modal frequency. Comparison with a new model using both sets;
- Case 2 – both sets are used for estimation, using linear regression and ARX models, considering the three inputs and first modal frequency.

4.2.5.1 Case1

This first case reflects only a static approach based on the model showed in Figure 69, where temperature and the first modal frequency are related. With a square correlation factor of 0.50, a linear correlation is obtained but with a quadratic polynomial the square factor increases to 0.52. The difference is not too big, but since the quadratic form is also simple, it was the chosen one to develop a model.

So, this model was determined using the first set of values from 22/12/2010 to 08/04/2010, from now one called Estimation data.

The next step is to calculate the response of the structure using the function of the model, in this situation:

$$\hat{y} = 0.0003x^2 + 0.0042x + 2.8506 \tag{22}$$

Where $\hat{y}$ is the estimated frequency and x is the temperature. After this step, the simulation error can be calculated, by subtracting the estimated frequency to the measured one. The final step for the simulation is establishing the 95% confidence interval for the simulation error, as shown in Figure **72**.

Using now the temperatures of the Validation data (the second set, from 11-04-2010 to 29-05-2010), the estimated frequencies are calculated applying function (**22**) and the residuals are calculated. They were plotted in Figure **72** to see how they behave relatively to the confidence intervals.

Observe that the model doesn’t respond already well to some points of the estimation data, since they are outside the confidence interval boundaries. For the validation data the situation is even worse, because a lot of the points especially the last ones are completely out of the interval.

In a normal situation, with a good model, let’s say with a correlation coefficient superior to 0,8, the present situation would mean that other input parameter is corrupting the response of the model. This

could be damage or for example the presence of another environmental effect, not take into account by the model. In this particular case, due to the initial low correlation coefficient, the reason is the bad quality of the model. Other aspect that can help to identify the quality of the model, is to analyse the simulation error and see if it's following a trend, which is clear in this case.

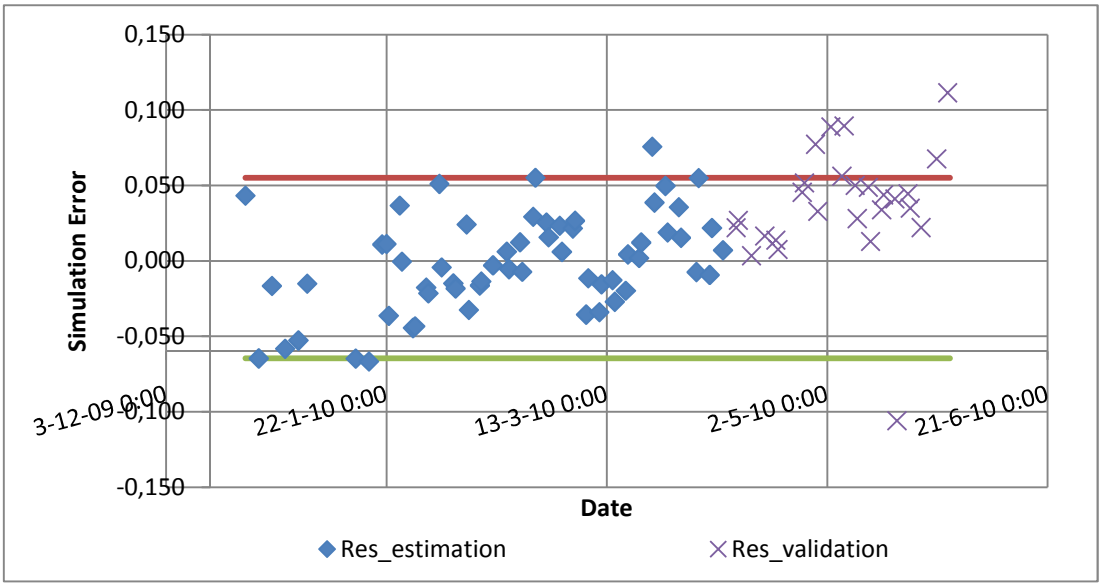

Figure 72 - Application of the validation data to the model

A first improvement and update is shown in Figure **73**, where both sets of data are used to determine the model. As one can see, the correlation factor increased from around 0.50 to 0.70, which was expected because the temperature is following the normal cycle and increasing value.

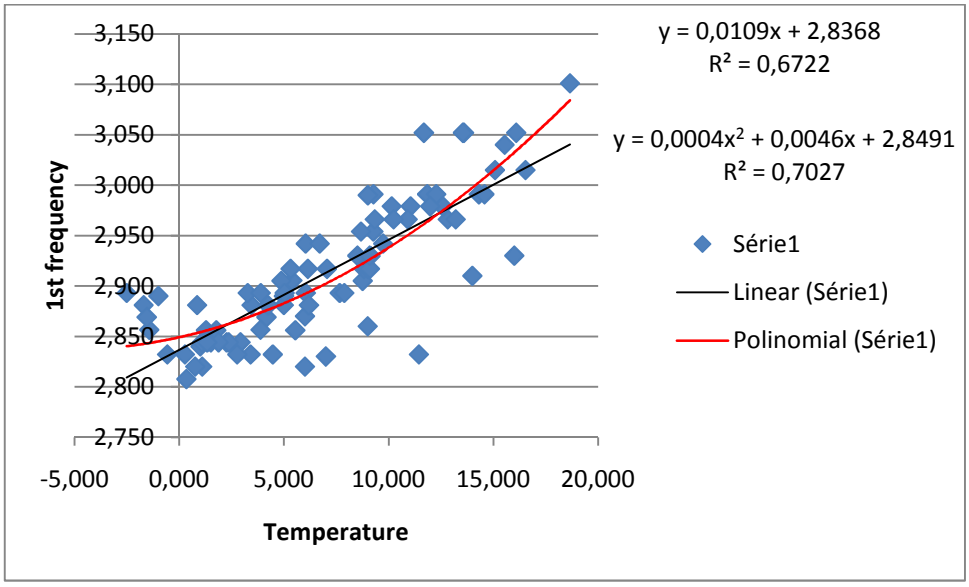

Figure 73 - Static models for the two sets of data

As done previously, the new simulation error was calculated considering a new quadratic expression, as well as the confidence interval. From Figure **74**, is possible to see that some points continue to be outside the boundaries of the confidence interval and the error still shows an approximated linear trend, meaning that the model in still not good enough. Although is clear that something happen in one of the second set frequencies, on 17/05/2010 at 20:00, since the value is really low and away from the crescent trend. Probably another environmental factor, besides temperature, affected the structure, since the frequencies determined later don't seem to be affected by it.

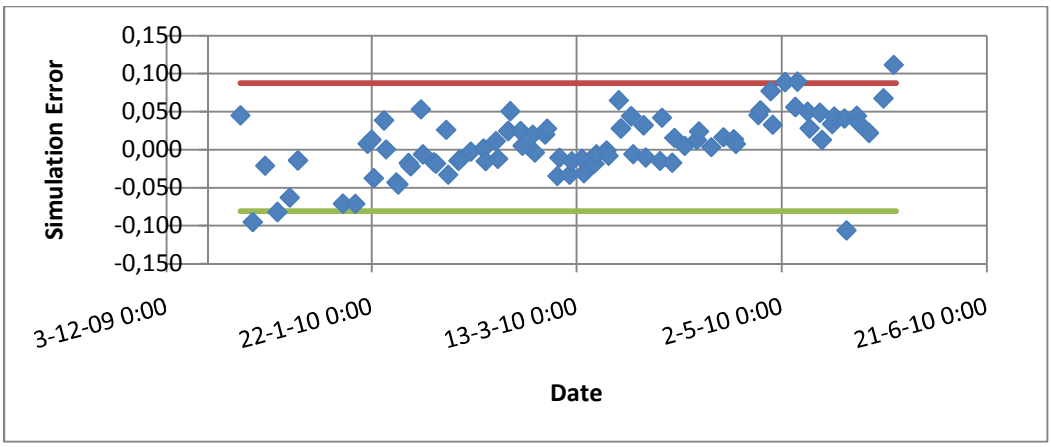

Figure 74 - Simulation error, considering the new quadratic model

4.2.5.2 Case 2

This case intends to show a possible approach, which is the ARX models, more than take real conclusions about the damage of the structure. Again, even using the two sets of data, as seen in the previous case, it's not enough to achieve a good model.

The procedure to implement is the one described in section 3.5.2., applied to a multi-input output-only set of data. To better understand the behaviour of the variables, the two sets of data are plotted together for each variable, as shown in Figure **75**. Now is very clear to see that frequency is increasing with temperature, which is starting to describe an annual cycle. The last values of the RMS are really high when compared to the average, meaning that some event increased the ground excitation those days. Table 10 presents the statistical parameters used to normalise all the variables, since is a procedure required by the first step of the sequence presented in section 3.5.2.

Table 10 - Statistical results of the variables

	Mean	Std
T	6.9291	5.0615
RH	72.7016	13.1669
RMS	0.0421	0.0080
ω1	2.9124	0.0674

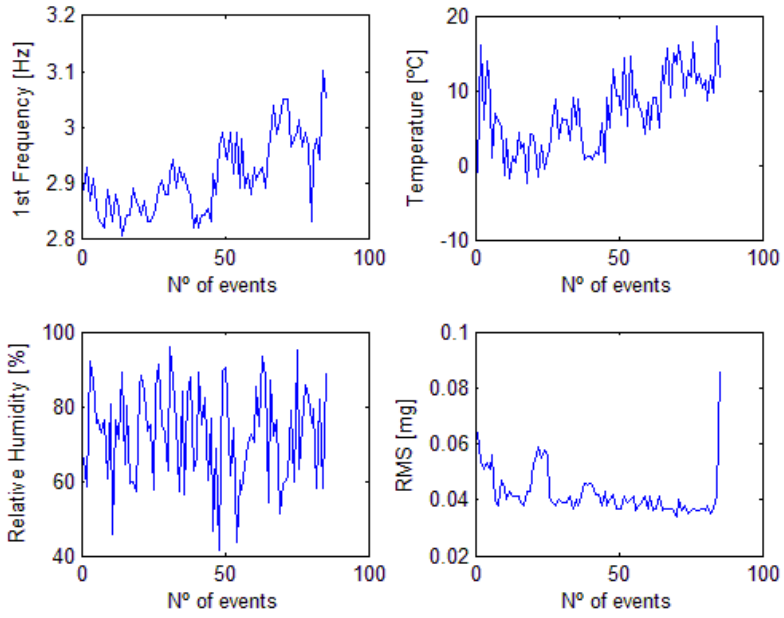

Figure 75 - Data of the two sets, regarding the first modal frequency, the temperature, the relative humidity and the RMS

To apply the ARX models, the software Matlab was used, since the arx function is already existent in the program. Since is multi-input model the coefficients are described by: one n_a (only one output), three n_b (three inputs) and three n_k (three inputs). They can be estimated with determined functions (like *delayest*) but the estimation only gives a starting point, and then trial and error can lead to the best model. Six different models were determined using the coefficients of Table **11**. The first one is a static model, since al the delays are zero.

Table 11 - Coefficients used in the different models

Models	na	nb_1	nb_2	nb_3	nk_1	nk_2	nk_3
ARX 1	0	1	1	1	0	0	0
ARX 2	0	1	1	1	0	12	0
ARX 3	5	2	3	5	0	12	0
ARX 4	5	10	3	5	0	12	0
ARX 5	5	10	7	8	0	24	1
ARX 6	5	11	7	8	0	24	1

By observing Table **12**, is possible to conclude that the best model is ARX 5, which presents the lower FPE and the highest correlation factor. ARX 1 and ARX 5 are plotted in Figure **76** and Figure **78**, respectively, accompanied by their simulation errors, Figure **77** and Figure **79**.

Table 12 - Statistical values calculated for six possible ARX models

Models	Std	R^2	V	FPE
ARX 1	0.5690	0.6763	0.3199	0.3425
ARX 2	0.5868	0.6700	0.1901	0.2035
ARX 3	0.4870	0.7658	0.1287	0.1742
ARX 4	0.4819	0.7749	0.1109	0.1710
ARX 5	0.4679	0.7964	0.0658	0.1123
ARX 6	0.4688	0.7961	0.0654	0.1130

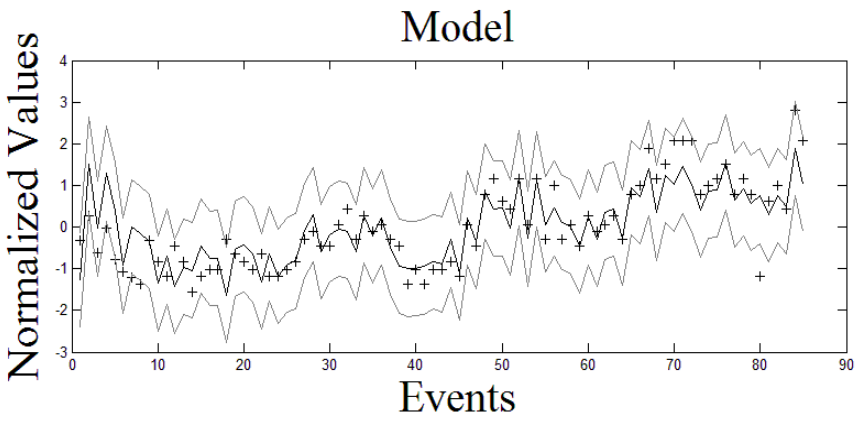

Figure 76 - ARX 1 model approximation with the respective confidence intervals

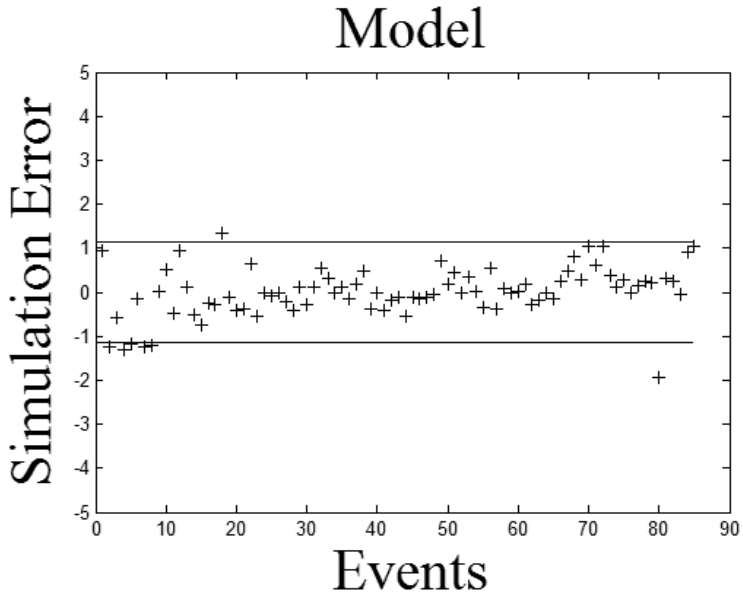

Figure 77 - Simulation residuals of ARX 1 model

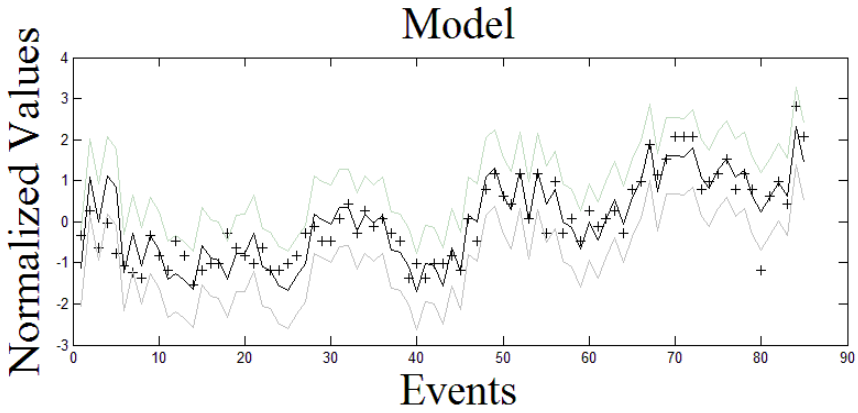

Figure 78 - ARX 5 model approximation with the respective confidence intervals

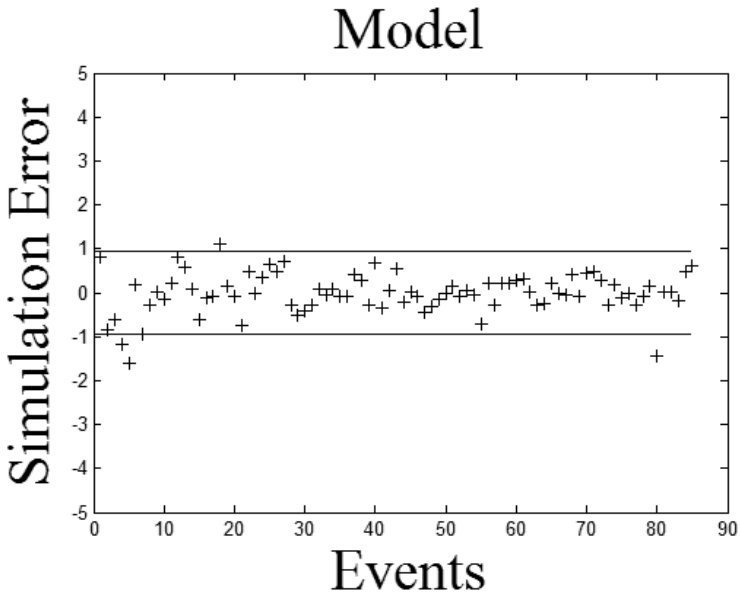

Figure 79 - Simulation residuals of ARX 5 model

ARX 1 presents a correlation factor around 0.68 and the ARX 5 presents a coefficient of 0.8, making them good approximations to the measured data. Theoretically, ARX 5 represents better the measured data and will behave better if validation data is introduced. Comparing the simulation error is possible to observe that the confidence interval of ARX 5 is narrower and fewer points are found outside its boundaries. Again the data of the day 17/05/2010 at 20:00, stands out, which can mean that other environmental factor, besides temperature, RH and RMS affected the frequencies of the structure. Since no shift in the modal frequency is recognizable, probably no damage is associated with this event.

4.2.6 Special Events

Other important aspect is to compare the modal frequencies detected with the monitoring with minor-tremors felt by the structure. The entire list of seismic events recorded by the Italian seismic network between 02/01/2010 and 30/04/2010 that could be relevant to the structure is in Annex II. From those, the events with magnitude superior to 2.5 and also some of the recordings with 2.2 in the district *Aquilano* were studied (see Table **13**).

Table **13** contains the RMS and the PGA for each minor tremor, being the biggest five pointed out. For this last group was determined the acceleration response spectrum for Channel1 (using a spreadsheet of Excel with the Duhamel's integral) and then all were compared with the spectrum recommended by the EC8.

Table 13 - Principal minor seismic events and respective characteristics

Date	Time (UTC)	Mag	Seismic District	RMS (m/s2)			PGA	
				CH1	CH2	Mean	CH1	CH2
22-01-2010	12:30:50	3.4	Valle dell'Aterno	0.002248	0.001462	0.001855	0.0058	0.0032
23-01-2010	13:11:07	2.8	Valle dell'Aterno	0.001073	0.000902	0.000988	0.0021	0.0011
26-01-2010	10:19:29	2.2	Aquilano	0.000111	0.000718	0.000415	0.0001	0.0001
30-01-2010	06:28:45	2.6	Valle dell'Aterno	0.000362	0.000717	0.000540	0.0009	0.0007
31-01-2010	21:21:30	3.2	Velino-Sirente	0.002194	0.001639	0.001917	0.0066	0.0042
16-02-2010	16:25:19	2.9	Gran Sasso	0.000754	0.000920	0.000837	0.0013	0.0012
18-02-2010	08:40:29	2.8	Valle dell'Aterno	0.001331	0.001550	0.001441	0.0032	0.0020
08-03-2010	23:32:11	2.7	Aquilano	0.003646	0.003363	0.003505	0.0091	0.0126
10-03-2010	23:56:26	2.7	Gran Sasso	0.000413	0.000785	0.000599	0.0008	0.0007
16-03-2010	05:51:43	2.7	Aquilano	0.002485	0.001520	0.002003	0.0081	0.0033
20-03-2010	01:17:19	2.5	Aquilano	0.001613	0.001665	0.001639	0.0049	0.0062
03-04-2010	21:11:58	2.2	Aquilano	0.000842	0.000898	0.000870	0.0020	0.0016

As visible in Figure 80, the peaks of the micro tremors are located in the horizontal branch of the EC8 spectrum, between 0.055s and 0.155s. Transforming the modal frequencies into periods, the values for each mode are: T1 = 0.347s; T2 = 0.243s; T3 = 0.188s and finally T4 = 0.117s. Only the fourth mode falls in the range of the minor tremors, which can cause damage in the last floor. This part of the exterior wall collapsed during the 6th April earthquake, due to an out-of-plane mechanism, which describes the fourth mode shape. All the periods, with the exception of the first, are in the interval of 0.05s to 0.25s, which comprehends the horizontal branch of the EC8 spectrum.

Finally, when comparing the frequencies of the minor-tremors with the models previous determined, these events seem to have no impact in the structure.

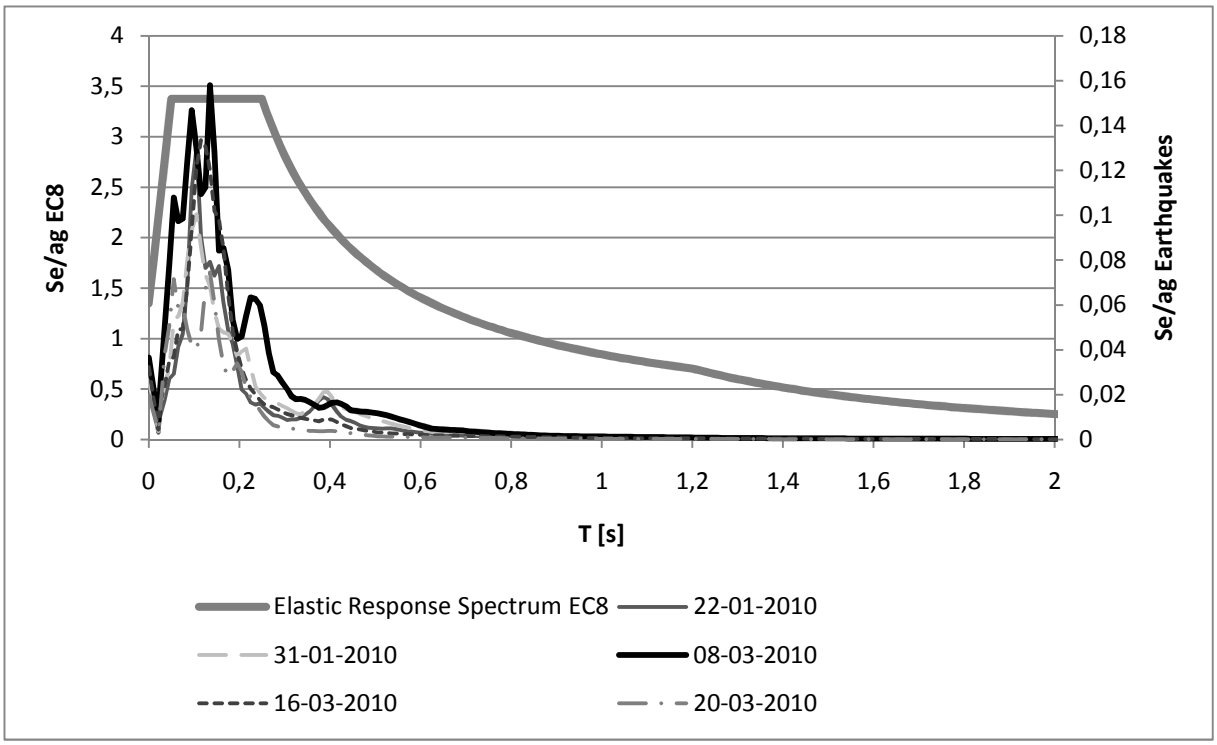

Figure 80 - Micro-tremors and the Elastic Response Spectrum EC8

5. CONCLUSIONS AND FUTURE WORKS

First let's have a particular look over each study case and then general conclusions are presented.

5.1 Case Study 1

In the case of San Domenico church, the FEM model created seems to reproduce the expected behaviour of such a structure when performed a static linear elastic analysis, considering only the self-weight and natural frequencies analysis.

The values of stresses and modal frequencies point out a stiff structure, with a range of principal stresses from 3MPa to -0.670MPa and values of the first four modal frequencies from 2.71Hz to 3.8Hz. These are a direct result of all the considerations and assumptions taken when constructing the model and attributing properties. Since any experimental campaigns were carried out till now, the values assumed were based in regulations, previous experiences with similar structures and "good sense".

All the information gathered before building the model, had a positive impact in the results. Since the model is based on hypothesis, the empirical information coming for historical background, damage mapping, detection of mechanisms and visual inspection brings the opportunity of validating some of the assumptions.

The determination of modal frequencies and shapes was the most important step of this case study, because they constitute the base to start designing possible monitoring programs. Regarding this, a preliminary proposal for the location of the sensors was proposed, as for the duration of the recording and expected range of frequencies and modal shapes, achieving the objectives proposed initially.

5.2 Case Study II

Regarding the monitoring phases, the Spanish fortress is in the third, for a period of 7 months, not yet describing one year (the minimum required for starting evaluating the behaviour of the structure). This fact had a great impact on the approach to the case study.

The first thing to do was to detect the modal frequencies and here the difficulty was high, since only the first mode was presenting itself clearly. The second and third mode, in some cases presented a good coherence but what really helped their detection was the visualization of the modal shape and phase angle. The last mode is uncertain in most of the cases and also, only the observation of the modal shape enabled its determination. These characteristics made the determination of the modes, very time consuming.

In any case, the modal frequencies detected are around: 2.883Hz, 4.111Hz, 5.328Hz and finally 8.531Hz.

This lack of quality of especially, the three last modes had also impact in the following procedure which would be the filtering the frequencies of the environmental and loading effects.

Low accuracy of the data conjugated with a small time interval made the establishment of reasonable correlations between data very difficult and not realistic. So, this confined the study of the environmental effects to the first modal frequency. The objective was to apply and show the possibilities that filtering the data from environmental and loading influence can bring for damage detection and especially in structures already severely damage, the progression of damage. This was accomplished successfully with the implementation of polynomial regressions and ARX models to two sets of data.

Temperature showed a good correlation with frequency, since when temperature increases, frequency also increases. For the relative humidity and the RMS, more data is necessary to evaluate the relation with frequency.

With the polynomial regression the steps to simulate and predict the behaviour of the structure were showed and what to consider to detect damage was also explained.

ARX models are more appropriate to describe frequency influenced by temperature because allow the consideration of thermal insulation. But also with other variables, the impact is positive since this type of models considers the previous states of the structure to calculate its behaviour at a determined time, which is closer to reality.

5.3 General

This thesis showed the enormous potential of monitoring to study and to assess structures and pointed out the importance of developing each of its stages: pre- and post-processing.

The pre-processing phase by giving some information prior to the installation of system, is contributing to improve its results, accuracy and reduce cost. Gathering as much information as possible about the structure and creating a FEM model is going without any doubt, not only improve the monitoring design, but also create a starting point to structural analysis and starting a cycle of calibration of the model.

The post-processing phase has enormous potential in damage detection, as seen previously, but has the disadvantage of needing long time spans for the models accurately recreate the behaviour of the structure. Nevertheless, filtering the environmental and frequency effect of the frequency is uncovering most of the times the presence of damage, allowing a faster intervention on the structure.

To conclude, the work of this thesis is a “work in progress”, since both study cases have the opportunity of being improved and more than just analysing two structures, what to retain are the procedures involved.

5.4 Future Works

As said before, both case studies can be improved and actions can be developed in order to create more information.

For Case 1, the main recommendations are start experimental campaigns, which allow determining with more accuracy some of the data necessary to build the model, material properties and boundary conditions. For example, flat jack tests and the double one, to evaluate the stress level and the E of the masonry, dynamic test to get empirical frequency data and conjugate it with the model, to come up with a better monitoring program, radar and sonic tests, etc.

Regarding, Case 2, definitely more data is necessary to improve the models. For the modal, identification other methods can be used besides the FDD to determine some of the hardest modes and also a parameter measuring the accuracy of the frequency should be added to the data to eliminate uncertainties.

By now, relative humidity didn't prove to have a big impact on the results, so in long term, the necessity of this variable should be evaluated. Maybe, data about wind velocity can be more interesting for the structure.

Especially, the last case study needs to be constantly being updated and improved to get to the point of possibility of damage detection.

6. REFERENCES

Barbat, A.H., Yépez, F., Canas, J.A, Damage scenarios simulation for seismic risk assessment in urban zones, Earthquake Spectra 1996; 12(3): 371-394.

Albini, P., Ambraseys, N.N., Historical data on earthquakes and active faulting. The contribution of IRRS and IC to EC progect Faust, Kick-off meeting, Bergamo, 15-16 January 1998.

Baptista, M.A.; Mendes, P.; Afilhado, A.; Agostinho, L.; Lagomarsino, S.; and Victor, L.M. (2004): Ambient Vibration Testing at N. Sra. do Carmo Church, Preliminary Results, Proceedings of the Fourth International Seminar on Structural analysis of Historical Constructions, Padova, Italy, Vol. 1, pp. 483-488

Basili, R., et al., Rilievi geologici nell'area epicentrale della sequenza sismica dell'Aquilano del 6 aprile 2009, Quaderni di Geofisica 2009, 70, INGV.

Belletti, B., Prime considerazioni sugli effetti del terremoto sulle strutture in muratura in alcune località dell'Aquilano, Ingegneria Sismica 2009.

Binda, L.; and Saisi, A. (2001): Non Destructive Testing Applied to Historic Buildings: The Case of Some Sicilian Churches, Proceedings of the 3rd International Seminar of Historical Constructions, Guimarães, Portugal, University of Minho, pp. 29-46

Borzi, B., Crowley, H., Colombi, M., Faravelli, M., Onida, M., Lopez, M., Polli, D., Meroni, F., Pinho, R., A comparison of seismic risk maps for Italy, Bulletin of Earthquake Engineering 2008.

Boschi, E., Favalli, P., Frugoni, F., Scalera, G., Smriglio, G., MACROZONAZIONE SISMICA DEL TERRITORIO ITALIANO, Mappa della massima intensità sismica risentita in Italia, INGV 1995.

Brincker, R.; Zhang, L.; and Andresen, P. (2000): Modal Identification from Ambient Responses using Frequency Domain Decomposition, Proceedings of the 18th Internation Seminar on Modal Analysis, San Antonio, Texas, 7-10 February

Caetano, E. (1992): Identificação Experimental de Parâmetros Dinâmicos em Sistemas Estruturais, Master Thesis, Engineering Faculty of University of Porto, Portugal

Casarin, F.; and Modena, C. (2007): Dynamic Identification of S. Maria Assunta Cathedral, Reggio Emilia, Italy, Proceedings of the 2nd Int. Operational Modal Analysis Conference, Copenhagen, Denmark, April 30 - May 2, 2007, pp. 637-644

Chopra, A.K. (2001): Dynamics of Structures, Theory and Applications to Earthquake Engineering, Second Edition, Prentice Hall

Clough, R.W.; and Penzien, J. (1993): Dynamics of Structures, Second Edition, McGraw- Hill international Editions

Costantini, E.A.C., Urbano, F., L'Abate, G., Soil regions of Italy, http://www.soilmaps.it/.

Di Capua, G., et al., Preliminary report on the seismological and geotechnical aspects of the april 6 2009 L'Aquila earthquake in central Italy, Geo-Engineering extreme events reconnaissance, 2009.

Dimitrov, D.S., Geophysical Journal International, Juill 2004. Istituto Nazinale di Geofisica e Vulcanologia, INGV, http://www.ingv.it/.

Ewins, D.J. (2000): Modal Testing, Theory, Practice and Aplication, Second Edition, Research Studies Press LTD, Baldock, Hertfordshire, England

Genovese, F.; and Vestroni, V. (1998): Identification of Dynamic Characteristics of Masonry Building, Proceedings of European Conference on Earthquake Engineering, Paris, France

Gentile, C.; and Saisi, A. (2004): Dynamic-based F.E. Model Updating to Evaluate Damage in Masonry Towers, Proceedings of the 4th International Seminar on Structural analysis of Historical Constructions, Padova, Italy, Vol. 1, pp. 439-449

Kouskouna, V., Makropoulos, K., Historical earthquake investigations in Greece, Department of Geophysics and Geothermics, National and Kapodistrian University of Athens, Greece 2004.

Ljung, L. (1999): System Identification: Theory for the User, Second edition, Prentice Hall, Upper Saddle River, NJ, USA

Lourenço, P.B.; and Krakowiak, K.J. (2003): Avaliação da estabilidade das abóbadas da Igreja do Mosteiro dos Jerónimos, Report 03-DEC/E-02, University of Minho

Lourenço, P.B.; Krakowiak, K.J.; Fernandes, F.M.; and Ramos, L.F. (2007): Failure analysis of Monastery of Jerónimos, Lisbon: How to learn from sophisticated numerical models?, Engineering Failure Analysis, 14(2), pp. 280-300

Lynch, J.P.; Law, K.H.; Kiremidjian, A.S.; Kenny, T.; and Carryer, E. (2002): A Wireless Modular Monitoring System For Civil Structures, Proceedings of IMAC XX, the 20th International Modal Analysis Conference, Los Angeles, CA, USA

Maia, N.M.; and Silva, J.M. (1997): Theoretical and Experimental Modal Analysis, Research Studies Press LTD, England

Modena, C.; Franchetti, P.; Zonta, D.; Menga, R.; Pizzigalli, E.; Ravasio, F.; Muti, M.; Meloni, R.; and Bordone, G. (2001): Static and Dynamic Analyses of "Maniace Castle" in Siracusa-Sicily, Proceedings of the 3rd International Seminar on Historical Constructions, Guimarães, Portugal, pp. 933-942

Miyamoto, K., et al., L'Aquila Italy earthquake, April 6, 2009, Earthquake field investigation report, 2009.

Oliveira, D.V.; Ramos, L.F.; Lourenço, P.B.; and Roque, J. (2005): Structural monitoring of the Monastery of Jerónimos, Proceeding of the International Conference on the 250th Anniversary of the 1755 Lisbon Earthquake, Lisbon, p. 466-473

Peeters, B. (2000): System Identification and Damage Detection in Civil Engineering, PhD Thesis, Catholic University of Leuven, Belgium

Ramos, L. (2000): Damage Identification on Masonry Structures Based on Vibration Signatures, PhD Thesis, Universidade do Minho, Portugal

Ramos, L.F.; Casarin, F.; Algeri, C.; Lourenço, P.B.; and Modena, C. (2006): Investigations Techniques Carried out on the Qutb Minar, New Delhi, India, Proceedings of the 5th International Conference of Structural Analysis of Historical Constructions, New Delhi, November 6-8, 2006, Vol. 1, pp. 633-640

Rovida. A. Et al (2009): Historical earthquakes in the area affected by the April 2009 seismic sequence. INGV, 2009

Slejko, D., Peruzza, L., Rebez, A., Seismic hazard maps in Italy, Trieste, 1998.

SVS (2006): ARTeMIS Extractor Pro User Manual, Release 3.5, Structural Vibration Solutions, Aalborg, Denmark

Valensise G., Alcune considerazioni sulla sismotettonica del terremoto del 6 aprile. INGV Internal

Welch, P.D. (1967): The use of Fast Fourier Transform for the Estimation of Power Spectra: a Method based on Time Averaging over short Modified Peridograms, IEEE Transaction on Audio and Electro-Acoustics, AU-15(2)

Il problema sismico in Italia, Dipartimento di protezione civile, http://www.protezionecivile.it/, 2008.

http://www.comune.laquila.it/

http://www.emsc-csem.org/index

http://cnt.rm.ingv.it/earthquakes_list.php?year=2009&month=04&ml_selection=3

http://itaca.mi.ingv.it/ItacaNet/

http://www.soilmaps.it/en/home.html

http://www.mi.ingv.it/#

http://zonesismiche.mi.ingv.it/

http://zonesismiche.mi.ingv.it/documenti/Pericolo_aq_090416.pdf

http://esse1.mi.ingv.it/

http://cnt.rm.ingv.it/earthquakes_list.php?year=2010&month=06&ml_selection=1

ANNEX I

AI.1 – Damage maps from Study Case 1

- Plan
- Detail A
- Section
- Elevation S-E
- Elevation S-W

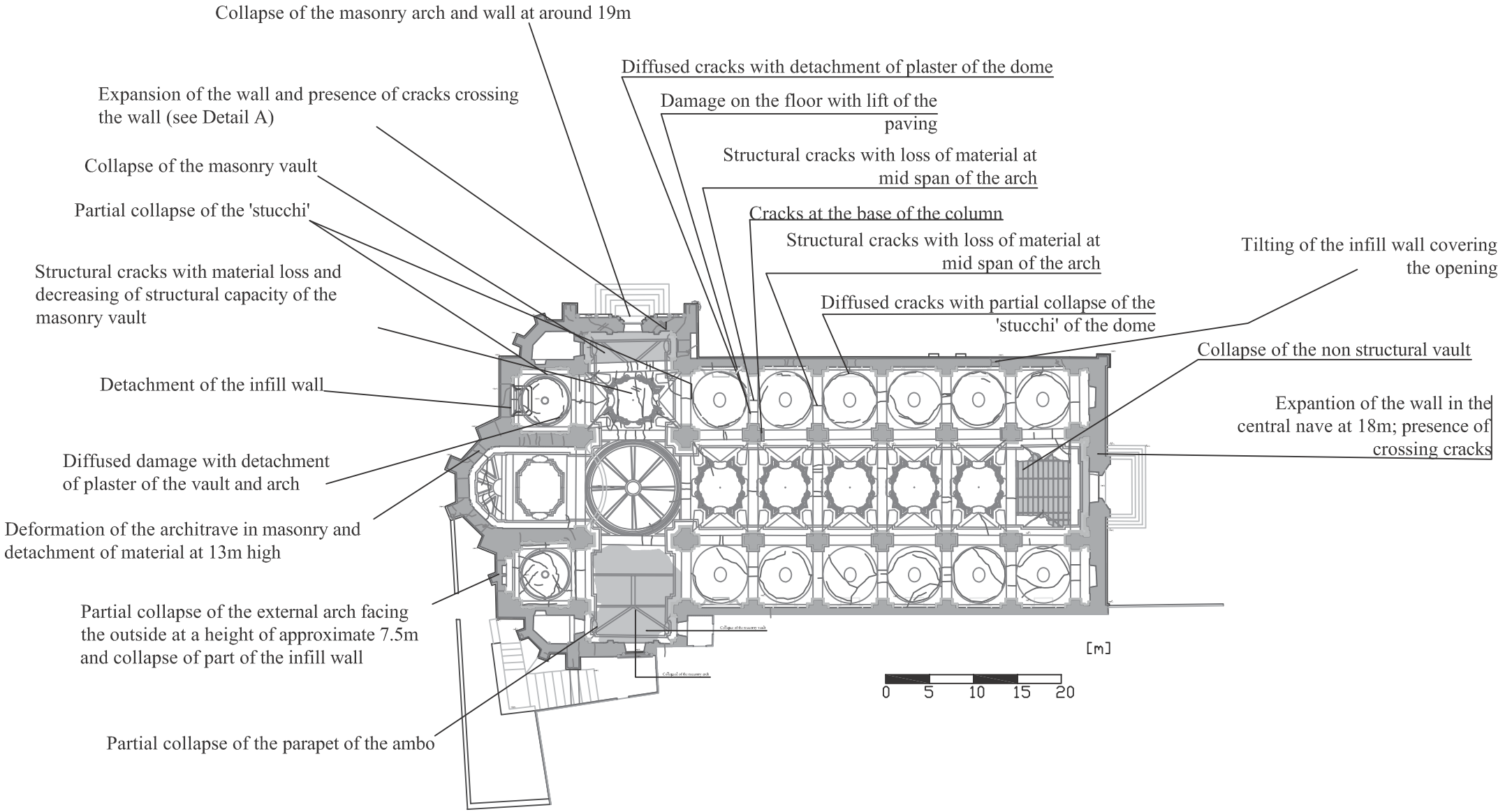
Collapse of the masonry arch and wall at around 19m
Diffused cracks with detachment of plaster of the dome
Expansion of the wall and presence of cracks crossing the wall (see Detail A)
Damage on the floor with lift of the paving
Collapse of the masonry vault
Structural cracks with loss of material at mid span of the arch
Partial collapse of the 'stucchi'
Cracks at the base of the column
Structural cracks with loss of material at mid span of the arch
Tilting of the infill wall covering the opening
Structural cracks with material loss and decreasing of structural capacity of the masonry vault
Diffused cracks with partial collapse of the 'stucchi' of the dome
Collapse of the non structural vault
Detachment of the infill wall
Expantion of the wall in the central nave at 18m; presence of crossing cracks
Diffused damage with detachment of plaster of the vault and arch
Deformation of the architrave in masonry and detachment of material at 13m high
Partial collapse of the external arch facing the outside at a height of approximate 7.5m and collapse of part of the infill wall
[m]
0 5 10 15 20
Partial collapse of the parapet of the ambo

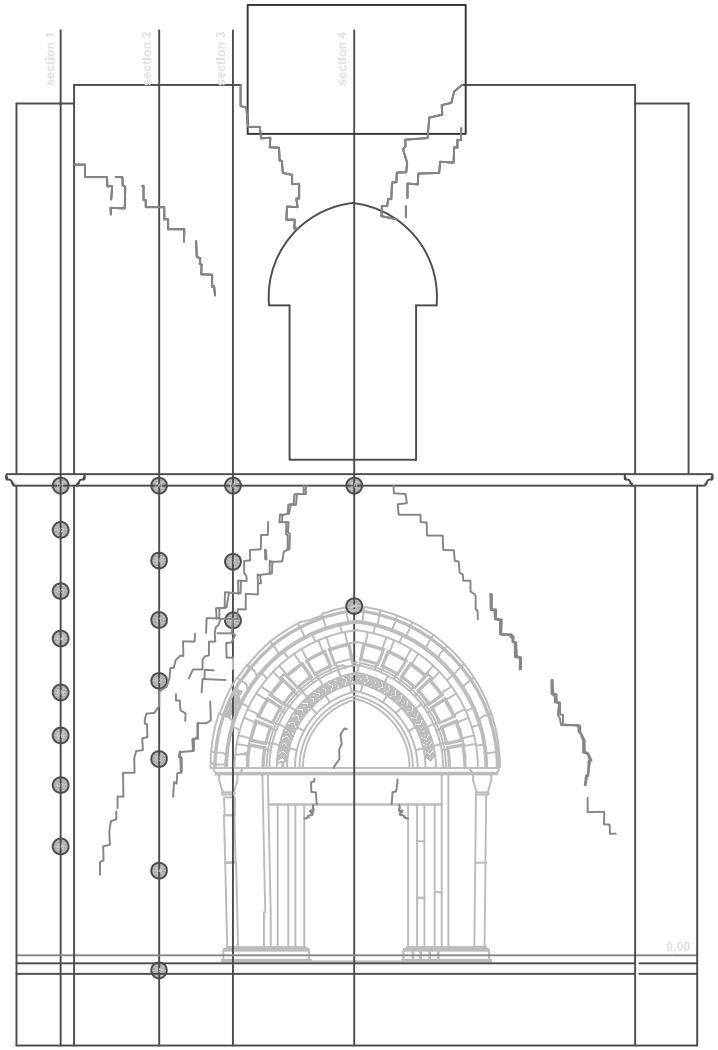
section 1
section 2
section 3
section 4
0,00

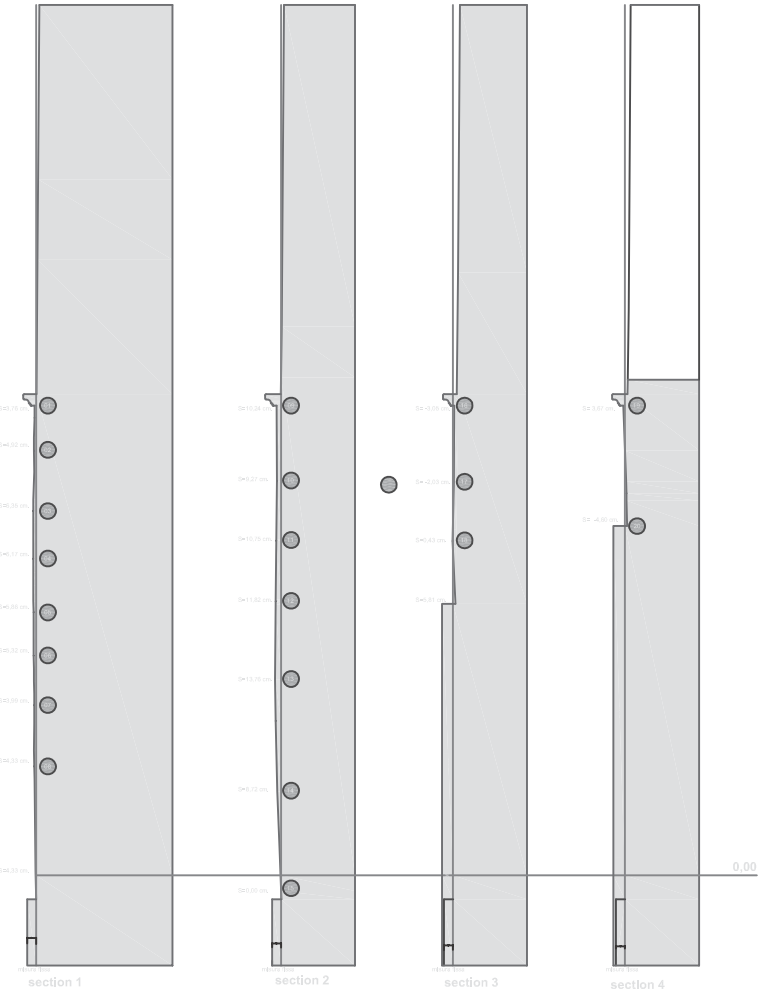
0,00
section 1
section 2
section 3
section 4

Detail A

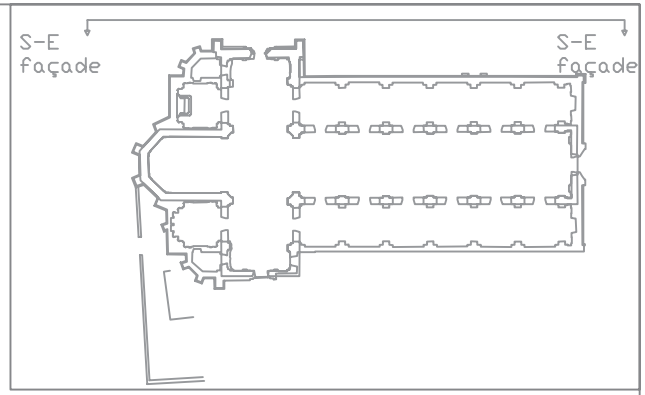

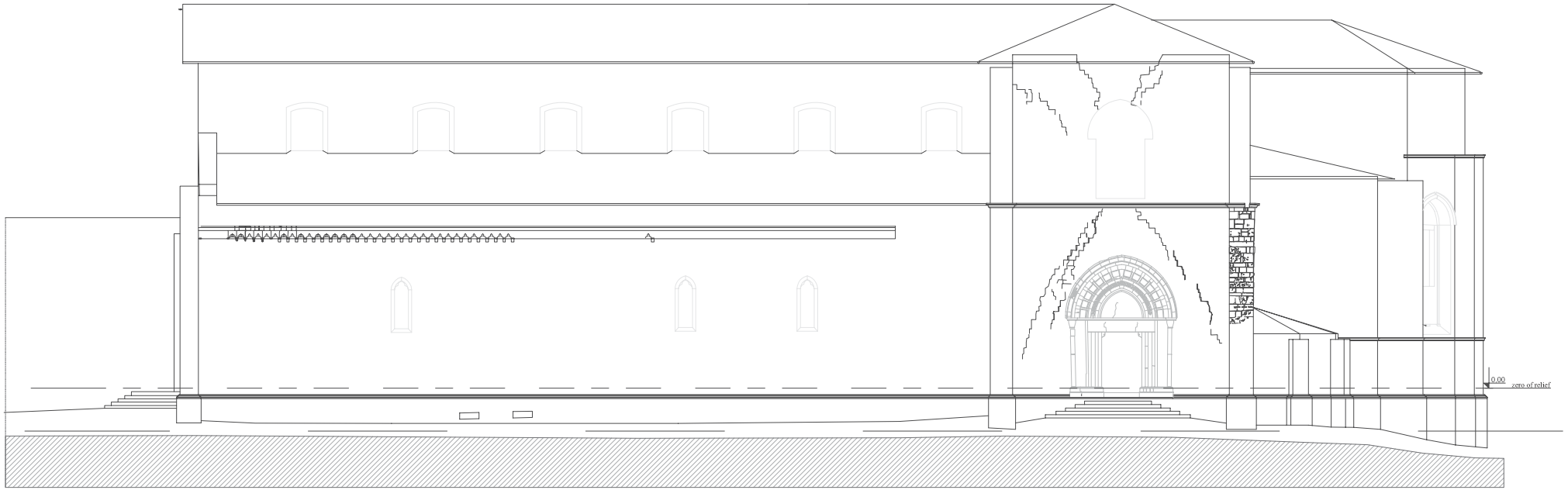

[m]

0 5 10 15 20

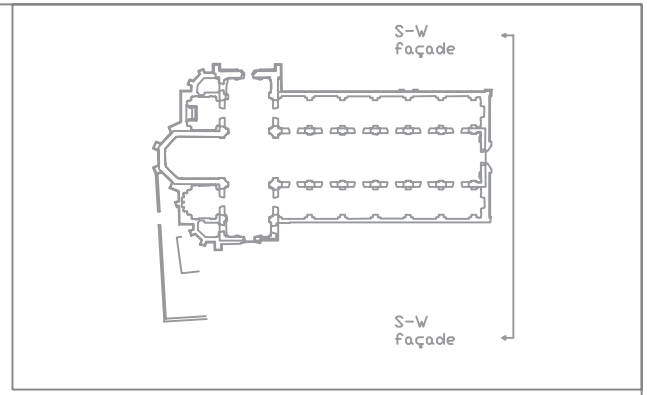

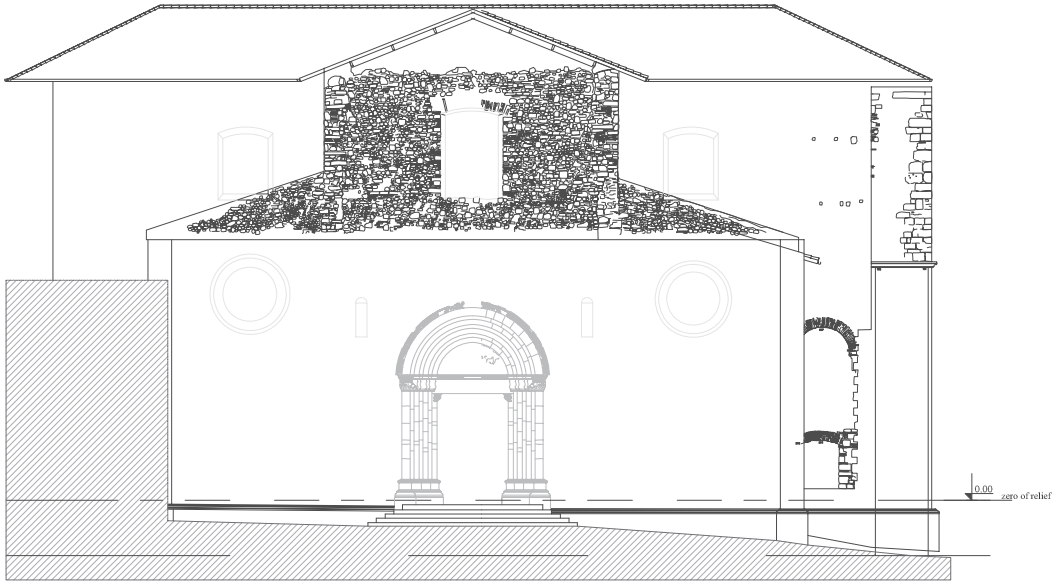

[m]

0 5 10 15 20

ANNEX II

AII.1 - Data from Study Case 2

- Frequency vs. Temperature (1st set of data)

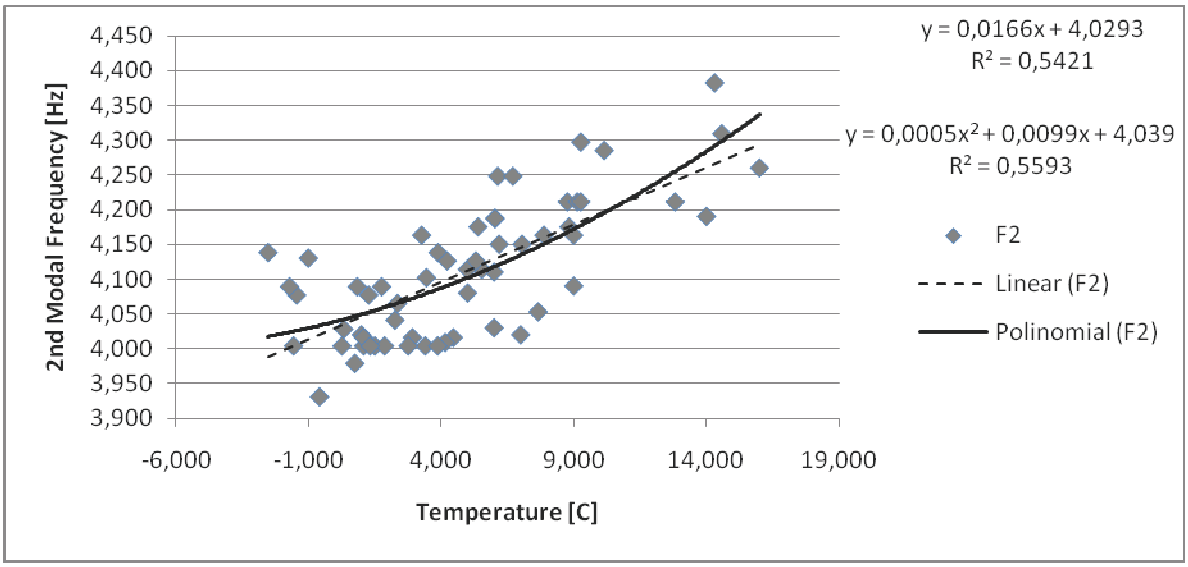

Figure 1 - Relation between 2nd modal frequency and Temperature

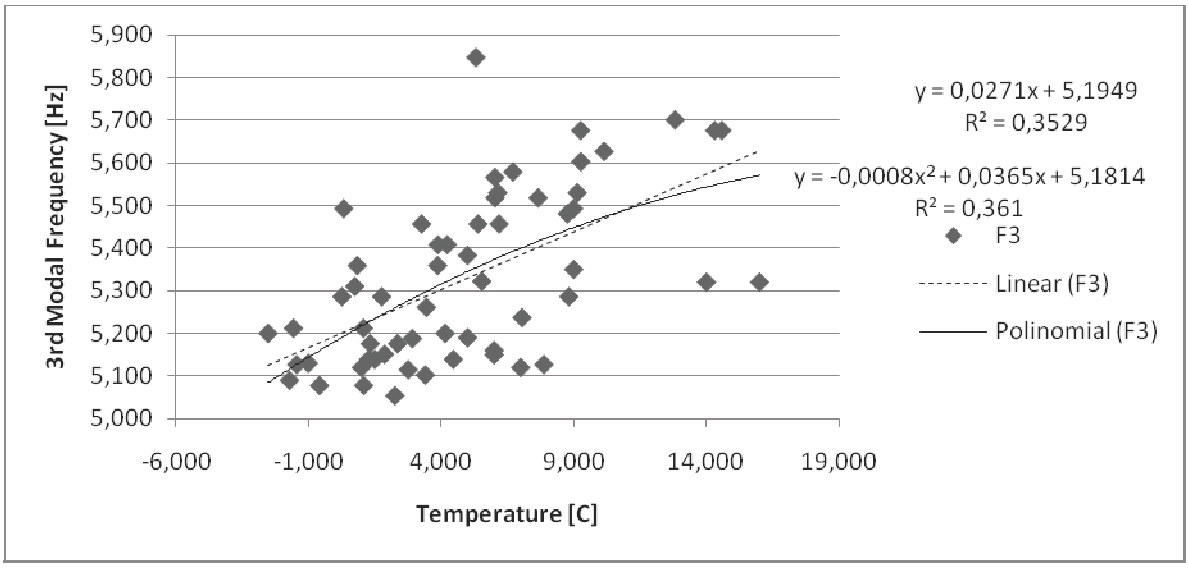

Figure 2 - Relation between 3rd modal frequency and Temperature

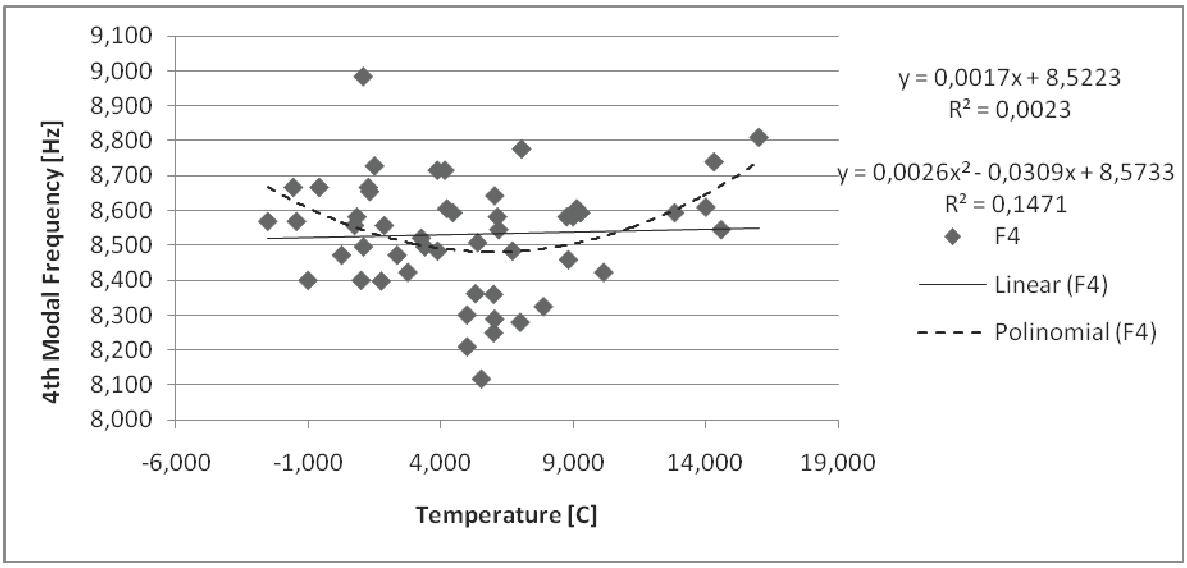

Figure 3 - Relation between 4th modal frequency and Temperature

- Frequency vs. Relative Humidity (1st set of data)

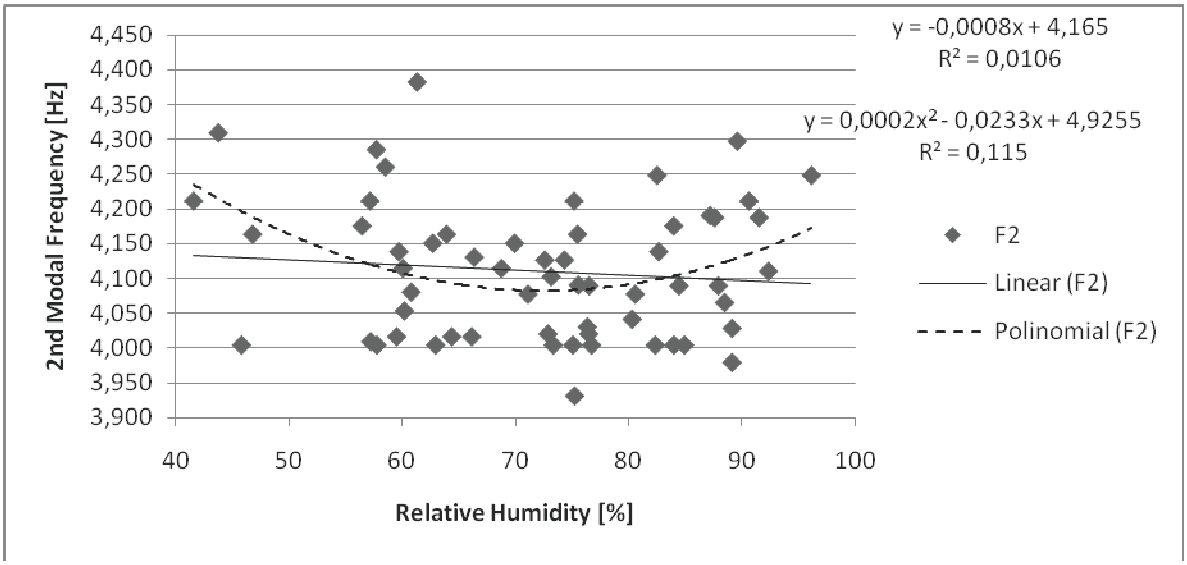

Figure 4 - Relation between 2nd modal frequency and Realtive Humidity

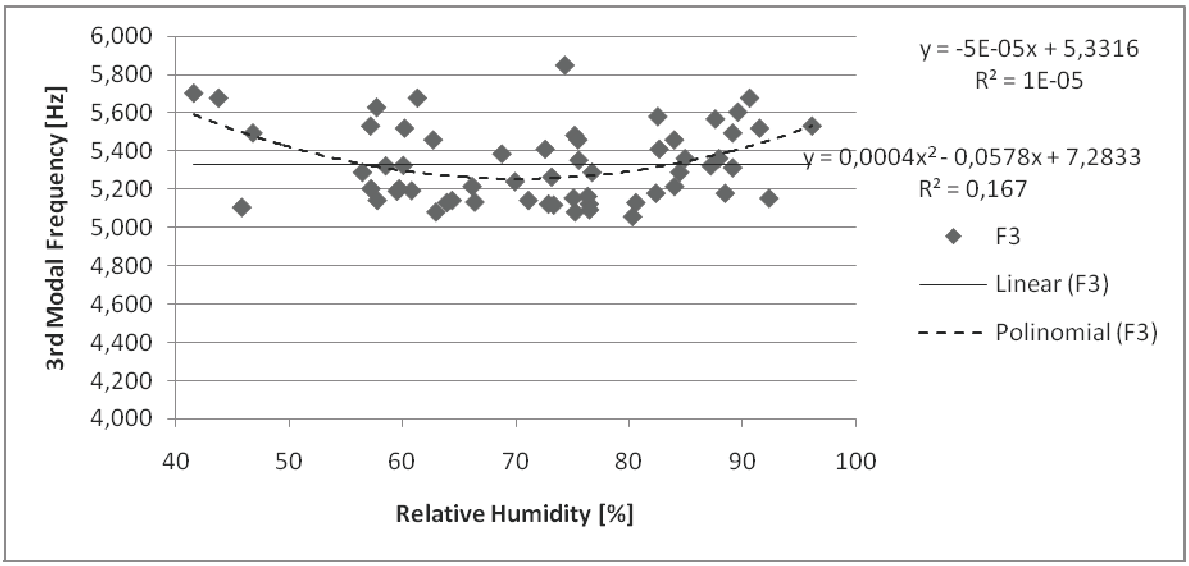

Figure 5 - Relation between 3rd modal frequency and Realtive Humidity

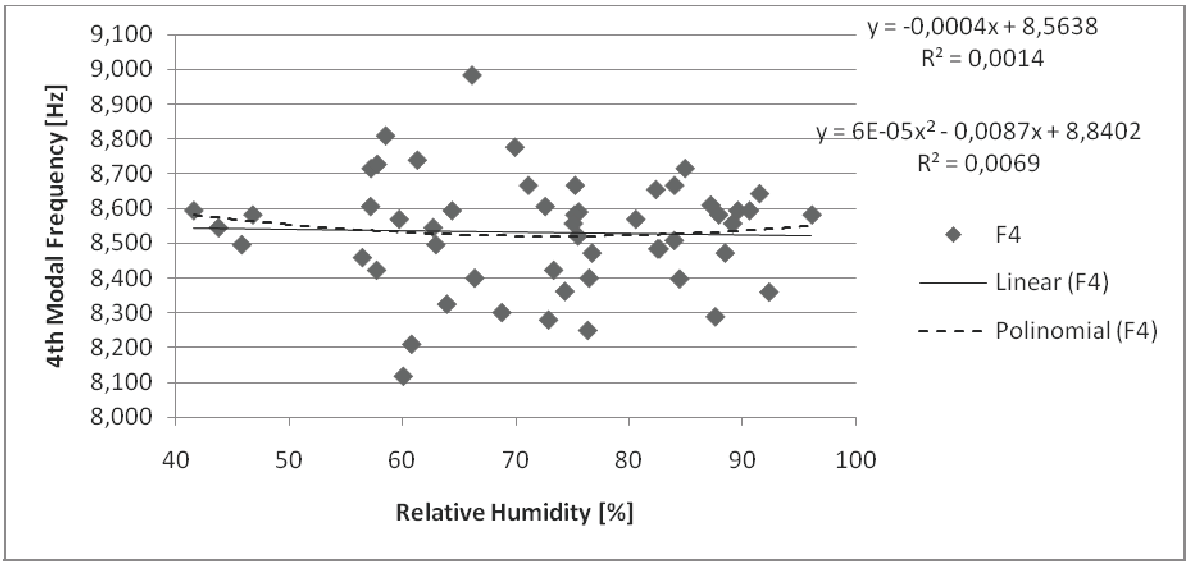

Figure 6 - Relation between 4th modal frequency and Realtive Humidity

- Frequency vs. RMS (1st set of data)

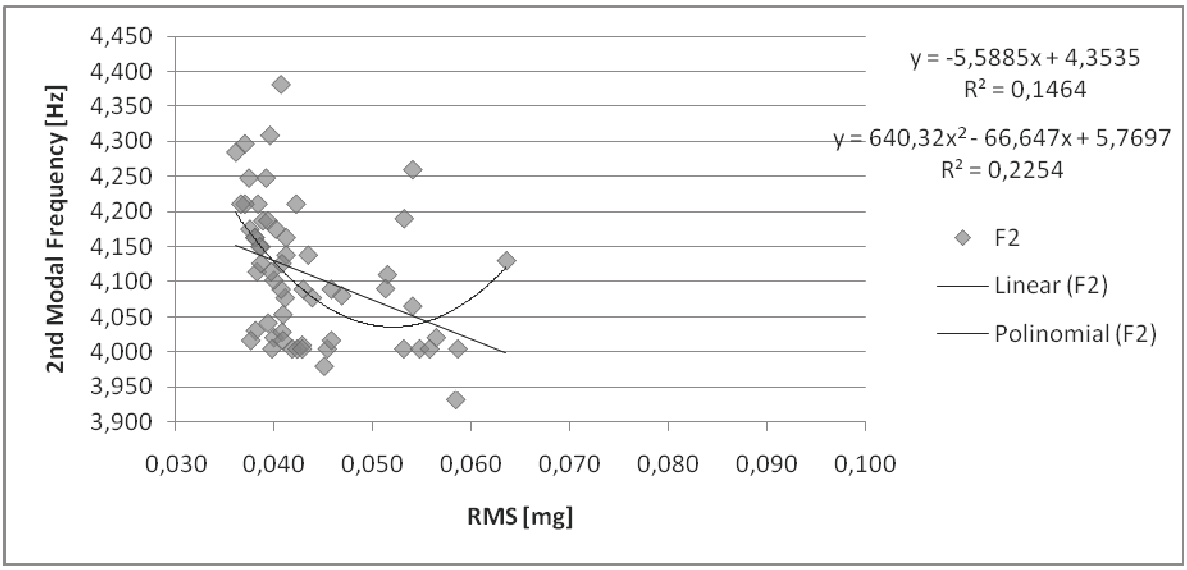

Figure 7 - Relation between 2nd modal frequency and RMS

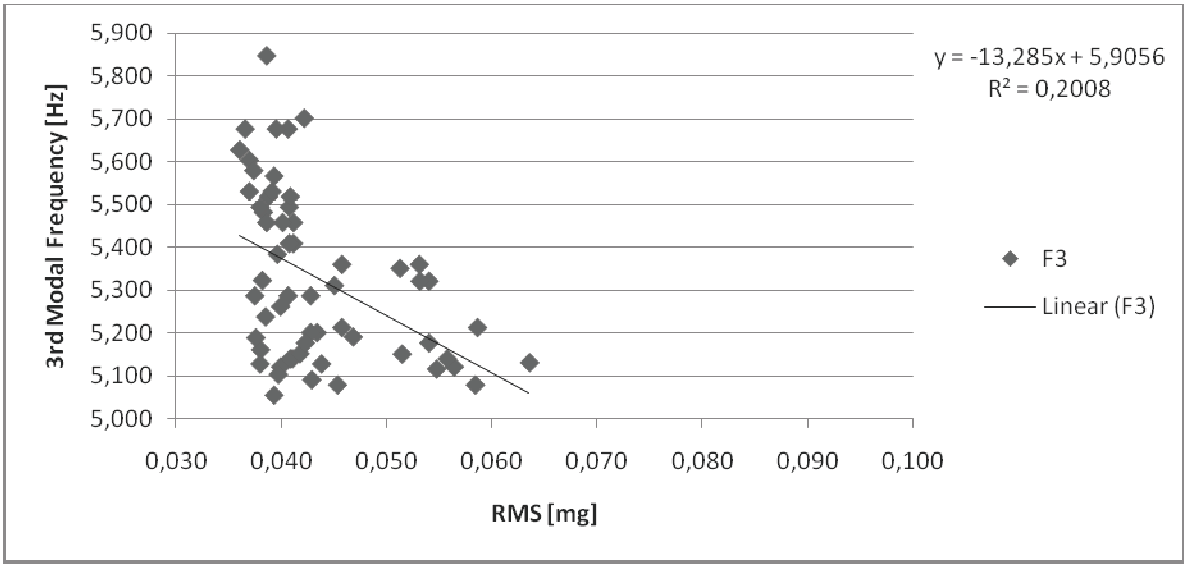

Figure 8 - Relation between 3rd modal frequency and RMS

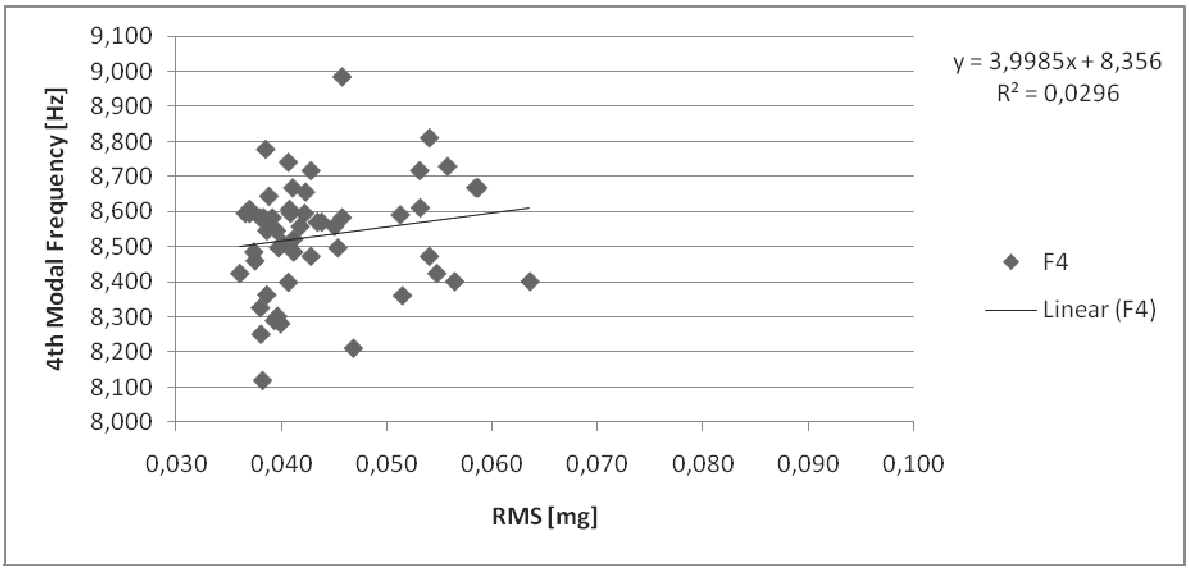

Figure 9 - Relation between 4th modal frequemcy and RMS

AII.2 – List of micro-tremors

(The events chosen for analysis are with grey filling)

Table 1 - List of micro-tremors

Event-Id	Date	Time (UTC)	Lat	Lon	Prof(Km)	Mag	Seismic District
2210400380	02-01-2010	03:18:54	42.378	13.384	9.2	2.4	Aquilano
2210521170	10-01-2010	12:37:36	43.134	13.416	35.8	**3.1**	Zona_Ascoli_Piceno
2210518730	10-01-2010	08:33:35	43.126	13.402	9	**3.9**	Zona_Ascoli_Piceno
2210521280	10-01-2010	12:51:55	42.235	13.548	10	2.2	Valle_dell'Aterno
2210550550	12-01-2010	13:35:44	43.129	13.438	24.1	**4.1**	Zona_Ascoli_Piceno
2210547450	12-01-2010	08:25:10	43.123	13.413	25.6	**4**	Zona_Ascoli_Piceno
2210567390	13-01-2010	17:39:32	42.367	13.398	9.7	2.2	Aquilano
2210676980	21-01-2010	08:18:33	42.474	13.369	9.8	**2.5**	Gran_Sasso
2210693900	22-01-2010	12:30:50	42.247	13.526	9.9	**3.4**	Valle_dell'Aterno
2210708710	23-01-2010	13:11:07	42.337	13.507	8.9	**2.8**	Valle_dell'Aterno
2210751310	26-01-2010	12:12:12	42.257	13.484	9.3	2.1	Velino-Sirente
2210750190	26-01-2010	10:19:29	42.368	13.423	9.5	2.2	Aquilano
2210775770	28-01-2010	04:58:21	42.485	13.379	11.2	2	Gran_Sasso
2210805480	30-01-2010	06:28:45	42.24	13.53	9.8	**2.6**	Valle_dell'Aterno
2210828810	31-01-2010	21:21:30	42.273	13.413	10.2	**3.2**	Velino-Sirente
2210881260	04-02-2010	12:46:56	42.344	13.518	10.2	2	Valle_dell'Aterno
2211056240	16-02-2010	16:25:19	42.355	13.519	8.4	**2.9**	Gran_Sasso
2211080400	18-02-2010	08:40:29	42.353	13.512	9.3	**2.8**	Valle_dell'Aterno
2211085890	18-02-2010	17:49:22	43.137	13.422	22.1	**2.5**	Zona_Ascoli_Piceno
2211239480	01-03-2010	09:48:26	42.361	13.401	10.1	2.4	Aquilano

Event-Id	Date	Time (UTC)	Lat	Lon	Prof(Km)	Mag	Seismic District
2211348520	08-03-2010	23:32:11	42.365	13.4	9.4	**2.7**	Aquilano
2211377560	10-03-2010	23:56:26	42.472	13.386	10.1	**2.7**	Gran_Sasso
2211453110	16-03-2010	05:51:43	42.299	13.382	10.6	**2.7**	Aquilano
2211519370	20-03-2010	20:17:54	42.359	13.333	10	1.5	Aquilano
2211509060	20-03-2010	03:06:26	42.359	13.332	9	2.2	Aquilano
2211508010	20-03-2010	01:21:59	42.349	13.316	8	2.3	Aquilano
2211507970	20-03-2010	01:17:19	42.357	13.322	9	**2.5**	Aquilano
2211535470	21-03-2010	23:07:43	42.271	13.477	0.7	1.2	Valle_dell'Aterno
2211544660	22-03-2010	14:27:35	42.381	13.34	8.8	0.8	Aquilano
2211541650	22-03-2010	09:26:19	42.367	13.328	10.3	1.9	Aquilano
2211540450	22-03-2010	07:26:53	42.349	13.288	10.3	1.7	Aquilano
2211538850	22-03-2010	04:45:23	42.272	13.548	10.1	2.2	Valle_dell'Aterno
2211538820	22-03-2010	04:42:40	42.232	13.517	6	1.5	Velino-Sirente
2211538650	22-03-2010	04:25:10	42.368	13.437	9.6	1.8	Aquilano
2211538550	22-03-2010	04:15:35	42.345	13.29	10.7	1.6	Aquilano
2211590980	25-03-2010	19:38:33	42.376	13.356	9.7	2	Aquilano
2211607450	26-03-2010	23:05:18	42.482	13.351	11.8	2.2	Gran_Sasso
2211625440	28-03-2010	05:04:54	42.329	13.513	10.8	2.1	Valle_dell'Aterno
2211700140	02-04-2010	09:34:53	42.466	13.345	10	2.2	Gran_Sasso
2211721510	03-04-2010	21:11:58	42.388	13.413	9.6	2.2	Aquilano
2211752570	06-04-2010	00:57:07	42.449	13.324	12	2.2	Gran_Sasso
2211767110	07-04-2010	01:11:55	42.45	13.337	14.3	2.3	Gran_Sasso
2211943790	19-04-2010	07:39:22	42.27	13.565	9.8	2	Valle_dell'Aterno
8211971830	21-04-2010	06:23:38	42.47	13.4	5	2.3	Gran_Sasso
2211971830	21-04-2010	06:23:20	42.461	13.385	9.4	2.3	Gran_Sasso
8211987790	22-04-2010	08:59:38	42.35	13.49	10.8	2	Valle_dell'Aterno
2211987790	22-04-2010	08:59:20	42.346	13.503	10.4	2.1	Valle_dell'Aterno
2212016030	24-04-2010	08:04:46	42.463	13.315	13.9	2.2	Gran_Sasso
2212047900	26-04-2010	13:10:32	42.466	13.309	10.9	2.1	Gran_Sasso
2212108070	30-04-2010	17:29:11	42.329	13.521	9.5	2.1	Valle_dell'Aterno
2212123400	01-05-2010	19:01:30	42.384	13.253	5	2.1	Aquilano
2212112500	01-05-2010	00:50:33	42.322	13.528	10.2	**2.6**	Valle_dell'Aterno
2212306190	14-05-2010	11:39:21	42.295	13.564	8.9	1.8	Valle_dell'Aterno
2212485770	26-05-2010	22:57:12	42.463	13.244	10.1	**2.5**	Aquilano
2212485640	26-05-2010	22:44:52	42.471	13.245	10.8	**2.9**	Aquilano
2212478680	26-05-2010	11:08:40	42.326	13.436	9.7	1.6	Aquilano
2212537740	30-05-2010	13:34:48	42.354	13.502	11.4	2.1	Valle_dell'Aterno
2212531010	30-05-2010	02:30:34	42.294	13.421	11.2	2.4	Aquilano
2212697350	10-06-2010	15:35:09	42.36	13.377	10.6	2.3	Aquilano
2212723110	12-06-2010	10:31:16	42.445	13.319	11.1	2.1	Aquilano
2212723040	12-06-2010	10:24:26	42.444	13.322	12.8	2	Aquilano

Event-Id	Date	Time (UTC)	Lat	Lon	Prof(Km)	Mag	Seismic District
2212751400	14-06-2010	09:40:45	42.375	13.33	10.4	**2.5**	Aquilano
2212761220	15-06-2010	02:02:56	42.499	13.302	10.7	2.1	Gran_Sasso
2212776530	16-06-2010	03:33:56	42.481	13.322	9.4	2.4	Gran_Sasso
2212809970	18-06-2010	11:18:33	42.461	13.201	9.2	**2.5**	Aquilano